SPINOPHILIN-DEPENDENT REGULATION OF THE PHOSPHORYLATION, PROTEIN INTERACTIONS, AND FUNCTION OF THE GLUN2B SUBUNIT OF THE NMDAR AND ITS IMPLICATIONS IN NEURONAL CELL DEATH

by

Asma Beiraghi Salek

A Dissertation

Submitted to the Faculty of Purdue University

In Partial Fulfillment of the Requirements for the degree of

Doctor of Philosophy

Department of Biology at IUPUI

Indianapolis, Indiana

December 2020

THE PURDUE UNIVERSITY GRADUATE SCHOOL
STATEMENT OF COMMITTEE APPROVAL

Dr. AJ Baucum II, Chair

Department of Biology

Dr. Theodore Cummins

Department of Biology

Dr. Nicolas Berbari

Department of Biology

Dr. Yvonne Lai

Department of Psychological and Brain Sciences

Dr. Andy Hudmon

Department of Medicinal Chemistry and Molecular Pharmacology

Dr. Jason Meyer

Department of Medical and Molecular Genetics

Approved by:

Dr. Theodore Cummins

هو هو

برای مادر و پدر

و برای روزبه

بخاطر عشق و حمایتهای بی دریغ و بخاطر بودنشان

خانم بشاش معلم عزیزم که با صبر و اشتیاق و درایت کنجکاویم برای علوم زیستی را پروراند

و دکتر جعفر وطن پرست که با شرافت و دانش و آگاهی شعله تحقیقات مغز و اعصاب را در ذهنم

برافروخت

اسرار ازل را نه تو دانی و نه من

وین حل معما نه تو خوانی و نه من

هست از پس پرده گفتگوی من و تو

چون پرده برافتد نه تو مانی و نه من

حکیم عمر خیام

If you keep knocking on a door long enough, sooner or later someone will answer you.

ACKNOWLEDGMENTS

I would like to acknowledge Dr. A.J. Baucum, my supervisor, for believing in me, for his help, advice, patience, guidance, and full support during my years in his lab. Also, Drs. Nicolas Berbari, Theodore Cummins, Yvonne Lai, Andy Hudmon, and Jason Meyer for serving on my advisory committee and providing much-needed feedback and constructive criticism. I would also like to acknowledge the Biology Department at IUPUI for giving me the opportunity to further my education in such a positive environment. Sue Merrell, Shari Dowell, Laura Flak, Angela Longfellow, Julie Driscol and Anita Sale for their care and help along the way.

I would like to acknowledge Drs Mike Edler and Sarah Ohlemacher for their help and advice during all these years. Thank you, Cameron, Kaitlyn and Darryl. I have learned so much from you. Thank you for your help and support and for creating a fun, positive and interactive environment in the lab. And thank you for setting the bar so high with being hardworking and caring at the same time.

I would also like to give my very special thanks to Indiana CTSI, Eli Lilly and Company and Stark Neurosciences research institute for believing in me and giving me the opportunity to focus on my research by selecting and generously supporting me as a Eli Lilly/Stark Neurosciences predoctoral fellow. Thank you to Dr. Lisa Jones and the Indiana School of Medicine Proteomics Core facility for mass spectrometry-based sequencing.

These studies were supported by NIH grant (K01NS073700/ R21/R33DA041876) IUPUI School of Science and Department of Biology to AJB and partly by the Stark Neurosciences Research Institute, the Indiana Alzheimer Disease Center, Eli Lilly and Company, and by the Indiana Clinical and Translational Sciences Institute to ABS, funded in part by grant # UL1TR002529 from the National Institutes of Health, National Center for Advancing Translational Sciences. The content is solely the responsibility of the authors and does not necessarily represent the official views of the National Institutes of Health.

TABLE OF CONTENTS

LIST OF TABLES

LIST OF FIGURES

LIST OF ABBREVIATIONS

aCSF: Artificial Cerebrospinal Fluid

Ala: Alanine

AMPAR: α-amino-3-hydroxy-5-methyl-4-isoxazolepropionic acid receptor

APVor AP5: 2-amino-5phosphonovaleric acid

Ara-C: Cytosine β-D-arabinofuranoside

Asp: Aspartate

AUC: Area under the curve

CaMKII: Calcium/Calmodulin dependent kinase II

CDK5: Cyclin-dependent kinase 5

cNB: Conditioned Neurobasal media

DG: Dentate gyrus

DIV: Days in vitro

EC: Entorhinal Cortex

EPSC: Excititiry post synaptic Current

EPSP: Excitotory post synaptic potential

FBS: Fetal Bovine Serume

GC: Granule cells

GPCR: G-protein Coupled Receptors

HEK293: Human Embryonic Kidney 293

HSS: High sucrose solution

IBMX: 3-isobutyl-1-methylxanthine

IST: Insulin/Selenite/Transferrin

LTD: Long Term Depression

LTP: Long Term Potentiation

MEM: Modified Eagle's Medium

MU: Mutant

MWM: Morris Water Maze

NLR: Novel Location Recognition

NMDA: N-Methyl, D-Aspartate

NMDAR: N-Methyl, D-Aspartate receptor

NOR: Novel Object Recognition

PBS: Phosphate-buffered Saline

PD: Pull down

Pen/Strep: Penicillin/Streptomycin

PKA: Protein Kinase A

PKAc: Catalytic subunit of Protein kinase A

PKC: Protein Kinase C

PP1: Protein Phosphatase 1

PSD: Postsynaptic density

RGS: Regulators of G protein signaling

rMWM: Reversal learning using Morris Water Maze

RRID: Research Resource Identifier.

SD: Standard deviation

SEM: Standard error of the mean

Ser: Serine

TBS: Tris Buffer Saline

ABSTRACT

Excitotoxicity, a major hallmark of neurodegeneration associated with cerebral ischemia, is a result of accumulation of extracellular glutamate. This excess glutamate leads to hyperactivation of glutamate receptors such as the N-methyl-D-asparate (NMDA) receptors (NMDARs) following the activation of α-amino-3-hydroxy-5-methyl-4-isoxazolepropionic acid (AMPA) receptor (AMPARs). Excessive activation of NMDARs causes an influx of calcium, which can eventually activate apoptotic pathways and lead to death of neurons. Regulation of NMDAR subunit composition, localization, surface expression, and activity can balance cell survival via activation of either pro-death or pro-survival pathways after a course of an ischemic insult. Specifically, phosphorylation of different NMDAR subunits defines their activity and downstream signaling pathways. NMDARs are phosphorylated by multiple kinases and dephosphorylated by different phosphatases. Besides phosphatases and kinases, per se, phosphorylation of synaptic proteins that regulate kinase or phosphatase targeting and activity also mediate NMDAR phosphorylation. Spinophilin, a major synaptic scaffolding and protein phosphatase 1 (PP1) targeting protein, mediates substrate phosphorylation via its ability to bind PP1. Our studies focus on delineating the role of spinophilin in the regulation of phosphorylation and function of the GluN2B subunit of the NMDA receptor as well as the role of spinophilin in modulating glutamate-induced neurotoxicity. Interestingly, our data demonstrate that spinophilin sequesters PP1 away from GluN2B thereby enhancing phosphorylation of GluN2B at Ser-1284. These changes impact GluN2B protein interactions, subcellular localization, and surface expression, leading to alterations in the amount of calcium entering the neuron via GluN2B-containing NMDARs. Our data show that spinophilin biphasically regulates GluN2B function. Specifically, Ser-1284 phosphorylation enhances calcium influx through GluN2B containing NMDA receptors, but spinophilin leads to dramatic decreases in the surface expression of the receptor independent of Ser-1284 phosphorylation. Moreover, in spinophilin knockout mice, we observe less PP1 binding to GluN2B and less phosphorylation of Ser-1284, but more surface expression of GluN2B and greater levels of caspase activity. Together, these observations suggest a potential neuroprotective role for spinophilin by decreasing GluN2B-containing NMDA receptor-dependent surface expression and thereby decreasing intracellular calcium and neuronal cell death.

CHAPTER 1. INTRODUCTION

1.1 Hippocampus, Hippocampal Function, And Behavior

The hippocampus is a major component of the vertebrate brain. Humans and other mammals have two hippocampi, one within each hemisphere of the brain. The hippocampus is known to be a key brain structure for the formation of memories. The hippocampus was implicated in human memory formation 60 years ago, when the patient H.M faced a pure memory deficit after surgical excision of the medial temporal lobe (including the hippocampus) as a treatment for epilepsy (Andersen, 2007). More specifically, the hippocampus stores shorter-term declarative memory from days to weeks while the ultimate storage site for all declarative memories is thought to be cerebral cortex. The circuitry of the hippocampus determines how it stores long lasting memories. The hippocampus is divided into multiple subfields designated as Ammon's horn (cornu ammonis; CA)1, CA2, CA3, CA4, and the dentate gyrus. (Andersen, 2007). The major hippocampal input comes from the entorhinal cortex (EC), while the major output is to the CA1 region which then synapses to the layer V and VI of the EC (Kandel, 2013). The EC sends inputs to the hippocampus through the direct and indirect perforant pathways. Through the direct pathway, the EC sends its inputs directly to the distal dendrites of the CA1 region. The indirect pathway projects to CA1 through a tri-synaptic pathway. In this pathway, EC axons synapse on granule cells (GC) in the dentate gyrus (DG). These cells project through the mossy fiber pathway to CA3 pyramidal cells, which then project through the Schaffer collaterals to the proximal dendrites of CA1 pyramidal neurons. Both the direct and indirect perforant pathways are believed to be important for learning and memory such that lesions to Schaffer collaterals impair complex spatial learning memory tasks while some forms of spatial learning remain intact. On the other hand, lesions to the direct perforant pathway do not interfere with memory formation but inhibit memory consolidation, a process of storing initial memories as long-term memories (Kandel, 2013). Studies on these pathways later showed that a brief, high-frequency train of stimuli leads to long-lasting increases in the excitatory post synaptic potentials (EPSPs), a process termed long-term potentiation (LTP) (Bliss & Lomo, 1973) . This form of plasticity is observed in GC to CA3 (Zalutsky & Nicoll, 1990), CA3 to CA1 (Morgan & Teyler, 2001a, 2001b), and EC to CA1 synapses (Remondes & Schuman, 2003). Interestingly, N-methyl-D-aspartate (NMDA) receptor

NMDAR function is believed to be critical for CA3 to CA1 LTP such that this LTP is abolished in the presence of the NMDAR antagonist, APV, while EC to CA1 synapses are not completely blocked with APV and are partially dependent on L-type calcium channels in addition to NMDARs (Remondes & Schuman, 2003). Furthermore, the GC to CA3 synapses are not blocked with AP5 treatment and do not require NMDAR activity. However, LTP at these synapses requires PKA and is blocked with the PKA inhibitor, H89 (Weisskopf, Castillo, Zalutsky, & Nicoll, 1994; Zalutsky & Nicoll, 1990). The role of the NMDAR at CA3 to CA1 synapses is critical in mediating downstream activation of the indirect perforant pathway and changes in synaptic strength. Specifically, glutamate released from presynaptic terminals that project from CA3 binds to AMPA receptors and NMDA receptors in the post synaptic cell within CA1. At resting membrane potentials, binding of glutamate to NMDARs does not fully activate NMDARs due to a blockage of the channel pore by magnesium. However, if sufficient glutamate is bound to AMPARs, the membrane will depolarize and permit removal of the magnesium block. With glutamate bound to the NMDAR and the magnesium block removed, cations such as sodium (Na+) and calcium (Ca2+) move into the cell. The conductance of NMDARs to calcium is higher than that of AMPARs to calcium and so activation of NMDARs is critical for activation of calcium-dependent pathways inside the cell (Kandel, 2013). Intracellular calcium acts via multiple pathways, such as activation of Calcium/Calmodulin-dependent kinase II (CaMKII), protein kinase C (PKC), Fyn (Malinow & Tsien, 1990) and nitric oxide synthase, to increase the cell's excitability in response to glutamate by increasing AMPARs on the surface (Malinow, 2003) and increasing presynaptic glutamate release (Tsien & Malinow, 1990). This enhanced excitability of the post synaptic cell leads to an "early LTP" that lasts for hours. In "late LTP," in which the cells stay potentiated for 24 hours, changes in gene expression by activation of Protein Kinase A (PKA) and subsequent phosphorylation of the cAMP response element binding protein (CREB), enhances the protein expression required for formation of new dendritic spines (Bolshakov, Golan, Kandel, & Siegelbaum, 1997). In contrast to enhanced glutamate signaling and LTP, if the post-synaptic cell receives prolonged periods of low-frequency stimulation from the pre-synapse, the synapse will eventually weaken. Interestingly, the smaller magnitude EPSP is not sufficient to relieve the magnesium block from NMDARs and results in dramatic decreases in the amount of calcium entering the cell. The low calcium levels will shift the balance of activation towards the calcium-dependent phosphatase, calcineurin, compared to kinases such as CaMKII due to the higher

affinity of the phosphatase, compared to CaMKII, to calcium. The activated calcineurin dephosphorylates key members of post synaptic density (PSD), such as AMPARs thus decreasing their surface expression. With this process, the post synaptic cell becomes less likely to be excited by the presynaptic input, leading to a depression of postsynaptic function termed, Long Term Depression (LTD) (Bear & Malenka, 1994; Dudek & Bear, 1992; Malenka & Bear, 2004). Both types of plasticity, LTP and LTD, are important in formation and storage of spatial memory (Kandel, 2013) and are heavily NMDAR-dependent, suggesting an important role for NMDARs in mediating hippocampal function. Furthermore, while NMDARs are not required in the LTP observed in DG-CA3 synapses (Weisskopf et al., 1994), selective knockout of the obligate GluN1 subunit of NMDARs in the granule cells of the DG abolishes pattern separation and the ability to distinguish similar contexts (McHugh et al., 2007) suggesting a role for NMDARs residing in DG in hippocampal-dependent behaviors. Taken together, these studies suggest the important role of the hippocampus in formation and storage of declarative/explicit memory and the integral role of NMDARs in mediating hippocampal plasticity and hippocampal function.

1.2 NMDA Receptor Subunits and Function

Glutamatergic synapses are the main excitatory synapses in mammalian brain and are critical for proper neuronal connectivity. In these synapses, glutamate released from the presynaptic terminals activates ionotropic glutamate receptors such as NMDA, AMPA and kainite receptors on the post synaptic dendrites (Dingledine, Borges, Bowie, & Traynelis, 1999; Hollmann & Heinemann, 1994). Glutamatergic transmission plays a critical role in mediating normal brain function and deficits in this transmission are associated with multiple neurological disorders such as Alzheimer disease, Parkinson disease, and schizophrenia (S. Cull-Candy, Brickley, & Farrant, 2001; Waxman & Lynch, 2005). NMDARs, as a main class of glutamate receptors, play an important role in systemic integrity of glutamatergic synapses. These receptors are heterotetramers and consist of subunits that are encoded by three main families of genes, *Grin1*, *Grin2*, and *Grin3*. These genes encode GluN1, GluN2, and GluN3 subunits, respectively (S. Cull-Candy et al., 2001). Various studies show that NMDARs consist of two obligatory GluN1 subunits and two GluN2 or one GluN2 and one GluN3 subunits (S. G. Cull-Candy & Leszkiewicz, 2004). Appropriate, functional channel assembly requires one GluN1 homodimer, and either a GluN2 or a GluN2-GluN3 dimer, to form a dimer of dimers (Karakas, Simorowski, & Furukawa, 2011; Qiu, Hua,

Yang, Chen, & Luo, 2005). Moreover, crystallographic and electrophysiological analysis indicates that GluN1/GluN2 heterodimers is the functional unit for formation of glutamate activated NMDARs (Furukawa, Singh, Mancusso, & Gouaux, 2005). Functional NMDARs are voltage-gated cation channels which also allow for calcium influx. Moreover, activation of these functional channels requires multiple steps due to receptor blockade by magnesium ions at resting membrane potentials. Specifically, binding of glutamate to GluN2 subunits and glycine, as a co-agonist, to GluN1 subunits along with depolarization caused by AMPA receptor activity, results in removal of the magnesium block and allows for inward calcium flow (Erreger, Chen, Wyllie, & Traynelis, 2004).

Transcriptional and translational control of different NMDAR subunits is complex. For example, the GluN1 subunit of NMDARs is encoded by a single gene (*Grin1*) which is alternately spliced into eight different variants (H. Liu et al., 2019). The GluN2 subunits, however, are encoded by four different genes (*Grin2a*, *Grin2b*, *Grin2c*, *Grin2d*). Moreover, NMDAR subunit composition is developmentally regulated (Monyer, Burnashev, Laurie, Sakmann, & Seeburg, 1994), and plays an important role in defining channel properties (S. G. Cull-Candy & Leszkiewicz, 2004; McKay et al., 2018; Sanz-Clemente, Nicoll, & Roche, 2013; Wyllie, Livesey, & Hardingham, 2013). The expression pattern of these subunits depends on the brain region and developmental stage of the animal (S. Cull-Candy et al., 2001). Specifically, studies of the rodent brain shows that GluN2C and GluN2D have a restricted expression pattern. The GluN2C subunit is expressed mostly in the cerebellum later in embryonic development, while the GluN2D subunit is expressed early in prenatal development in the thalamus, hypothalamus, and brain stem. Unlike GluN2C and GluN2D, the GluN2A and GluN2B subunits of NMDARs are more ubiquitously expressed in the brain (Monyer et al., 1994). GluN2B constitutes most of the NMDARs early in development since GluN2B is identified as a key regulator of synapse maturation (S. Cull-Candy et al., 2001). Later in adulthood, GluN2B is found in hippocampus, cortex, striatum and other brain regions. GluN2B-containing NMDARs are localized at synaptic and extrasynaptic sites early in development but become more enriched at extrasynaptic sites after maturation (B. Li et al., 2002; Tovar & Westbrook, 1999). Interestingly, GluN2B-containing NMDRs have higher surface mobility compared to GluN2A-containing NMDARs (Groc et al., 2006). The GluN3 subunits on the other hand, are only incorporated in a subpopulation of the NMDARs in the neocortex, hippocampal CA1 region, olfactory bulb, cerebellum, and nuclei of the amygdala, thalamus,

hypothalamus and brainstem and exhibit lower channel conductance (S. G. Cull-Candy & Leszkiewicz, 2004).

Structurally, each NMDAR subunit, consists of multiple domains such as an N-terminal extracellular domain, 3 membrane spanning domains, a pore loop, and an intracellular C-terminal domain or tail region (S. Cull-Candy et al., 2001). Specifically, the C-terminal cytosolic tail is highly variable depending on the subunit and splice variant. The C-terminal tail region is a key component in defining proper receptor trafficking, localization, and receptor interacting proteins. For example, interactions of NMDARs with members of the PSD, such as SynGap (Kim, Dunah, Wang, & Sheng, 2005) and CaMKII (Barria & Malinow, 2005; Baucum, Shonesy, Rose, & Colbran, 2015; Halt et al., 2012; Sanz-Clemente, Gray, Ogilvie, Nicoll, & Roche, 2013; Stein, Donaldson, & Hell, 2014) are required for different forms of synaptic plasticity (Barria & Malinow, 2005). Furthermore, multiple post-translation modifications, in particular phosphorylation, on the tail region of the NMDAR or on NMDAR interacting proteins are critical modulators of receptor activity, protein interactions, and membrane localization (Cercato et al., 2016; J. A. Murphy et al., 2014; Sanz-Clemente, Gray, et al., 2013; Sanz-Clemente, Nicoll, et al., 2013; Tavalin & Colbran, 2017; Vieira et al., 2016; Wyllie et al., 2013).

1.3 The Balance Between Protein Kinases and Phosphatases

Protein phosphorylation is a key mechanism required for normal cellular function and is regulated by two main groups of enzymes, kinases and phosphatases. In eukaryotes, these proteins are widely expressed throughout the body. The human genome encodes ~500 kinases (Manning, Whyte, Martinez, Hunter, & Sudarsanam, 2002) and ~150 phosphatases (Cohen, 2002), suggesting a discrepancy in the number of phosphatases compared to the number of kinases. However, a balance between these processes is critical for the dynamic regulation of phosphorylation. Moreover, in the vertebrate nervous system, the appropriate balance and shift in the balance of the activity of these enzymes are specifically important for myriad functions, including: modulation of neuronal activity, axon and dendrite formation, and synaptic plasticity (Soderling, 2000).

Kinases and phosphatases are categorized into different families. One specific family is the serine/threonine family of kinases and phosphatases which regulate the phosphorylation of serine and/or threonine residues on various substrates. The human genome encodes for, ~385 serine/threonine kinases (Manning et al., 2002), but only ~40 known serine/threonine phosphatases

(Cohen, 2002). Given the low number of phosphatases compared to kinases, and the promiscuous nature of phosphatases, phosphatases require a greater diversity of targeting or regulatory proteins in order to obtain substrate specificity that balances kinase activity (Cohen, 2002; Janssens, Longin, & Goris, 2008; J. D. Scott & Pawson, 2009).

PKA and CDK5 are among the kinases active in the nervous system. Specifically, PKA is one of the key regulators of glutamate receptor phosphorylation (Tingley et al., 1997) and this phosphorylation underlies various neurological processes such as neuronal plasticity changes such as LTP and LTD (Raymond, Blackstone, & Huganir, 1993; Roche, Tingley, & Huganir, 1994). Besides this, PKA plays an important role in cellular development and its activation is important in neurite formation required for proper neuronal connectivity (Vogt Weisenhorn, Roback, Kwon, & Wainer, 2001). CDK5, another Ser/Thr kinase is known to be a key regulator of cell cycle and cellular development specifically in Central Nervous System (CNS) (Dhavan & Tsai, 2001) such that its removal in mice is known to be fatal due to improper cortex formation. Interestingly, this effect was specific to CNS since formation of other organs was unaffected (Ohshima et al., 1996) most probably due to its importance in neurite growth and neuronal cell development. Besides CDK5's importance in cell development, it is also believed to be one of the important contributors to Tau phosphorylation and aggregation observed in Alzheimer disease (Baumann, Mandelkow, Biernat, Piwnica-Worms, & Mandelkow, 1993). Furthermore, CDK5 can phosphorylate Protein phosphatase inhibitor-1 which results in PP1 being in an active state (Bibb et al., 2001).

Phosphatases, on the other hand, have also strongly been implicated in synaptic plasticity and in mechanisms such as LTP and LTD. For example, as stated above LTP in the CA1 region of hippocampus requires activity of cAMP/PKA and is sensitive to both pharmacological and genetic inhibition of the cAMP/PKA cascade. One mechanism by which the PKA pathway participates in LTP is to suppress PP1 activity, thus allowing for greater stimulus-evoked kinase activity (Winder & Sweatt, 2001). Besides LTD, it has been shown that phosphatases are strongly associated with mechanisms underlying CA1 LTD. Studies show that the induction of LTD in CA1 is associated with a transient increase in PP1 activity for ~35 minutes after LTD induction(Norman, Thiels, Barrionuevo, & Klann, 2000). However, when protein phosphatase 2A (PP2A) is activated with the same stimulus, it remains active for ~65 minutes (Thiels, Kanterewicz, Knapp, Barrionuevo, & Klann, 2000; Thiels, Norman, Barrionuevo, & Klann, 1998). Interestingly, pretreatment with NMDAR antagonists completely abolishes these changes in phosphatase activity. Consistent with

activity-dependent changes in phosphatase activity, direct evidence suggests substrate dephosphorylation with LTD-inducing stimulation. For example, studies show that PKC activity decreases in the CA1 in response to LTD-producing stimuli. This decrease is accompanied by decreased phosphorylation of Ser657/660 on PKC-α and PKC-β (Thiels et al., 2000). However, this change is blocked by treatment with the PP1 and PP2A inhibitor, okadaic-acid, which links this LTD to protein phosphatase activation. These studies show that LTD-producing stimuli evokes PP1/PP2A-mediated dephosphorylation of PKC. Along with PKC, a similar decrease in the phosphorylation on Ser845 of GluR1 subunit of AMPARs, which regulates AMPAR trafficking (Y. Liu et al., 2009), is observed after LTD-producing stimulation which is blocked with pretreatment of Okadaic acid (H. K. Lee, Barbarosie, Kameyama, Bear, & Huganir, 2000).

1.4 NMDA Receptor Phosphorylation

Protein kinases and phosphatases are main groups of enzymes that promote and inhibit, respectively, the phosphorylation state of proteins like NMDAR subunits. Many studies, have focused on investigating NMDAR subunit phosphorylation by multiple kinases such as: PKA, Protein Kinase B (PKB), PKC, CDK5, CaMKII, and Casein Kinase II (CKII) (Mammen, Kamboj, & Huganir, 1999; Roche et al., 1994; Salek, Edler, McBride, & Baucum, 2019; Sanz-Clemente, Gray, et al., 2013; Swope, Moss, Raymond, & Huganir, 1999). To limit phosphorylation, studies have observed phosphatase-dependent regulation of NMDAR phosphorylation (Chiu et al., 2019; Salek et al., 2019). In addition to kinases and phosphatases, per se, phosphorylation of synaptic proteins that modulate kinase or phosphatase targeting also regulate NMDAR phosphorylation (Lan et al., 2001; Sigel, Baur, & Malherbe, 1994; Zheng, Zhang, Wang, Bennett, & Zukin, 1999).

Differential phosphorylation of NMDARs is important in regulating channel properties such as conductance, function, and subcellular localization (H.-K. Lee, 2006). For example, PKC promotes NMDAR activity by increasing the rate of NMDAR opening and the surface expression of NMDARs (Lan et al., 2001; W. Y. Lu et al., 1999). PKC can modulate the phosphorylation of multiple NMDAR subunits, including GluN1, GluN2A and GluN2B. Specifically, PKC-dependent phosphorylation of Ser890 on GluN1 disrupts GluN1 clustering (Tingley et al., 1997) while phosphorylation of GluN1 by PKC at Ser896 has no effect on clustering of GluN1. Moreover, coordinated phosphorylation of GluN1 at Ser896 by PKC and at Ser897 by PKA, increases receptor surface expression (D. B. Scott, Blanpied, Swanson, Zhang, & Ehlers, 2001). Furthermore,

PKC-dependent regulation of GluN2A phosphorylation on Ser1291 and Ser1312 leads to a decreased threshold for activation of the NMDAR (Grant, Guttmann, Seifert, & Lynch, 2001; Jones & Leonard, 2005). PKC also phosphorylates Ser1416 on GluN2A which reduces its binding affinity to CaMKII (Gardoni, Bellone, Cattabeni, & Di Luca, 2001) which may impact NMDAR subcellular localization. PKC also phosphorylates GluN2B at Ser1303 and Ser1323 which inhibits CaMKIIα binding and potentiates channel currents (Liao, Wagner, Hsu, & Leonard, 2001). Therefore, PKC is a critical modulator of NMDAR phosphorylation and function.

In addition to PKC, PKA modulates neuronal plasticity by mediating NMDAR function. Specifically, PKA, increases calcium permeability and synaptic targeting of NMDARs thereby enhancing NMDAR-mediated excitatory post synaptic currents (EPSCs) in order to promote synaptic connectivity (Crump, Dillman, & Craig, 2001; Raman, Tong, & Jahr, 1996; Skeberdis et al., 2006). As stated above, PKA phosphorylation of GluN1 at Ser897 along with PKC-dependent phosphorylation at Ser896 contributes to receptor surface expression (D. B. Scott et al., 2001). PKA also mediates phosphorylation of GluN2B at various sites. For example, phosphorylation at S1166 (J. A. Murphy et al., 2014) is critical in synaptic NMDAR function and Ca2+ signaling in spines. We have also found that PKA can regulate the phosphorylation of Ser929/930, Ser940, and Ser1050 on GluN2B in heterologous cells (Salek et al., 2019); however, the functional consequences of regulating phosphorylation at these sites is unknown.

CDK5, is an additional protein kinase that regulates phosphorylation of Ser1232 on GluN2A and increases functionality of GluN2A-containing NMDARs by increasing NMDAR activity (B. S. Li et al., 2001). Besides GluN2A, GluN2B is regulated by CDK5. Specifically, Y1472 (Zhang, Edelmann, Liu, Crandall, & Morabito, 2008), S1116 (Plattner et al., 2014) and S1284 (W. Lu et al., 2015) are recently characterized phosphorylation sites that are either indirectly or directly phosphorylated by CDK5 and can modulate NMDAR function.

CaMKII regulates the phosphorylation of GluN2B at Ser1303 which promotes slow dissociation of CaMKII-NR2B complex, destabilizes CaMKII and reduces NMDAR desensitization to low Cl2 conditions (Omkumar, Kiely, Rosenstein, Min, & Kennedy, 1996; Prabhu Ramya, Suma Priya, Mayadevi, & Omkumar, 2012; Tavalin & Colbran, 2017).

CKII phosphorylates GluN2B on Ser1480 and thus disrupts GluN2B/PSD95 interaction. Disruption of this interaction maintains GluN2B in the extrasynaptic sites (Chiu et al., 2019; Sanz-Clemente, Gray, et al., 2013).

Besides protein kinases, PP1 regulates the phosphorylation of GluN2B. Ser1480 is a PP1 site on GuN2B and is important for NMDAR translocation and trafficking (Chiu et al., 2019; Chung, Huang, Lau, & Huganir, 2004; Sanz-Clemente, Gray, et al., 2013). Besides Ser1480, we have identified Ser-1284 as another PP1 dephosphorylation site on GluN2B. While the phosphorylation on this site is known to be regulated under ischemic conditions (Ai et al., 2017; W. Lu et al., 2015; Salek et al., 2019), the functional consequence of phosphorylation of this site is yet to be determined.

1.5 Spinophilin Function and Localization

The diversity of phosphatase targeting proteins is most apparent in regulation of PP1. There are ~200 PP1 binding proteins in vertebrates that balance phosphatase activity by targeting PP1 to substrates or inhibiting PP1 activity by limiting its ability to access substrates (Heroes et al., 2013). PP1 interacts with many regulatory proteins via an R-V-x-F motif on the targeting protein (Ceulemans & Bollen, 2006; Meiselbach, Sticht, & Enz, 2006).

Spinophilin is the most abundant PP1 binding protein in the PSD (Colbran et al., 1997) and it regulates the phosphorylation state of various target proteins by either targeting PP1 to the substrates (Allen, Ouimet, & Greengard, 1997), or sequestering PP1 away from substrates (Salek et al., 2019). Modulation of substrate phosphorylation can subsequently modulate protein-protein interaction in the PSD. Specifically, PP1-spinophilin dissociation leads to AMPAR dephosphorylation resulting in a decreased channel activity (Yan et al., 1999). Other studies have reported that the PP1-dependent regulation of NMDARs is abolished in the absence of spinophilin (Feng et al., 2000).

Spinophilin was discovered in brain PP1 immunoprecipitates in 1997 and was observed to be structurally similar to another PP1 binding protein known as neurabin (Satoh et al., 1998). Therefore, spinophilin is sometimes referred to as neurabin-II and neurabin is sometimes referred to as neurabin-I. Due to its high abundance in spines (Allen et al., 1997) it was later referred to as spinophilin. Neurabin and spinophilin are very similar in their structural motifs and their PP1 binding ability (Egloff et al., 1997). The spinophilin gene, *PPP1R9B* (gene ID 84687) is localized on chromosome 17q21.33 and consists of 10 exons. Analysis of PP1 holoenzyme of rat brain shows that neurabin and spinophilin both associate with different isoforms of PP1 (MacMillan et

al., 1999) and that these proteins are two of the most abundant PP1 binding proteins within the postsynaptic density region of rodent forebrains (Colbran et al., 1997).

Comparing the expression pattern of spinophilin across brain regions, the highest levels of spinophilin are in hippocampus, olfactory bulb, olfactory tubercle, and striatum and lower levels are observed in cortex, cerebellum and brain stem (Allen et al., 1997; Ouimet, Katona, Allen, Freund, & Greengard, 2004). Within the hippocampus, spinophilin is present in both principal cells and spiny interneurons and a significant number of symmetric GABAergic hippocampal and pallidal synapses. However, the dentate gyrus has less spinophilin immunoreactivity, indicating lower spinophilin expression in this region (Allen et al., 1997; Ouimet et al., 2004). Other studies looking at the spinophilin expression pattern in macaque prefrontal cortex show that the intensity of spinophilin immunoreactivity is the highest in PSD and spine (Muly, Smith, Allen, & Greengard, 2004) where spinophilin strongly co-localizes with neurabin (Muly, Allen, et al., 2004). Spinophilin reactivity is shown in significant number of dendritic shafts and less frequently in unmyelinated preterminal axons , large myelinated neurons, and glia (Muly, Smith, et al., 2004). Interestingly, one other study using drosophila Neuro-Muscular Junction (NMJ), showed that spinophilin can be present at presynaptic terminals and regulate neurexin/neuroligin signaling (Muhammad et al., 2015). Other than the nervous system, spinophilin is also found at the adherence junction fraction of rat liver as well as Cadherin based cell-cell adhesion sites of Madin-Darby canine kidney cells, explaining its role in associating cell membrane to actin cytoskeleton (Satoh et al., 1998).

Structurally, spinophilin is known to have 817 amino acids and consists of multiple domains including an N-terminal actin-binding domain, a PP1-binding domain, a PSD-95/discs large/zona occludens-1 (PDZ) domain, and a C-terminal coiled-coil region (Sarrouilhe, di Tommaso, Metaye, & Ladeveze, 2006).

The N-terminal actin domain: Spinophilin binding to F-actin anchors a pool of PP1 to the PSD, where it regulates glutamatergic neurotransmission and plasticity (Allen et al., 1997; Feng et al., 2000; Satoh et al., 1998; Yan et al., 1999). Phosphorylation of spinophilin by PKA at Ser94, Ser177, and Ser100 (Hsieh-Wilson et al., 2003), CaMKII at Ser100 (Grossman et al., 2004), CDK5 at Ser17, and ERK2 at Ser15 and Ser205 (Futter et al., 2005) can modulate this interaction of spinophilin with F-actin. Specifically, PKA phosphorylation of spinophilin at Ser94 and Ser177 (in rat spinophilin) suppresses the spinophilin-actin interaction (Grossman et al., 2004; Hsieh-

Wilson et al., 2003). However, since Ser177 is not conserved in either human or mouse spinophilin, its relevance is less clear. However, Ser94 is present in all species and can also suppress this interaction (Uematsu et al., 2005). Studies show that residues 1-154 on spinophilin, despite being intrinsically unstructured, are sufficient for actin binding. Interestingly, at low molar ratios (4:1, F actin: spinophilin) spinophilin in known to bundle F actin. However, at higher molar ratios, (1:1, F actin: spinophilin), it creates short actin filaments and can act to cap F-actin (Schuler & Peti, 2008).

The PP1 binding domain: The PP1 binding domain is located between amino acids 417-494. Specifically, the primary R-V-x-F PP1 binding site that is conserved in all PP1 binding proteins (Bollen, 2001) is RKIHF on spinophilin and is located between amino acids 447 and 451. Mutation of the Phe residue at position 451 to an alanine attenuates spinophilin binding to PP1 (Yan et al., 1999). Ragusa et. al in 2010 showed that spinophilin is unstructured in its unbound state. However, upon interaction with PP1 it becomes structured. This protein reorganization blocks one of PP1's putative substrate binding sites, limiting its activity and increasing its substrate specificity (M. J. Ragusa et al., 2010).

The PDZ domain: The PSD-95-Disks Large-ZO1 (PDZ) domain is a structural domain that permits interactions of transmembrane proteins that contain a PDZ ligand, such as NMDARs, with intracellular synaptic proteins to help organize the PSD (Gomperts, 1996). In 2007, Kelker et al showed that, both spinophilin and neurabin PDZ domains are categorized as class V PDZ domains. Using NMR titration experiments they showed that spinophilin and Neurabin can both interact with NMDA and AMPA receptors (Kelker et al., 2007). In 2011, Ragusa et al, indicated the presence of a flexible linker between spinophilin PP1 binding domain and its PDZ domain (Ragusa, Allaire, Nairn, Page, & Peti, 2011). They suggested that this flexibility is congruent with the finding that spinophilin PDZ domain does not increase PP1 binding or substrate recognition (Hsieh-Wilson, Allen, Watanabe, Nairn, & Greengard, 1999; Kelker et al., 2007).

The Coiled-Coil region: It has been suggested that the coiled-coil region of spinophilin is important in putative scaffolding function within the spine. Furthermore, the amino acid terminus of spinophilin is rich in Proline and contains consensus sequence for binding of Src homology 3 domain binding (SH3) (Mayer & Eck, 1995). This region has also been shown to be important in dimerization with neurabin, and other synaptic proteins such as densin-180 (Baucum et al., 2010) and CaMKII (Baucum, Strack, & Colbran, 2012).

Functionally, spinophilin targets PP1 to specific neuronal substrates (Grossman et al., 2004; Michael J. Ragusa et al., 2010; Sarrouilhe et al., 2006; Terry-Lorenzo et al., 2002). As stated before, spinophilin regulates PP1-dependent substrate phosphorylation not only by targeting PP1 to dephosphorylate substrates, but it can also inhibit PP1 activity towards certain substrates by binding tightly to PP1 (Mathieu Bollen, Wolfgang Peti, Michael J. Ragusa, & Monique Beullens, 2010; Michael J. Ragusa et al., 2010). As stated before, spinophilin interacts with F-actin and through this interaction, can modulate spine morphology and dynamics. Specifically, spinophilin-actin interaction has been shown to affect spine maturation and maintenance, and synaptic plasticity (Feng et al., 2000; Nakanishi et al., 1997; Zito, Knott, Shepherd, Shenolikar, & Svoboda, 2004). Other than F-actin, ion channels and various receptors such as NMDA and AMPA receptors are known to interact with spinophilin. The GluA1, GluA2, and GluA3 subunit of the AMPAR (X. Wang et al., 2005; Yan et al., 1999) and the GluN1 and GluN2B subunit of the NMDAR interact with spinophilin (Baucum et al., 2012; Salek et al., 2019).

Spinophilin through interactions with multiple synaptic proteins and PSD members such as PP1, F-actin, NMDAR, AMPAR, CaMKII, G-protein coupled receptors (GPCRs) (Richman et al., 2001; Smith, Oxford, & Milgram, 1999) and RGS (regulator of G-protein family) protein (Luo, Popov, Bera, Wilkie, & Muallem, 2001; X. Wang et al., 2005) may affect normal synaptic function and spine morphology. Consistent with this hypothesis, studies using spinophilin knockout mice report a smaller brain size specifically in the hippocampus region with decrease spine density in the hippocampus (Evans, Robinson, Shi, & Webb, 2015) and alterations in filopodia formation (Feng et al., 2000). Furthermore, spinophilin KO mice experience altered coritcostriatal and hippocampal LTD (Allen et al., 2006; Di Sebastiano et al., 2016), which, along with LTP, is considered to be essential for synaptic plasticity and are underling mechanisms for learning and memory (Bear & Malenka, 1994; Malenka & Bear, 2004). Moreover, other studies have shown that cocaine and amphetamine locomotor sensitization is lost in spinophilin KO animals (Areal, Hamilton, Martins-Silva, Pires, & Ferguson, 2019; Morris, Watkins, Salek, Edler, & Baucum, 2018) as well as altered Conditioned Taste Aversion learning (Stafstrom-Davis et al., 2001) and anxiety-like behavior (H. Wu et al., 2017).

1.6 Hypothesis

Given the important role of NMDAR in hippocampal plasticity, function, and behavioral output as well as NMDAR subunit phosphorylation in regulating protein function, we hypothesize that spinophilin modulates NMDAR subunit phosphorylation and function thereby impacting NMDAR-dependent behaviors and pathology.

CHAPTER 2. SPINOPHILIN REGULATES PHOSPHORYLATION AND INTERACTIONS OF THE GLUN2B SUBUNIT OF THE N-METHYL-D-ASPARTATE RECEPTOR

Salek, A.B., et al., *Spinophilin regulates phosphorylation and interactions of the GluN2B subunit of the N-methyl-d-aspartate receptor.* J Neurochem, 2019.

2.1 Abstract

N-methyl-D-Aspartate receptors (NMDARs) are abundant postsynaptic proteins that are critical for normal synaptic communication. NMDAR channel function is regulated by multiple properties, including phosphorylation. Inhibition of protein phosphatase 1 in hippocampal neurons increases NMDAR activity, an effect abrogated by loss of spinophilin, the major protein phosphatase 1 (PP1)-targeting protein in the postsynaptic density (PSD). However, how spinophilin regulates PP1-dependent NMDAR function is unclear. We hypothesize that spinophilin regulates PP1 binding to the NMDAR to alter NMDAR phosphorylation. Our data demonstrate that spinophilin interacts with the GluN2B subunit of the NMDAR. In HEK293 cells, activation and/or overexpression of protein kinase A increased the association between spinophilin and the GluN2B subunit of the NMDAR. Functionally, we found that spinophilin overexpression decreased PP1 binding to the GluN2B subunit of the NMDAR and attenuated the PP1-dependent dephosphorylation of GluN2B at Ser-1284. Moreover, in postnatal day 28 (P28) hippocampal lysates isolated from spinophilin KO compared to WT mice, there was increased binding of GluN2B to PP1, decreased phosphorylation of GluN2B at Ser-1284, and altered GluN2B protein interactions with PSD-enriched proteins. Together, our data demonstrate that spinophilin decreases PP1 binding to GluN2B and concomitantly enhances the phosphorylation of GluN2B at Ser-1284. The putative consequences of these spinophilin-dependent alterations in GluN2B phosphorylation and interactions on synaptic GluN2B localization and function are discussed (Salek et al., 2019).

2.2 Introduction

Normal signaling in neurons requires a proper balance between kinases and phosphatases. While serine/threonine (ser/thr) kinases use protein interactions for dynamic localization of

specific substrates (Welch, Jones, & Scott, 2010), substrate specificity is obtained by consensus sequences located around the phosphorylation site (Brinkworth, Breinl, & Kobe, 2003). In contrast to ser/thr kinases, ser/thr phosphatases are more promiscuous. These differences in promiscuity are due, in part, to a ~6-8-fold greater number of ser/thr kinases compared to phosphatases and a lack of easily defined consensus dephosphorylation sites (Cohen, 2002; Morrison, Murakami, & Cleghon, 2000). The greater promiscuity and lower number of phosphatases require phosphatases such as protein phosphatase 1 (PP1) to rely more heavily on targeting and regulatory proteins for substrate specificity (Esteves, Domingues, da Cruz e Silva, Fardilha, & da Cruz e Silva, 2012).

The most abundant PP1 targeting protein in the postsynaptic density (PSD) is spinophilin (Colbran et al., 1997). Spinophilin associates with and bundles F-actin (Grossman et al., 2004; Hsieh-Wilson et al., 2003; Satoh et al., 1998) as well as interacts with multiple different synaptic proteins (Baucum, Brown, & Colbran, 2013; Baucum et al., 2010; Baucum et al., 2012; Bielas et al., 2007; Muhammad et al., 2015; Sarrouilhe et al., 2006; Smith et al., 1999). Specifically, spinophilin interacts with and/or regulates the function of multiple classes of glutamate receptors (Allen et al., 2006; Di Sebastiano et al., 2016; Feng et al., 2000; Morris et al., 2018; Yan et al., 1999), synaptic proteins that are critical mediators of normal synaptic communication and underlie processes such as long-term potentiation (LTP) and long-term depression (LTD) (Bear & Malenka, 1994; Malenka & Bear, 2004). Whereas spinophilin co-immunoprecipitates with the N-methyl, D-Aspartate receptor (NMDAR) (Baucum et al., 2013; Hiday et al., 2017) to modulate NMDAR channel properties (Allen et al., 2006), the mechanisms and consequences of this regulation are unknown.

We used a heterologous expression system to control interacting partners and show that spinophilin associates with the GluN2B subunit of NMDARs. Mechanistically, the spinophilin interaction with GluN2B is enhanced by protein kinase A (PKA) expression and activity. Consequences of regulating the spinophilin/NMDAR interaction may be to regulate PP1 binding to GluN2B as we found that spinophilin displaces PP1 from GluN2B and that this displacement occurs concurrently with enhanced GluN2B phosphorylation at Ser-1284. Whereas the above studies were performed in heterologous cells, we have identified spinophilin as a critical *in vivo* regulator of PP1 binding to, and dephosphorylation of, GluN2B. Specifically, spinophilin KO animals had increased association of PP1 with GluN2B, decreased GluN2B Ser-1284

phosphorylation, and enhanced interaction of GluN2B with specific PSD-enriched proteins. Understanding mechanisms that regulate NMDAR phosphorylation at Ser-1284 may have implications in multiple pathologies as this site is decreased under ischemic conditions, increased following reperfusion, and enhanced by acute stress (Ai et al., 2017; W. Lu et al., 2015). Moreover, mechanisms that regulate GluN2B interactions may modulate GluN2B subcellular localization. This is important as GluN2B localization at synaptic and extrasynaptic sites is linked to pro-survival and proapoptotic processes, respectively (Hardingham & Bading, 2010).

2.3 Materials and Methods

2.3.1 Materials

All custom materials will be shared upon reasonable request. Experiments were approved by the institutional biosafety committee (IBC-1594 and IN-1000). cDNAs: Templates used for generation of expression vectors were: human PP1α (PBC004482, Transomic Technologies, Huntsville, AL), rat PP1γ1 (Carmody, Baucum, Bass, & Colbran, 2008), human spinophilin (Hiday et al., 2017), human GluN2B (BC113618; Transomic Technologies), human PKAc - pDONR223-PRKACA, (PKAc was a gift from William Hahn & David Root (Johannessen et al., 2010) (Plasmid RRIDs: Addgene_23495). Transfection Reagent: PolyJet (SignaGen Laboratories, Rockville, MD) was used for transfections. Antibodies: Antibodies used for IPs and/or primary blotting: goat polyclonal anti-Neurabin II (spinophilin) (A-20, SC14774, RRID:AB_2169477, Santa Cruz Biotechnology, Dallas, TX), rabbit monoclonal anti-NMDAR2B (GluN2B) (D15B3, RRID:AB_2112463 or D8E10, RRID:AB_2798506, 4212 or 14544, Cell Signaling Technology), Rabbit Phospho-NMDA Receptor 2B (GluN2B) (Ser-1284) (RRID:AB_10922589), goat polyclonal anti-V5 tag (A190-119A, RRID:AB_67317, Bethyl Laboratories, Montgomery, TX), goat polyclonal anti-HA tag (A190-107A, RRID:AB_66970, Bethyl Laboratories), goat polyclonal anti-Myc tag (A190-104A, RRID:AB_66864, Bethyl Laboratories), goat polyclonal anti-PP1γ (sc-6108, RRID:AB_2168091, Santa Cruz Biotechnology), mouse monoclonal anti-PP1 (E-9, sc-7482, RRID:AB_628177, Santa Cruz Biotechnology), rabbit polyclonal anti-V5 (G-14, sc-83849, RRID:AB_2019670, Santa Cruz Biotechnology) and mouse monoclonal anti-Myc (9E10, sc-40, RRID:AB_627268, Santa Cruz Biotechnology). Secondary antibodies used were: Alexa Fluor 790-conjugated AffiniPure Donkey Anti-Mouse IgG (715-655-150,

RRID:AB_2340870, Jackson ImmunoResearch Laboratories, West Grove, PA), Alexa Fluor 790-conjugated AffiniPure Donkey Anti-Rabbit IgG (711-655-152, RRID:AB_2340628, Jackson ImmunoResearch Laboratories), Alexa Fluor 790-conjugated AffiniPure Donkey Anti-Goat IgG (705-655-147, RRID:AB_2340441, Jackson ImmunoResearch Laboratories), Alexa Fluor 680-conjugated donkey anti-Goat (A-21084, RRID:AB_2535741, Thermo-Fisher Scientific) and Alexa Fluor 680-conjugated donkey anti-Rabbit (A10043, RRID:AB_2534018, Thermo-Fisher Scientific).

2.3.2 Mutagenesis

Mutagenesis reactions were performed using QuikChange site-directed mutagenesis (Agilent Technologies, Santa Clara, CA). Reactions were carried out using Q5 DNA buffer and 1 µl DNA polymerase in the presence of 5 µM DNTPs and 10 ng of template DNA. The following reaction protocol was performed: 1) an initial denaturation of 98°C for 2 minutes, 2) a 45-second denaturation at 98°C, 3) a 1-minute annealing reaction at a primer-specific temperature, 4) a 15-minute elongation at 68°C. Steps 2-4 were repeated 18 times. To eliminate template DNA, 10 µl of each reaction mixture was digested using 1 µL of DpnI for ~2 hours at 37°C. PCR product (1 µl) was transformed in competent DH5α *E. coli.* Vectors were then sequence verified (GENEWIZ, Inc South Plainfield, NJ.) for the mutations.

2.3.3 Mammalian Protein Expression

Human embryonic kidney 293 FT cells (HEK293; Thermo-Fisher Scientific, Waltham MA RRID: CVCL_6911) were used for mammalian protein expression. Cells were purchased, split to passage 7, and frozen down. HEK293 cells are not listed by the International Cell Line Authentication Committee and have not been authenticated after purchase. Cells were used only to passage 23. Cell incubation and growth was performed in Dulbecco's modified Eagle's medium (DMEM) that contained 10% FBS, 584 mg/L L-glutamine, 1 mM Sodium Pyruvate, 100 U/mL penicillin and 100 µg/mL streptomycin. 25 mm^2 culture flasks were incubated at a constant 37°C and 5% CO_2 (Panasonic Healthcare; Secaucus, NJ). Cells were counted and approximately 1,000,000 cells were plated into 25 mm^2 flat-bottomed culture flasks and left for overnight growth. Typically, cells were transfected the next day at ~70-80% confluency. Confluency was measured

by estimating cell coverage on the bottom of the flask. DNA (0.5 - 5 µg per DNA vector) was added to 250 µL of serum-free DMEM in a 1.7 mL microcentrifuge tube. In a separate microfuge tube, transfection reagent was added to 250 µL of serum-free DMEM. Polyjet was used in a 3:1 volume: mass ratio (e.g. 18 µL of Polyjet was used with 6 µg DNA). For each experiment, DNA concentrations were equalized using an empty DNA vector, so that each condition in the same experiment had an equal mass of DNA and equal amount of transfection reagent. The transfection reagent containing mixture was then added to the tube containing DNA and incubated at room temperature for 15 minutes. The entire mixture was then added to the proper flask and cells were incubated overnight. Following overnight incubation, DMEM was aspirated off and cells were washed with 6 mL of cold 1X phosphate-buffered saline (PBS). PBS was aspirated and cells were lysed in 1.5 mL KCl lysis buffer (150 mM KCl, 1 mM DTT, 2 mM EDTA, 50 mM Tris-HCl pH 7.5, 1% (v/v) Triton X-100, 20 mM sodium fluoride, 20 mM β-glycerophosphate, 20 mM sodium orthovandate, 10 mM sodium pyrophosphate, 1X protease inhibitor cocktail; Thermo-Fisher Scientific or Bimake, Houston TX) then transferred into 2 mL microcentrifuge tubes. If a high percentage of cells were unattached, they were re-suspended in DMEM, then transferred to 15 mL centrifuge tubes and centrifuged at 250 x g for 5 minutes. After aspiration of media, 6 ml of cold PBS was added to cells and the pellet was triturated, which was followed by an additional centrifugation. PBS was then aspirated, and cells were lysed in KCl lysis buffer. Cells were sonicated at 25% amplitude for 15 seconds at 4°C using a probe sonicator (Thermo-Fisher Scientific) and centrifuged (4°C for 10 minutes at 16,900 x g). Cell lysates were then used for Ips .

2.3.4 Mice

Experiments were approved by the School of Science Institutional Animal Care and Use Committee (SC229R, SC239R, SC270R) and performed in accordance with the Guide for the Care and Use of Laboratory Animals and under the oversight of the Indiana University-Purdue University, Indianapolis (IUPUI). Animals were provided food and water ad libitum. Spinophilin KO mice were initially purchased from Jackson Laboratories (Bar Harbor, ME; Stock #018609; RRID: MMRRC_049172-UCD) and a breeding colony has been maintained at IUPUI. Male or female, WT, C57Bl6, (Jackson laboratories) or spinophilin knockout mouse brains were dissected at Postnatal day 28-30 (P28). Animals were group housed and WT and KO littermates were used (WT and KO animals were from heterozygote x heterozygote breeding pairs). Animals were

weaned ~P21. 12 total animals were used and animals were euthanized in a randomized order. Animals were euthanized by decapitation without anesthesia. Euthanasia was performed in the afternoon.

2.3.5 Tissue homogenization

Hippocampal or cortical tissue was flash-frozen in liquid nitrogen. Each brain region was homogenized in 2 mL of low ionic buffer containing 1% Triton X-100 buffer (2 mM Tris pH 7.5, 2 mM EDTA, 1 mM DTT, 1X protease inhibitor, 20 mM sodium fluoride, 20 mM sodium orthovanadate, 10mM sodium pyrophosphate, 20 mM β-Glycerophosphate) using fifteen up-and-down movements of a pestle in a 2 mL tight-fitting glass homogenizer. Tissue homogenates were then transferred to a 2 mL microcentrifuge tube and were sonicated at 25% amplitude for 15 seconds at 4°C using a 505 probe sonicator with 0.3 cm diameter probe (Thermo-Fisher Scientific) and centrifuged (4°C for 10 minutes at 16,900 x g) to reduce non-specific binding. Immunoprecipitations (IPs) were then performed as described below.

2.3.6 IPs

Human Embryonic Kidney 293 (HEK293) cell lysate or brain homogenates were transferred to a microcentrifuge tube for IPs (400-500 µL) or for a total input (75 µl). For the input, 25 µL of 4X sample buffer (0.2 M Tris HCl pH 6.8, 40% glycerol, 0.1 M DTT, 8% SDS w/v, 0.04% bromophenol blue w/v in water) was added to 75 µL of each input sample, vortexed and stored at -20°C. For the IPs, the appropriate IP antibody (1 – 3 µg) was added to the lysates and incubated at 4°C for approximately 1 hour. After 1-hour incubation of IP antibodies with samples, 25 µL of protein G magnetic beads (Dynabeads 10009D, Invitrogen) that had been previously washed in IP buffer (50 mM Tris HCl, 150 mM NaCl, 0.5% Triton X-100) was added to each sample and incubated rotating overnight at 4°C.

Following incubation, samples were magnetically separated and washed three times with IP wash buffer. Then 40 µL of 2x sample buffer (4x buffer diluted 1:2 with Milli-Q water) was added to each of the samples, vortexed and stored at -20°C until they were analyzed by immunoblot.

2.3.7 Immunoblotting

Protein IPs or cell lysates were used for western blotting. All samples including IPs and inputs were heated at 70°C for 10 minutes, then IP samples were placed on a magnet prior to loading on the gel to separate magnetic beads out of suspension. 10 µL of input or 10 µL of IP sample were loaded onto a 1-1.5 mm hand-cast 10% polyacrylamide gel or, 26-well, pre-cast Criterion 4-15% polyacrylamide gradient gel (Bio-Rad Laboratories, Hercules, CA) or a 15 well 4-15% Mini-Protein TGX polyacrylamide gradient gel (Bio-Rad Laboratories). The precast gels were typically electrophoresed at 165 V for 1 hour and hand-cast gels were generally electrophoresed at 75 V for 15 minutes and 165 V for approximately 1 hour.

Proteins were transferred to nitrocellulose membranes using either a wet transfer or the Trans-Blot Turbo (Bio-Rad Laboratories). For wet transfer, proteins were transferred to a nitrocellulose membrane using an N-cyclohexyl-3-aminopropanesulfonic acid (CAPS) transfer buffer (10% MeOH, 0.01 M CAPS pH 11). The transfer was performed in a transfer tank attached to a cooling unit set at 4°C and transfer was operated at a constant 1.0 Amps for 1.5 hours. For Trans-Blot Turbo, gels were transferred to nitrocellulose membrane using cold TransBlot Turbo transfer buffer with 20% ethanol. The transfer was performed at 9 V for 30 minutes.

Membranes were stained with a 2 mg/ml Ponceau S stain dissolved in 10% Trichloroacetic acid for 5 minutes to normalize inputs for equal loading where applicable. Following Ponceau staining, membranes were scanned and subsequently washed with deionized water. Membranes were blocked in Tris-buffered saline with Tween (TBST; 50 mM Tris pH 7.5, 150 mM NaCl, 0.1% (v/v) Tween-20) containing 5% (w/v) nonfat dry milk in. Blocking was performed 3 times, 10 minutes each, for a total of 30 minutes. Membrane was incubated with primary antibodies diluted in 5% milk in TBST overnight at 4°C with gentle shaking. Primary antibodies for Myc-tag (1:1000-1:10,000), HA-tag (1:1000-1:10,000), PP1 (1:1000-1:2000), GluN1 (1:1000-1:2000), spinophilin (1:1000-1:2000), GluN2B (1:1000-1:2000), and Ser-1284 (1:1000) were the same as used above for IP. After incubation, membranes were washed 3 times for 10 minutes per wash with TBST containing 5% milk. Appropriate secondary antibodies in TBST containing 5% milk were added to the membranes following the washes. Jackson ImmunoResearch antibodies were typically diluted 1:50000 and Invitrogen antibodies were generally diluted 1:10000. Secondary antibodies were incubated with membranes for one hour at room temperature shaking in darkness. Membranes were washed three times with Tris-Buffered saline without Tween for 10 minutes for

each wash. Fluorescence scans were performed using the Odyssey imaging system (LiCor, Lincoln, NE) and data analysis was done using Image Studio software (LiCor). We have previously shown linearity of fluorescence intensity using these conditions for multiple proteins and antibody pairs (Edler et al., 2018; Morris et al., 2018).

2.3.8 Mass Spectrometry

Samples collected from SDS-PAGE were de-stained with 25 mM ammonium bicarbonate in 50 % acetonitrile (ACN). For all digestion steps, a volume sufficient to cover the gel pieces were used. Next, 10 mM DTT in 25 mM ammonium bicarbonate was added to reduce disulfide bonds. 25 mM iodoacetamide was then added to alkylate free sulfhydryl groups. After addition of iodoacetamide, the reaction was incubated in the dark for 45 minutes. Gel pieces were incubated in 25 mM ammonium bicarbonate. The gel pieces were then dehydrated with 25 mM ammonium bicarbonate in 50% ACN. The samples were then placed in a rotary vacuum and centrifuged until dry and subsequently digested with 12.5 ng/µl trypsin in 25 mM ammonium bicarbonate at 37ºC overnight. The supernatant was collected from all samples. The remaining gel pieces were washed with 5% formic acid in 50% ACN and were vortexed and sonicated for 5 minutes. The supernatants were collected and pooled with previous supernatants and were submitted to the Indiana University Proteomics Core Facility for analysis. Digested peptides were loaded onto an Acclaim PepMap C18 trapping column and eluted on a PepMap C18 analytical column with a linear gradient from 3 to 35% acetonitrile (in water with 0.1% formic acid) over 120 minutes in-line with an Orbitrap Velos Pro or Qexactive plus mass spectrometer (Thermo-Fisher Scientific). Raw files generated from the run were analyzed using Thermo-Fisher Proteome Discoverer (PD) 2.2. SEQUEST HT (as a node in PD 2.2) was utilized to perform database searches as previously described (Smith-Kinnaman et al., 2014) with a few modifications: trypsin digestion, 2 maximum missed cleavages, precursor mass tolerance of 10 ppm, fragment mass tolerance of 0.8 Da, a fixed modification of +57.021 Da on cysteine, and a variable modification of +15.995 Da on methionine. The spectral false discovery rate (FDR) was set to ≤ 1% as previously described (Mosley et al., 2011). The FASTA database used was a mouse proteome downloaded from Uniprot on January 9, 2017 with addition of 72 common contaminants. Data was further analyzed in Scaffold Q+ (Proteome Software, Portland, OR) using an FDR cutoff of ≤ 1% for both proteins and peptides. MS/MS spectra of tryptic fragments matching specific phosphorylation sites were validated and the area

under the curve (AUC) of the extracted ion chromatogram (XIC) was calculated for both the phosphorylated and non-phosphorylated peptide as previously described (Baucum et al., 2015; Hiday et al., 2017). The XIC reflects the abundance of a specific peptide that has a specific mass. The AUCs of the XICs of the phosphorylated peptide were normalized to the non-phosphorylated peptide AUC of the XIC to create a phosphorylation ratio. The generated ratios were compared across different groups.

2.3.9 Statistical Analyses

Image Studio software was used for quantification of the integrated fluorescence intensities detected in the western blots. To measure changes in expression, we normalized inputs to total ponceau stain a well-validated approach (Fosang & Colbran, 2015). To calculate associations, we divided the integrated fluorescence intensity for the co-immunoprecipitated protein by the integrated fluorescence intensity for the immunoprecipitated protein. In order to normalize for any differences in protein expression, we took the above normalized value and divided it by the input value for the co-immunoprecipitated protein. To compare different conditions across gels, we normalized the above ratio from the experimental condition by the ratio generated on the same gel for the control condition. The formula for this ratio is EXPERIMENTAL((Intensity co-IP $protein_{Precipitate}$/Intensity IP $protein_{Precipitate}$)/(Intensity co-IP $protein_{input}$))/CONTROL((Intensity co-IP $protein_{Precipitate}$/Intensity IP $protein_{Precipitate}$)/(Intensity co-IP $protein_{input}$)) as we have previously utilized (Edler et al., 2018; Hiday et al., 2017; Morris et al., 2018). If gels were run on different days, this ratio was averaged across multiple transfections, with each transfection corresponding to a unique biological replicate (transfections performed on different days). The N values for each individual experiment correspond to the number of unique biological replicates. To compare between groups, a one-column t-test was performed to compare the experimental condition to a theoretical value of 1. If data were all analyzed on the same gel, a t-test was used. If more than two groups were compared, a one-way ANOVA was used to determine significance. Where appropriate, a two-way ANOVA was used to compare across two different conditions. ANOVA's were followed by a 1-column t-test for normalized values or a Tukey's multiple comparison test. All graphs were generated in Prism (Version 8, GraphPad Software, La Jolla, CA). All graphs show the mean +/- standard deviation and all individual data points. All text values show mean +/- standard error of the mean. No inclusion criteria were predetermined. For exclusion, if an outlier

was detected by a Grubb's outlier test, a single outlier was removed from a group. No animals were excluded from the studies. Normality was not evaluated.

2.3.10 Randomization, Preregistration, and Blinding

Given the study design using cell lines and non-treated animals, the study was not pre-registered, study groups were not randomized, and no blinding was performed. No sample calculation was performed.

2.4 Results

2.4.1 Spinophilin Associates With GluN2B Subunit Of NMDARs

We immunoprecipitated spinophilin, or GluN2B from P28 WT and spinophilin KO cortical lysates. Whereas GluN2B (**Figure 1A**) associated with spinophilin in WT animals, no GluN2B co-immunoprecipitated with the spinophilin antibody in the KO lysates where spinophilin was not present. For all figures, the immunoblots for either the inputs or the immunoprecipitates for each protein were performed on the same gel and are shown at the same signal intensity. These data suggest a specific interaction between spinophilin and GluN2B.

As the NMDAR is a heterotetramer with an obligate GluN1 subunit, we utilized a heterologous expression system to delineate if spinophilin binds specifically to the GluN2B subunit of the NMDAR. As full-length GluN2B is trapped in the ER in the absence of GluN1 (Das et al., 1998); we expressed the C-terminal, cytosolic tail of GluN2B ($GluN2B_{Tail}$; amino acids 839-1484) which is not trapped in the ER and is localized to the cytosol. HA-tagged spinophilin and V5-tagged $GluN2B_{Tail}$ were overexpressed in HEK293 cells and subsequently immunoprecipitated. We detected $GluN2B_{Tail}$ in spinophilin immunoprecipitates and spinophilin in $GluN2B_{Tail}$ immunoprecipitates (**Figure 1B**). As above, this interaction was specific as spinophilin was not detected in $GluN2B_{Tail}$ immunoprecipitates when $GluN2B_{Tail}$ was absent and $GluN2B_{Tail}$ was not detected in spinophilin immunoprecipitates when spinophilin was absent.

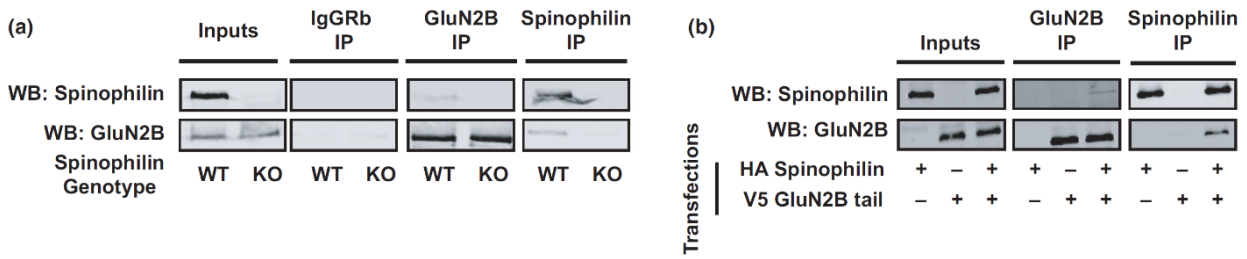

Figure 1 Spinophilin and NMDAR interaction. Spinophilin interacts with the GluN2B subunit of NMDARs in brain and HEK293 cells. **1A**: GluN2B is present in spinophilin immunoprecipitates from P28 cortical lysates of WT, but not spinophilin KO mice. Conversely, spinophilin is detected in GluN2B immunoprecipitates isolated from WT, but not spinophilin KO mice. No signal was detected in the IgG IPs. **1B** HEK293 cells were transfected with HA-spinophilin and V5-GluN2B$_{Tail}$. Western blot results show an association between spinophilin and GluN2B$_{Tail}$. Images are representative of 3 animals (A) or 3 independent cell culture preparations (B). Immunoblots for inputs or immunoprecipitates for each protein were taken from the same gel.

2.4.2 Overexpression Of The Catalytic Subunit Of PKA (PKAc) In HEK293 Cells Increases Spinophilin And GluN2B Interaction

PKA phosphorylates both spinophilin and NMDA receptor subunits (Hsieh-Wilson et al., 2003; J. A. Murphy et al., 2014) and our previous studies have found that PKA can regulate spinophilin interactions (Hiday et al., 2017). V5-tagged GluN2B$_{Tail}$ and HA-tagged spinophilin were co-expressed in HEK293 cells alone or alongside a Myc-tagged form of the catalytic subunit of protein kinase A (PKAc). Overexpression of PKAc led to the appearance of multiple bands in the GluN2B input blot, suggesting multiple GluN2B species (most likely differentially phosphorylated forms) (**Figure 2A**). PKAc overexpression increased the association of spinophilin and GluN2B$_{Tail}$. Quantified data show a PKAc-dependent increase of GluN2B$_{Tail}$ in the spinophilin IP (Figure 2B; ***2.142*** ± ***0.3329, **p=0.0089,)*** and spinophilin in the GluN2B$_{Tail}$ IP (**Figure 2C**) ***(10.6 ± 1.513, ***p=0.0002)***.

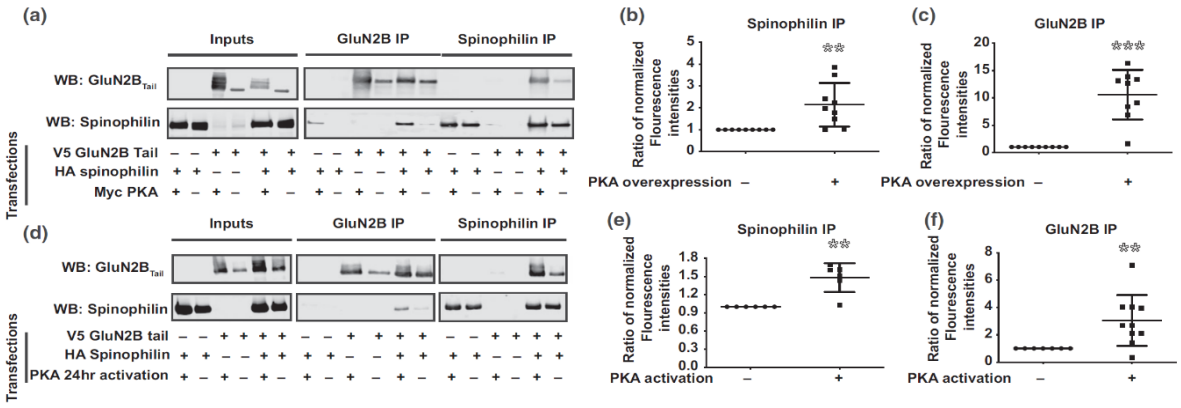

Figure 2. PKA activity enhances spinophilin-NMDAR interaction. Overexpression of the catalytic subunit of PKA (PKAc) and long-term activation of PKA enhances the spinophilin-NMDAR interaction. **2A**: HEK293 cells were transfected with HA-spinophilin and V5-GluN2B$_{Tail}$ with/without overexpression of Myc-PKA and immunoprecipitated and immunoblotted. **2B-C:** There is a significant increase in the spinophilin- GluN2B$_{Tail}$ interaction when PKAc is overexpressed (n=10). **2D:** HEK293 cells were transfected with HA-spinophilin and V5-GluN2B$_{Tail}$ and endogenous PKA was activated using forskolin and IBMX for 24 hours. **2E-F:** There is a significant increase in the spinophilin- GluN2B$_{Tail}$ interaction when PKAc is overexpressed (n=6 independent cell culture preparations). Graphs show the mean +/- the standard deviation. **p<0.01, ***p<0.001.

2.4.3 Activation Of Endogenous PKA Increases The Interaction Between Spinophilin And The GluN2B Subunit

While overexpression of PKAc enhanced the spinophilin-GluN2B interaction, we wanted to determine if PKA activity is responsible for this effect. IBMX and forskolin were used to pharmacologically increase intracellular levels of cAMP to activate endogenous PKA. V5-tagged GluN2BTail was transfected alone or together with HA-tagged spinophilin and cells were incubated for 24 hours. Subsequently, cells were treated with IBMX/forskolin or vehicle alone for 16-20 hours to activate PKA. Long-term activation of endogenous PKA increased the association of spinophilin with GluN2BTail (**Figure 2D**). Quantitatively, GluN2BTail and spinophilin levels were significantly increased in the HA (***1.48 ± 0.09710, **p=0.0043***) and V5 IPs (***3.046 ± 0.5874, **p=0.0069***), respectively (**Figure 2E, 2F**) compared to a theoretical value of 1.

2.4.4 Spinophilin-GluN2B Interaction Domains

To determine the region on $GluN2B_{Tail}$ that interacts with spinophilin, HEK293 cells were transfected with V5-tagged $GluN2B_{Tail}$ fragments containing amino acids 839-1088, 1038-1484 and 1268-1484 (**Figure 3A**), along with HA-tagged spinophilin. We also transfected Myc-tagged PKA in all the conditions to enhance the interaction between spinophilin and the $GluN2B_{Tail}$ fragments. Data demonstrate an interaction of HA-tagged spinophilin with the first fragment of $GluN2B_{Tail}$ containing amino acids 839-1088 (**Figure 3B**). This suggests an interaction of spinophilin with the first 250 amino acids of $GluN2B_{Tail}$.

To determine the domain on spinophilin on which GluN2B binds, we generated three spinophilin truncation fragments with deletions in the C-terminus of the protein (Morris et al., 2018): amino acids 1-817 (full length A), 1-301 (fragment B), 1-460 (fragment C), and 1-670 (fragment D) on spinophilin (**Figure 3A**). We co-transfected HEK293 cells with V5-tagged $GluN2B_{Tail}$ and HA-tagged spinophilin fragments. When full-length or spinophilin fragments are immunoprecipitated (Figure 3C middle panel), we detect $GluN2B_{Tail}$ in immunoprecipitates containing full-length spinophilin (* in lane 7 (A fragment)). There is little association of $GluN2B_{Tail}$ with the 1-301 fragment (* in lane 8 (B fragment)) and no detectable binding to the 1-460 or 1-670 spinophilin fragments (Lanes 9 and 10 (C and D fragments)) (**Figure 3C middle panel**). Conversely, when we immunoprecipitated $GluN2B_{Tail}$ we observed full-length spinophilin (* in lane 7 (A fragment)). There was some 1-301 fragment (* in lane 8 (B fragment)) and no

detectable 1-460 or 1-670 spinophilin fragments (Lanes 9 and 10 (C and D fragments)) in the GluN2B$_{Tail}$ immunoprecipitates (Figure 3C far right panel). The major band marked by the arrowhead is predicted to be a non-specific IgG heavy chain. These data suggest that the C-terminal coiled-coiled region (amino acids 665-817) of spinophilin is required for complete association of spinophilin with GluN2B. However, when we expressed only the coiled-coil region, we did not detect consistent binding of spinophilin with GluN2B$_{Tail}$, suggesting it is not sufficient for an interaction (data not shown)

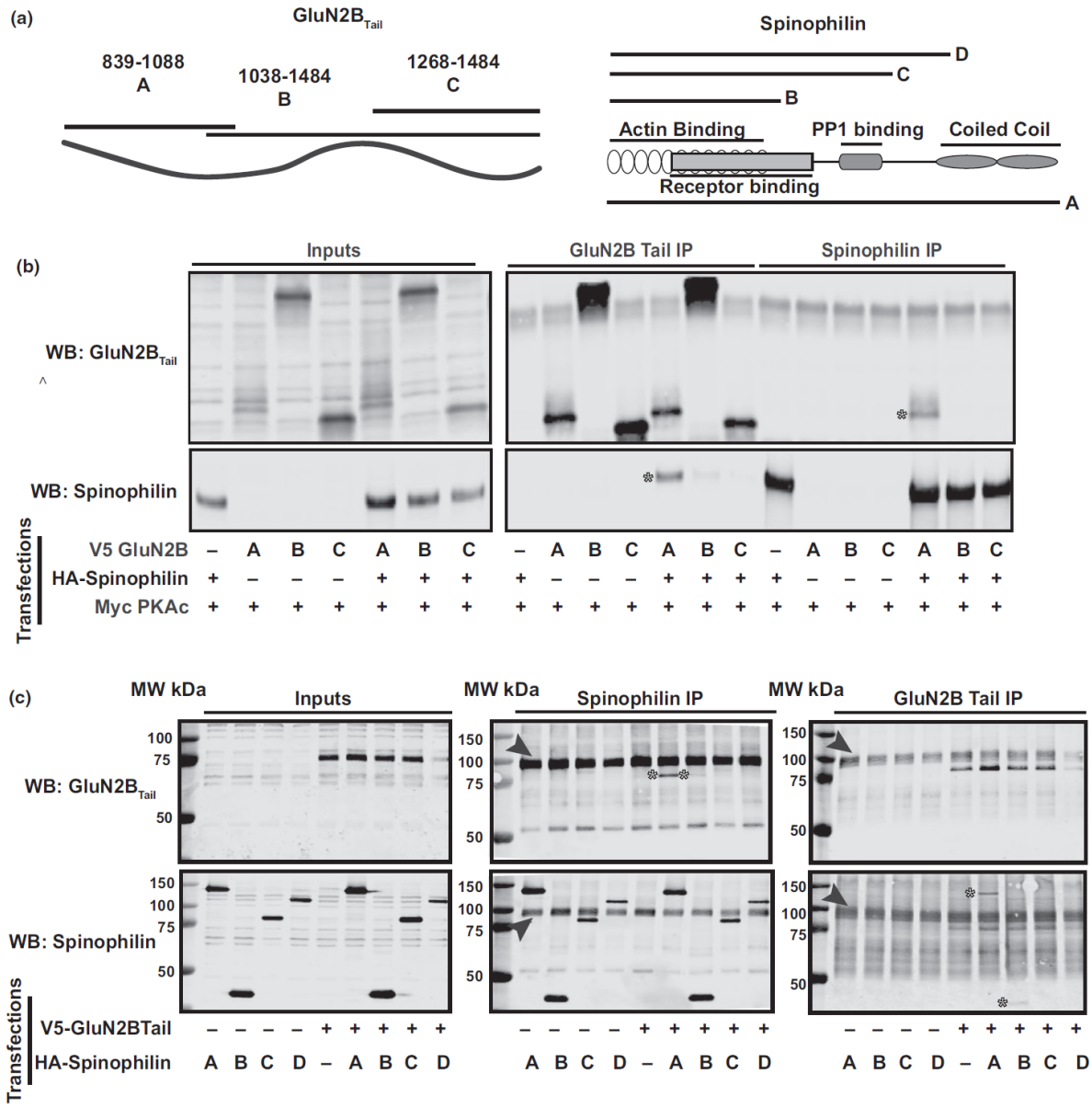

Figure 3. Spinophilin and GluN2B$_{Tail}$ interacting domains. HEK293 cells were transfected with V5-tagged GluN2B$_{Tail}$ fragments in the absence or presence of HA-tagged spinophilin. **3A:** Schema of fragments for GluN2B$_{Tail}$ (left) and spinophilin (right) used for the co-IP experiments. **3B:** Immunoblots of GluN2B$_{Tail}$ fragments using a V5-antibody and spinophilin using an HA antibody. **3C:** Immunoblots of GluN2B$_{Tail}$ and spinophilin fragment inputs and immunoprecipitations. Both images are representative of 5 independent cell culture preparations. * are used to highlight co-precipitated protein bands. Arrows are pointing to nonspecific band representing IgG heavy chain.

2.4.5 Spinophilin Decreases The Association Of PP1 With GluN2B$_{Tail}$

As spinophilin is critical in modulating PP1 targeting and PP1 activity, we wanted to determine if spinophilin targets PP1 to GluN2B$_{Tail}$. Both PP1α and PP1γ1 associated with GluN2B$_{Tail}$ in the absence of spinophilin, suggesting that both isoforms of PP1 can associate with GluN2B$_{Tail}$ directly or via a HEK-cell expressed targeting protein (**Figure 4A**).

As the major PP1-targeting protein in PSDs, we investigated whether spinophilin overexpression enhances PP1 co-IPs with GluN2B$_{Tail}$. V5-GluN2B$_{Tail}$ along with Myc-PP1γ1 was transfected in the presence and absence of WT and a mutant (F451A) HA-spinophilin that has reduced PP1 binding (M. J. Ragusa et al., 2010) (**Figure 4B; 0.3786 ± 0.1574, *p=0.0168**). There was a significant difference across groups for these data (**Figure 4D; F(2, 18)=4.899, *p=0.0200).** Surprisingly, overexpression of spinophilin decreased the abundance of PP1γ1 bound to GluN2B$_{Tail}$ (**Figure 4C, D; 0.3564 ± 0.1228, **p=0.0019)**. Conversely, the F451A mutant spinophilin had no effect on the association of PP1γ1 with GluN2B$_{Tail}$ (**Figure 4C, D; 1.218 ± 0.3283, p=0.5318**).

Given the unexpected effect of spinophilin on PP1γ1-GluN2B interaction, we investigated whether spinophilin and PP1γ1 are competing for the same site on GluN2B$_{Tail}$. (Spinophilin immunoprecipitates*: **2.178 ± 0.4227, p=0.0686;** GluN2B*$_{Tail}$ immunoprecipitates: ***6.402 ± 1.171, *p=0.0192***). Moreover, when we co-expressed GluN2B$_{Tail}$ fragments containing amino acids 839-1088, 1038-1484 and 1268-1484 along with PP1γ1, we observed PP1γ1 predominantly binding the second fragment of GluN2B (amino acids 1038-1484; * in **Figure 4E**). These data suggest that PP1 and spinophilin are binding to different regions on GluN2B, with spinophilin predominantly binding amino acids 839-1088 and PP1 predominantly binding amino acids 1038-1268. Together, these data suggest that spinophilin is neither targeting PP1 to GluN2B, nor is it directly displacing PP1 from, GluN2B.

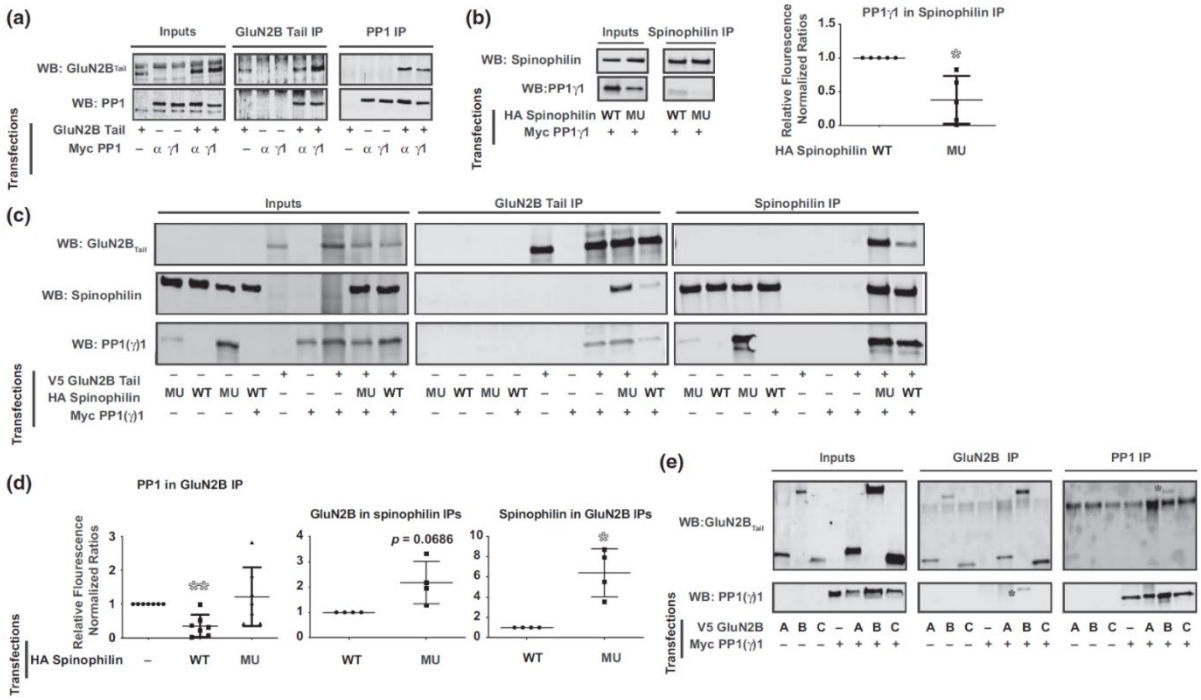

Figure 4. Spinophilin sequesters PP1 away from GluN2B$_{Tail}$. HEK293 cells were transfected with PP1γ1 and/or PP1α and GluN2B$_{Tail}$ (Myc and V5 tags respectively). **4A:** Immunoblots of GluN2B$_{Tail}$ and PP1 in inputs, GluN2B$_{Tail}$ immunoprecipitates, and PP1 immunoprecipitates and the experiment is representative of 4 independent experiments. **4B:** F451A mutant spinophilin has abrogated binding to overexpressed PP1γ1 (n=5). **4C:** GluN2B$_{Tail}$, PP1γ1, WT, and/or F451A (MU) spinophilin were co-transfected in HEK293 cells, immunoprecipitated for GluN2B$_{Tail}$ or spinophilin, and immunoblotted. **4D:** WT, but not F451A mutant, spinophilin overexpression decreased the association of PP1γ1 with GluN2B$_{Tail}$ (n=7). **4E:** PP1 precipitated with the GluN2B fragment containing residues 1038-1484 and the experiment is representative of 3 independent cell culture preparations. Graphs show the mean +/- the standard deviation. *p<0.05, **p<0.01.

2.4.6 Spinophilin Rescues PP1-Dependent Dephosphorylation Of Ser-1284 On GluN2B$_{Tail}$

To determine functional implications of decreasing PP1 targeting to GluN2B$_{Tail}$, we transfected V5-tagged GluN2B$_{Tail}$ along with Myc-tagged PP1γ1 with and without HA-tagged spinophilin in the presence of Myc-tagged PKAc to increase the interaction between spinophilin and GluN2B$_{Tail}$. Using mass spectrometry on the GluN2B$_{Tail}$ immunoprecipitates separated by SDS-PAGE, several PKA phosphorylation sites on GluN2B$_{Tail}$ were observed. Phosphorylation was detected at Ser- 929/930 (**Figure 5A**), Ser-940 (**Figure 5B**), Ser-1050 (**Figure 5C**), Ser-1303 (**Figure 5D**), and Ser-1284 (**Figure 5E**). Ser-929/930, Ser-940, and Ser-1050 were only observed in the presence of overexpressed PKA. In contrast, Ser-1284 and Ser-1303 were present under all conditions. Of note, Ser-1284 phosphorylation was regulated by spinophilin ***(F (4, 10) = 139.8, ****p<0.0001)***. Interestingly, overexpression of PP1γ1 decreased Ser-1284 phosphorylation on GluN2B$_{Tail}$ (**Figure 5E; *GluN2B$_{Tail}$ (20.39% ± 0.2537%) vs. GluN2B$_{Tail}$+PP1 (3.447% ± 0.2049%), ****p <0.0001).** Overexpression of PKA alone or along with PP1γ1 did not increase Ser-1284 phosphorylation, suggesting that this is not a PKA sensitive site, consistent with other data suggesting it is a CDK5 site (W. Lu et al., 2015). Co-expression of spinophilin along with PKA and PP1γ1 attenuated the PP1-dependent decrease in Ser-1284 phosphorylation (**Figure 5E; *GluN2B$_{Tail}$+PP1+PKA (4.948% ± 0.3837%) vs GluN2B$_{Tail}$+PP1+PKA+Spinophilin (14.24% ± 0.7482%), ****p<0.0001)***. To determine the role of spinophilin in regulating Ser-1284 phosphorylation in the absence of PKA, we overexpressed PP1α or PP1γ1 with GluN2B$_{Tail}$ in the absence or presence of spinophilin without overexpressing PKA in the cells. Consistent with the above spinophilin-dependent regulation of GluN2B phosphorylation at Ser-1284, there was a significant effect of spinophilin co-expression on phosphorylation of Ser-1284 (**Figure 5F**) ***(F(1,10) = 8.717, *p=0.0145)*** but no significant individual differences**.**

To validate mass spectrometric detection of the Ser-1284 site, we used a S1284A mutant GluN2B$_{Tail}$. We were able to quantify (**Figure 6A**) and validate by MS/MS the non-phosphorylated (**Figure 6B**) and phosphorylated (**Figure 6C**) peaks in the WT condition. We did not detect a peak matching the YPQSPTNSK peptide (phosphorylated or nonphosphorylated; **Figure 6D**) in the S1284A mutant. However, we did detect a strong peak matching the mass of the YPQAPTNSK tryptic peptide (**Figure 6E**). Moreover, we validated the MS/MS of this tryptic peptide (**Figure 6F**).

In addition to validation of the mass spectrometry, we utilized a Ser-1284 antibody to measure phosphorylation under different transfection conditions (**F3, 12 = 46.55, P<0.0001**). PP1 overexpression decreased phosphorylation of GluN2B by 63.8% (**Figure 5G**). Moreover, WT spinophilin abrogated the PP1-dependent decrease in phosphorylation (70.7% increase over PP1 condition) whereas the F451A mutant only attenuated this effect (35.1% increase over PP1 condition) (**Figure 5G**).

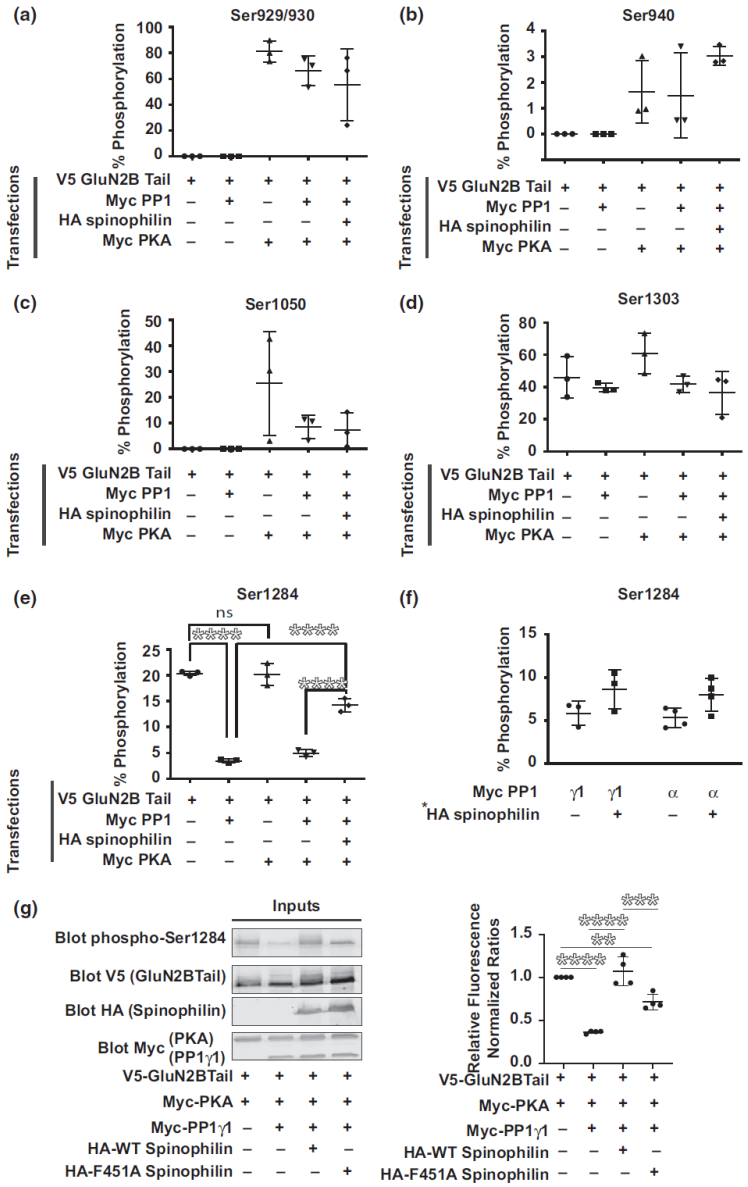

Figure 5 Spinophilin and PKA regulate GluN2B phosphorylation. HEK293 cells were transfected with V5-GluN2B$_{Tail}$ in presence or absence of Myc-PKA, HA-spinophilin, and/or Myc-PP1γ1. Immunoprecipitations were performed with V5-tag antibodies. Area under the curve of extracted ion chromatograms matching GluN2B$_{Tail}$ phosphorylation sites at **(A)** Ser-929/930, **(B)** Ser-940, **(C)** Ser-1050, **(D)** Ser-1303, and **(E)** Ser-1284. (n=3)**.** (**F**) GluN2B$_{Tail}$ and either PP1γ1 or PP1α were transfected in the absence or presence of overexpressed spinophilin and Ser-1284 phosphorylation was quantified. There was a significant effect ($p<0.05$) of spinophilin overexpression on the phosphorylation of Ser-1284. (n=3-4 cell culture preparations). (**G**) HEK293 cells were transfected with GluN2B$_{Tail}$, PKA, PP1γ1, and/or WT or F451A spinophilin and immunoblotted for protein expression and Ser-1284 phosphorylation (n=4 cell culture flasks per group from 2 cell culture preparations). Graphs show the mean +/- the standard deviation. **p<0.01, ***p<0.001, ****p<0.0001

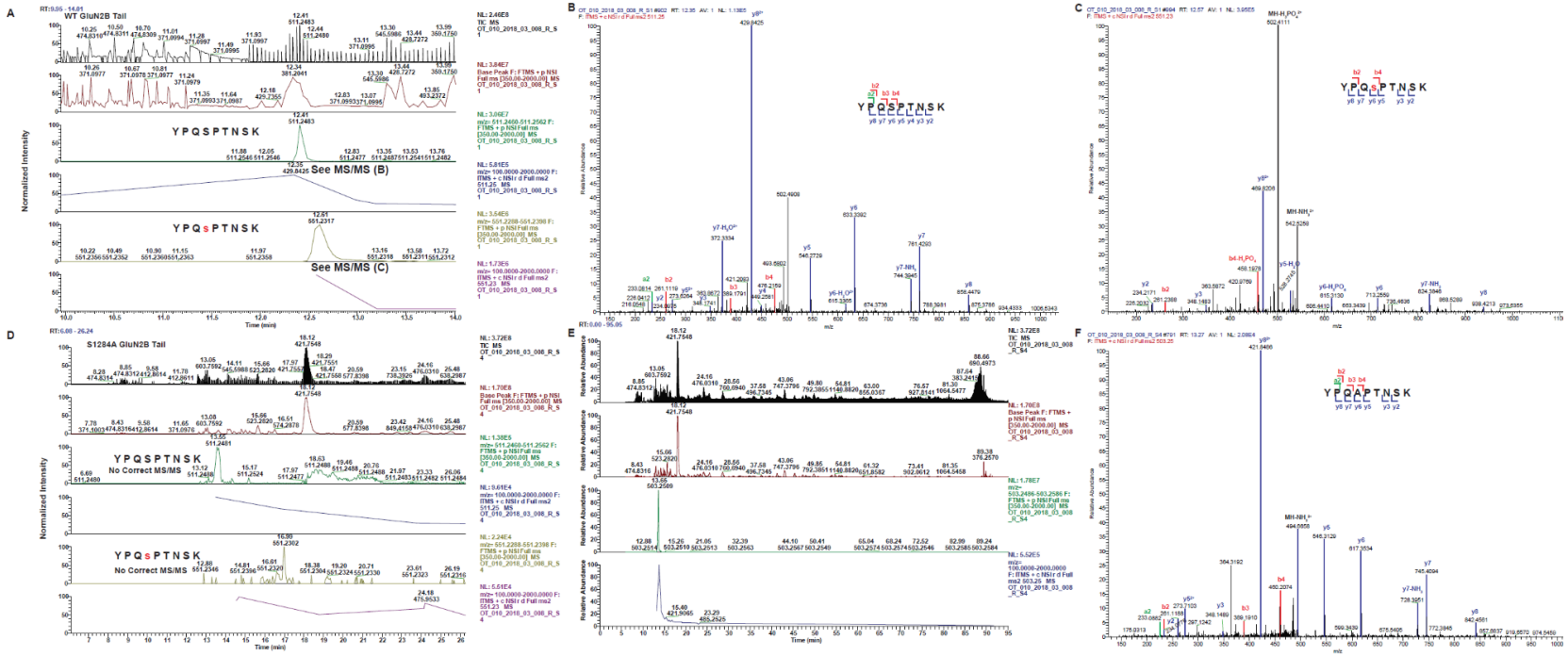

Figure 6. Validation of MS/MS spectra for Ser-1284 non-phosphorylated and phosphorylated tryptic peptide. 6A: Chromatograms matching the total ion current, base peak, non-phosphorylated peptide YPQSPTNSK, and phosphorylated Ser-1284 peptide (YPQ*s*PTNSK) are shown. MS/MS spectra matching the non-phosphorylated peptide YPQSPTNSK **(B)**, and phosphorylated Ser-1284 peptide (YPQ*s*PTNSK; **6C:** Chromatograms showing no proper peak for either the non-phosphorylated peptide YPQSPTNSK or phosphorylated Ser-1284 peptide (YPQ*s*PTNSK) in a sample containing mutant S1284A GluN2B$_{Tail}$. **6E:** Chromatogram showing the S1284A mutant tryptic peptide (YPQAPTNSK). **6F:** MS/MS matching the S1284A mutant tryptic peptide (YPQAPTNSK).

2.4.7 Spinophilin KO Mice Have Enhanced GluN2B-PP1 Interaction And Decreased Ser-1284 Phosphorylation In P28 Mouse Hippocampus

While the above data suggest that spinophilin can regulate GluN2B phosphorylation in a heterologous cell system, we next wanted to determine if loss of spinophilin regulates the PP1-GluN2B interaction and GluN2B phosphorylation at Ser-1284 *in vivo.* To achieve this, we used hippocampus dissected from postnatal day 28-30 (P28) wildtype (WT) and global spinophilin KO mice. P28 animals were used since spinophilin expression peaks between P21 and P26 (Allen et al., 1997) and GluN2B expression wanes somewhat into adulthood (McKay et al., 2018). Furthermore, since we are using global, constitutive spinophilin KO animals, we wanted to reduce the period of time that animals lack spinophilin to mitigate potential compensatory changes. As previously observed in striatal lysates (Allen et al., 2006), there were decreases in PP1 expression in hippocampal lysates isolated from the spinophilin KO animals. Specifically, PP1α expression was significantly decreased ***(WT (4.254 ± 0.5317) vs KO (2.128 ± .08013), **p=0.0051)*** (**Figure 7A-B**) whereas PP1γ1 expression trended towards a significant decrease ***(WT (1.531 ± 0.1461) vs KO (1.059 ± 0.1346), p=0.0761)*** (**Figures 7C-D**). Furthermore, PP1α and PP1γ1 were immunoprecipitated and PP1 immunoprecipitates were immunoblotted for GluN2B and spinophilin. When normalized to PP1 in the immunoprecipitate and GluN2B in the input, there was a greater association of GluN2B and PP1α ***(WT (4.505 ± 0.1826) vs KO (7.265 ± 0.9420), *p=0.0451*)*** (**Figure 7A-B**) and between GluN2B and PP1γ1 (**Figure 7C-D**) ***(WT (1.680 ± 0.2916) vs KO (4.015 ± 0.4585), *p=0.0127)*** in PP1 IPs isolated from KO compared to WT hippocampus

To determine if loss of spinophilin and enhanced PP1 binding correlate with alterations in GluN2B phosphorylation, GluN2B immunoprecipitates were separated by SDS-PAGE, Coomassie stained, and the GluN2B bands were digested and Ser-1284-containing tryptic peptides were analyzed by mass spectrometry (**Figure 7E**) for Ser-1284 phosphorylation on GluN2B. Consistent with overexpression of spinophilin in HEK293 cells increasing Ser-1284 phosphorylation on GluN2B, when normalized to the non-phosphorylated form, Ser-1284 phosphorylation was decreased in spinophilin KO hippocampus ***(WT (27.93% ± 1.332%) vs KO (20.60% ± 0.6658%), **p=0.0079)*** (**Figure 7F**), suggesting that spinophilin acts to limit Ser-1284 dephosphorylation *in vivo*.

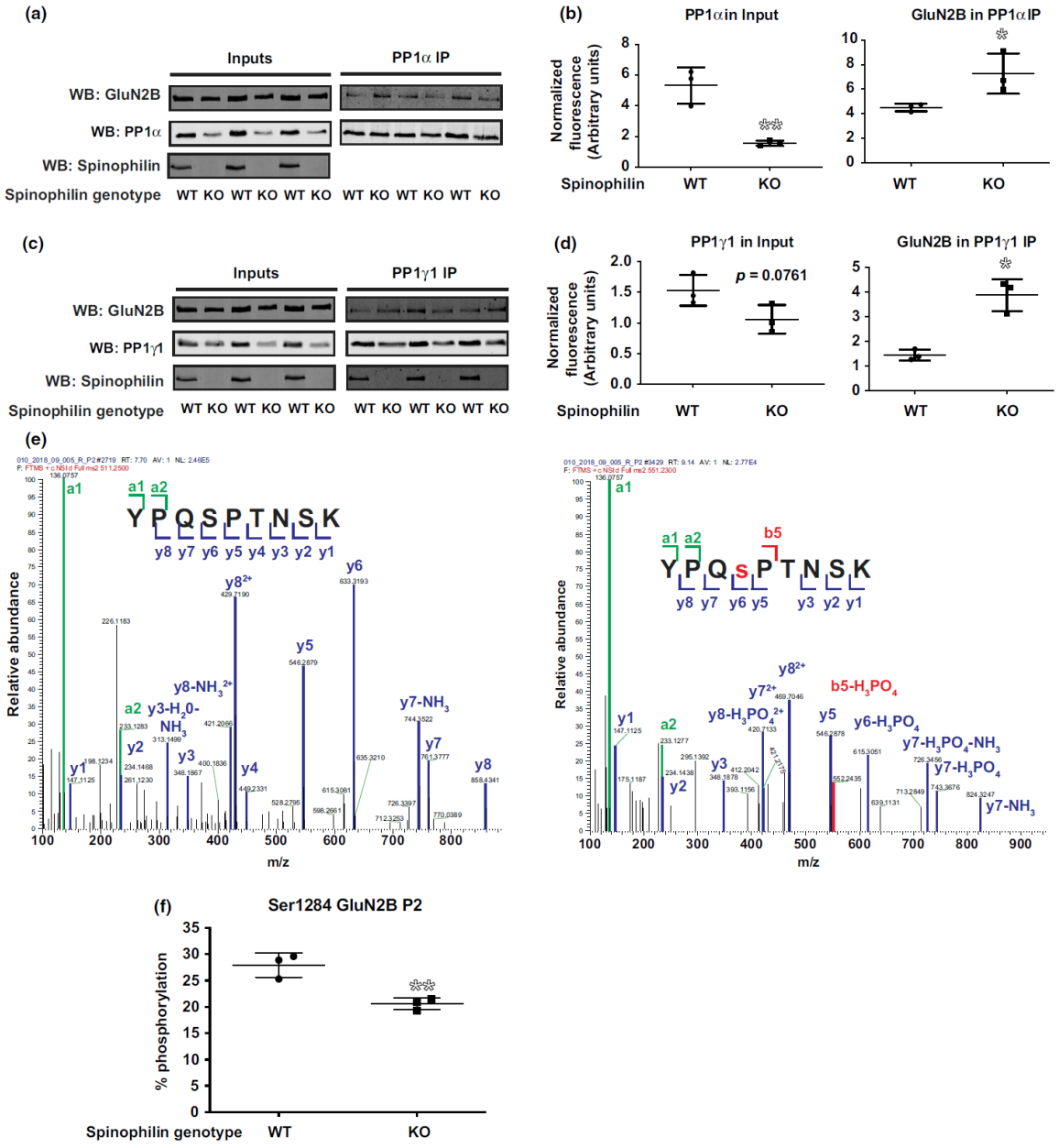

Figure 7. GluN2B-PP1 interaction is enhanced and Ser-1284 phosphorylation is diminished in P28 spinophilin KO hippocampus. PP1 and GluN2B were immunoprecipitated from hippocampal lysates generated from P28 WT and spinophilin KO animals. **7A-B:** Western blotting results show that the levels of PP1α are decreased and the amount of GluN2B in PP1α IP are increased in spinophilin KO animals. **7C-D:** There was a trend for lower levels of PP1γ1 and a significantly increased PP1γ1-GluN2B interaction in spinophilin KO hipopocampi. **7E:** MS/MS spectra showing the fragmented ions matching the non-phosphorylated (left) and phosphorylated (right) tryptic peptide YPQSPTNSK. **7F:** Ser-1284 phosphorylation is diminished in spinophilin KO hippocampus. One cohort of an n of 3 mice per group were used for the PP1 IPs and a separate N of 3 mice per group were used for the Ser-1284 phosphorylation. Graphs show the mean +/- the standard deviation. *p<0.05, **p<0.01.

2.4.8 Spinophilin KO Modulates The P28 GluN2B Interactome

To determine how spinophilin dependent changes in GluN2B phosphorylation and PP1 interaction regulate GluN2B interactions in brain, GluN2B interacting proteins isolated from WT and spinophilin KO P28 GluN2B immunoprecipitates were separated by SDS-PAGE and Coomassie stained. The GluN2B band (**Figure 8 red box**) and the other gel regions (black boxes) were excised, digested with trypsin and analyzed by mass spectrometry. We identified multiple proteins in the GluN2B IP. To begin to delineate a role for spinophilin in modulating the GluN2B interactome, we combined data from both the GluN2B band and interacting band (**Figure 8 red and black boxes on the gel**). To normalize for GluN2B abundance in the IP, the total number of spectral counts for each interacting protein was divided by the total number of spectral counts matching GluN2B from the same samples. Next, the normalized spectral counts from the WT and spinophilin KO hippocampus immunoprecipitates were summed and a ratio was generated by dividing the KO value by the WT value. To address non-specific interactions, we searched our identified interacting proteins against the CRAPome database (Mellacheruvu et al., 2013). Table 1 shows the 7 proteins that have a total decreased ratio of ≤ -0.5 and the 6 proteins that have an increased ratio of ≥ +0.5. This table only show proteins detected in at least 3 samples and having passed filtration via the CRAPome database. It is important to note that this is an initial screen of potential changes in the GluN2B interactome and follow-up immunoblotting or more quantitative mass spectrometry studies will need to confirm these initial interaction changes.

Using the string-db program, we input the 7 decreased (**Figure 8B**) and 6 increased (**Figure 8C**) interacting proteins and divided them into scaffolding, signaling, and cytoskeletal categories. Interestingly, loss of spinophilin increased the interaction of GluN2B with CaMKII isoforms, SAPAP3, PSD-95, and PSD-93 whereas it decreased the interaction of GluN2B with the other SAPAP isoforms (1,2,4) and myosin-Va.

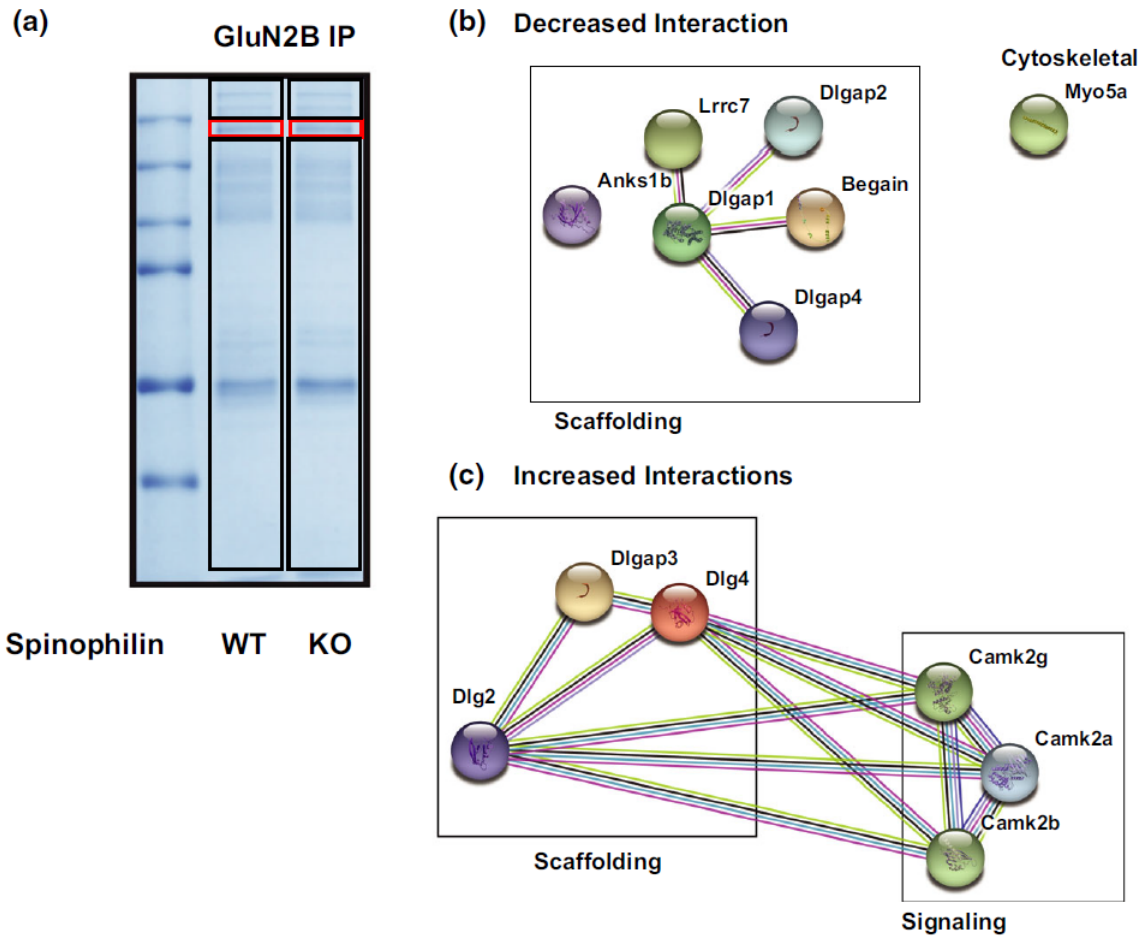

Figure 8. **Spinophilin modulates the P28 mouse hippocampal GluN2B interactome.** GluN2B immunoprecipitates isolated from P28 WT and spinophilin KO hippocampal lysates were separated by SDS-PAGE and Coomassie stained **(A).** Spectral counts of proteins in GluN2B IPs from WT and spinophilin KO mice were normalized to spectral counts matching GluN2B. A ratio (KO/WT) of normalized spectral counts matching GluN2B interacting proteins was generated. **8B**: The 8 proteins that had a decreased interaction with GluN2B in the KO mice were input into the string db and assigned to categories based on their function. **8C**: The 7 proteins that had an increased interaction with GluN2B in the KO mice were input into the string db and assigned to categories based on their function. n = 3 mice per group (same mice used in Figure 6F).

Table 1 Proteins having decreased interaction with GluN2B in P28 spinophilin KO/WT mice

Table 1			
Protein	Gene	Total PSMs	KO/WT Log2
ADP/ATP translocase	Slc25a4	6	-2.79
SAPAP4	*Dlgap4*	37	-1.59
Ankyrin repeat and sterile alpha motif domain-containing protein 1b	Anks1b	20	-1.33
SAPAP2	Dlgap2	31	-1.22
SAPAP1	Dlgap1	48	-1.04
Myosin Va	Myo5a	34	-0.95
Brain-enriched guanylate kinase-associated protein	Begain	14	-0.71
Leucine-rich repeat-containing protein 7	Lrrc7	48	-0.68

Table 2 Proteins having increased interaction with GluN2B in P28 spinophilin KO/WT mice

Table 2			
Protein	Gene	Total PSMs	KO/WT Log2
SAPAP3	Dlgap3	57	1.52
CaMKII beta	Camk2b	138	0.92
CaMKII alpha	Camk2a	273	0.75
CaMKII gamma	CaMK2g	88	0.75
PSD-93	Dlg2	153	0.72
PSD-95	Dlg4	414	0.59
Actin, cytoplasmic 1	Actb	32	0.5

2.5 Discussion

2.5.1 Mechanisms Regulating The Spinophilin-GluN2B Interaction

While spinophilin has been identified in NMDA receptor complexes (Baucum et al., 2013; Swartzwelder et al., 2016), our current data demonstrate that spinophilin interacts specifically with the GluN2B subunit. While expression of the individual NMDAR subunit suggests a direct interaction, we cannot rule out that a HEK cell-expressed protein is bridging this interaction. Moreover, spinophilin may interact with other NMDAR subunits within a triheteromeric receptor (e.g. GluN1 and GluN2A).

Spinophilin has been previously shown to target PP1 to specific substrates (Allen et al., 1997; M. J. Ragusa et al., 2010). Spinophilin binding to $GluN2B_{Tail}$ was increased in the presence of overexpressed PKAc. Moreover, activation of endogenous PKA using IBMX, a phosphodiesterase inhibitor (Francis, Turko, & Corbin, 2001) and forskolin, an adenylyl cyclase activator (Seamon & Daly, 1981) enhanced spinophilin binding to NMDARs. Furthermore, the intensity of $GluN2B_{Tail}$ protein band in both PKA activated and/or overexpressed blots is higher compared to control condition. This suggests that activation and/or overexpression of PKAc may either increase $GluN2B_{Tail}$ protein expression or stabilize the protein. However, when we normalize for the increased expression, we still observe a significant increase in the $GluN2B_{Tail}$-spinophilin interaction when PKAc is activated or overexpressed. Together, these data suggest that PKA activity is regulating the spinophilin NMDAR interaction; however, future studies will need to determine if this is due to phosphorylation of spinophilin, the NMDAR, or an additional protein.

To inform future studies, we input the coiled-coil region of spinophilin, a region critical for the spinophilin/GluN2B interaction, into the NetPhos 3.1 algorithm (Blom, Gammeltoft, & Brunak, 1999; Blom, Sicheritz-Ponten, Gupta, Gammeltoft, & Brunak, 2004). Three putative PKA sites on spinophilin were detected with this algorithm: Ser-694, Ser-758, and Ser-814. When we added PKA to our samples, we observed multiple GluN2B species that migrated differently on the gel, suggesting that the $GluN2B_{Tail}$ is phosphorylated at multiple sites. The mass spectrometry results revealed PKA phosphorylation sites on Ser-929/930, Ser-940 and Ser-1050 on GluN2B, that were within the spinophilin binding region. In addition, Ser-882, was determined as a predicted PKA site using the NetPhos prediction algorithm (Blom et al., 1999; Blom et al., 2004).

Future studies will need to detail if phosphorylation of any PKA site(s) on spinophilin and/or GluN2B regulate the interaction of these two proteins.

2.5.2 Spinophilin Attenuates PP1 Targeting To GluN2B

Inhibition of PP1 in the presence, but not absence, of spinophilin increases NMDAR currents (Feng et al., 2000). Spinophilin directly binds PP1 (Allen et al., 1997; Colbran et al., 1997) and can alter the phosphorylation state of various proteins by either targeting (Grossman et al., 2004; M. J. Ragusa et al., 2010; Terry-Lorenzo et al., 2002) or inhibiting PP1 activity (M. Bollen, W. Peti, M. J. Ragusa, & M. Beullens, 2010; M. J. Ragusa et al., 2010). PP1 associates with ~200 targeting/inhibitor proteins and it is not thought to exist in an unbound form; therefore, PP1 catalytic activity is exclusively dependent upon these associated proteins (M. Bollen et al., 2010; Cohen, 2002; Virshup & Shenolikar, 2009). We found that spinophilin overexpression decreases PP1γ1 association with $GluN2B_{Tail}$ in heterologous cells. Our results suggest that this effect of spinophilin is not due to competition between PP1 and spinophilin interaction domains. Therefore, we posit that decreased PP1 binding to GluN2B is a result of greater affinity of PP1 for spinophilin compared to GluN2B such that when spinophilin is present, it sequesters PP1 away from GluN2B. However, when spinophilin is low or absent, unbound PP1 will find a binding partner (e.g. GluN2B). Spinophilin-dependent sequestration of PP1 is not an overexpression artifact as we observed greater association of GluN2B with PP1 in spinophilin KO compared to WT mice, suggesting an *in vivo* role of spinophilin. Of note, we have previously found that spinophilin binding to PP1 is regulatable by kinases, such as CDK5 (Edler et al., 2018). Therefore, modulation of the spinophilin/PP1 interaction may regulate PP1 binding to, or activity at, synaptic substrates.

2.5.3 Spinophilin Enhances GluN2B Phosphorylation At Ser-1284

In order to determine the functional consequences of the spinophilin/GluN2B interaction and/or spinophilin expression on GluN2B phosphorylation, we utilized MS/MS-based approaches to identify and ratiometrically quantify various phosphorylation sites on $GluN2B_{Tail}$ in the absence or presence of overexpressed PP1γ1 and spinophilin. Interestingly, our mass spectrometry and immunoblotting results show a significant decrease in GluN2B Ser-1284 phosphorylation caused by overexpression of PP1γ1. This decrease was partially rescued when spinophilin was mutually

overexpressed along with PP1γ1. Moreover, PKA overexpression enhanced the association of spinophilin with $GluN2B_{Tail}$ and also led to a greater attenuation of the PP1-induced decrease in Ser-1284 phosphorylation in HEK293 cells both by mass spectrometry and using a Ser-1284 antibody. Of note, the F451A mutant spinophilin which has attenuated binding to PP1γ1 and does not displace PP1 from GluN2B, had a less robust attenuation of the PP1-dependent dephosphorylation of Ser-1284. Together these data suggest that in the absence of spinophilin, PP1 binds GluN2B and dephosphorylates it at Ser-1284. However, when spinophilin is present it displaces PP1 from GluN2B. Moreover, the greater attenuation of Ser-1284 by spinophilin in the presence of PKA suggests that even though the spinophilin-PP1 complex may be bound to GluN2B, in this spinophilin bound state, PP1 cannot dephosphorylate Ser-1284 as readily. Moreover, less Ser-1284 phosphorylation in spinophilin KO compared to WT P28 animals suggest a similar *in vivo* role for spinophilin. Together, these data suggest that spinophilin acts as an inhibitor of PP1 binding to GluN2B to maintain Ser-1284 phosphorylation (Figure 8). These data are of interest as phosphorylation at this site is altered in ischemic conditions as well as acute stress conditions (W. Lu et al., 2015). However, the roles of Ser-1284 on regulating GluN2B-containing NMDAR channel activity and localization need to be further evaluated.

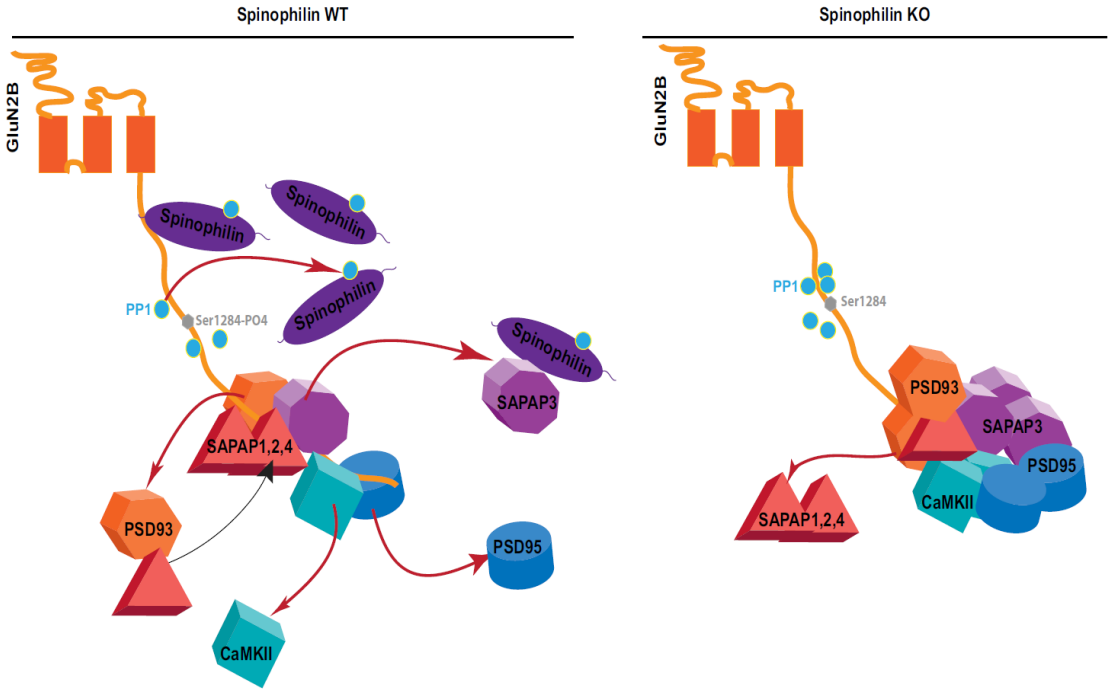

Figure 9 Schema showing spinophilin regulation of GluN2B protein interactions and GluN2B phosphorylation at Ser-1284. In WT conditions, spinophilin limits PP1 binding to GluN2B thereby maintaining GluN2B phosphorylation at Ser-1284 in a high state. Moreover, spinophilin limits the association of PSD-enriched proteins such as PSD95, CaMKII, and SAPAP3. In spinophilin knockout mice spinophilin no longer limits PP1 binding and therefore, there is a greater interaction of PP1 with $GluN2B_{Tail}$ that occurs concurrently with decreased phosphorylation of GluN2B at Ser-1284. Moreover, spinophilin no longer limits the association of proteins such as PSD95, CaMKII, and SAPAP3, which increase their association with GluN2B while concomitantly decreasing the association of the other SAPAP proteins

2.5.4 Loss Of Spinophilin Alters GluN2B Phosphorylation And The GluN2B Interactome *in vivo*

Spinophilin expression and/or regulation of GluN2B phosphorylation may impact its protein interactions. Using an initial proteomics approach, we found that spinophilin KO mice had altered GluN2B protein interactions. Gel-based proteomics studies may be limited in their ability to detect lowly expressed or lowly interacting proteins and we did not observe PP1 or spinophilin in our dataset possibly be due to low levels of interaction. However, we did observe increased GluN2B interaction with synaptic proteins such as CaMKII isoforms, PSD-95, PSD-93 and SAPAP3, but decreased association with different scaffolding proteins such as SAPAP1, SAPAP2, and SAPAP4 and the cytoskeletal protein, myosin Va. SAPAP3 interacts with spinophilin (Morris et al., 2018) and here we report that the association of SAPAP3 with GluN2B is greater in spinophilin KO compared to WT animals. All four SAPAPs are expressed in hippocampus (Kindler, Rehbein, Classen, Richter, & Bockers, 2004) and therefore spinophilin may normally act to sequester SAPAP3 away from GluN2B to allow for binding of other SAPAP isoforms (Figure 8).

We have observed spinophilin-dependent changes in protein binding to GluN2B that are in the range of 1.5- to 3-fold. It is important to note that these changes in interactions may be due to alterations in protein expression, changes in protein interaction, or both. Moreover, as spinophilin is the major PP1 targeting protein in the PSD, it may be surprising that these changes are not higher. However, compensatory changes, such as decreased PP1 expression in spinophilin KO mice may mitigate these changes. Furthermore, the spinophilin homolog, neurabin, is also highly abundant in the PSD which may limit the effects of spinophilin KO.

The mechanisms and functional consequences of spinophilin-dependent regulation of GluN2B protein interactions are unclear. As stated above, spinophilin KO animals have decreases in Ser-1284 phosphorylation and Ser-1284 phosphorylated GluN2B may be higher in PSD fractions of hippocampal lysates isolated from adult mice (W. Lu et al., 2015). Functionally, previous studies report that disturbing the CaMKII-GluN2B interaction protects primary hippocampal cultures against ischemic-dependent cell death (Vieira et al., 2016); therefore, regulation of this interaction may have effects on neurotoxicity. Of note, synaptic, compared to extrasynaptic, expression of the NMDAR is associated with neuronal survival (Hardingham & Bading, 2010). Pathologically, the GluN2B interactome is implicated in various conditions such

as hypoxia-ischemia (F. Lu et al., 2018). Given the important role of GluN2B interaction with synaptic proteins and GluN2B phosphorylation in ischemic neurotoxicity (W. Lu et al., 2015; Vieira et al., 2016), future studies will need to delineate if spinophilin-dependent regulation of GluN2B is an important modulator of ischemic neurotoxicity in brain.

2.6 Summary

Taken together our data demonstrate that spinophilin attenuates PP1 binding to GluN2B and that this decreased binding enhances Ser-1284 phosphorylation on GluN2B. Moreover, loss of spinophilin enhances GluN2B interactions with PSD-enriched proteins such as PSD-95 and CaMKII.

CHAPTER 3. SPINOPHILIN-DEPENDENT REGULATION OF GLUN2B CONTAINING NMDA RECEPTORS AND GLUTAMATE TOXICITY

3.1 Abstract

Excitotoxicity is a major hallmark of neuronal damage associated with cerebral ischemia. Excitotoxicity is a result of accumulation of extracellular glutamate, resulting in hyperactivation of glutamate receptors such as N-methyl-D-Aspartate receptors (NMDARs). Phosphorylation of NMDAR subunits defines receptor activity, downstream signaling pathways, and localization and modulation of NMDAR phosphorylation and its consequences could mitigate excitotoxicity-induced pathology. NMDAR phosphorylation is dynamically controlled by a balance of kinase and phosphatase activity. Spinophilin is a scaffolding and protein phosphatase 1 (PP1) targeting protein that modulates phosphorylation of various substrates via targeting or inhibition of PP1. Spinophilin limits NMDAR functionality in a PP1-dependent manner. We have previously shown that spinophilin sequesters PP1 away from the GluN2B subunit of the NMDAR, which results in increased phosphorylation of Ser-1284. However, how spinophilin-mediated Ser-1284 phosphorylation modulates NMDAR function is unclear. Herein, we detail that while Ser-1284 phosphorylation increases the channel activity, overexpression of spinophilin decreases GluN2B-containing NMDAR activity while also decreasing GluN2B-containing NMDAR surface expression. Moreover, in hippocampal neurons isolated from spinophilin knockout animals there is greater cleaved caspase levels. Taken together, our data demonstrate a unique mechanism by which spinophilin modulates GluN2B containing NMDAR phosphorylation, channel function, and trafficking to potentially mitigate NMDAR-dependent neuronal cell death.

3.2 Introduction

Stroke is the fifth leading cause of death in the USA and ischemic stroke accounts for ~87% of all strokes (Benjamin et al., 2017). Glucose and oxygen deprivation (OGD) caused by shortage of blood supply to the brain, leads to neuronal death in various brain regions though both necrosis and apoptosis (Gorter et al., 1997; Kirino, 1982; Petito, Feldmann, Pulsinelli, & Plum, 1987). The sudden loss of energy supply due to OGD in the brain leads to a breakdown and depolarization of

neuronal and astro-glial membrane potentials. In neurons, the membrane depolarization leads to vesicular glutamate release from axonal terminals (Graham, Shiraishi, Panter, Simon, & Faden, 1990). The overload of glutamate eventually leads to excitotoxicity (Arundine & Tymianski, 2004; Forder & Tymianski, 2009). Excitotoxicity, a main feature of ischemic pathology results in hyper-activation of α-amino-3-hydroxy-5-methyl-4-isoxazolepropionic acid (AMPA) (Gorter et al., 1997; S. Liu et al., 2004; Pellegrini-Giampietro, Gorter, Bennett, & Zukin, 1997) and N-methyl-D-aspartate (NMDA) receptors (Arundine & Tymianski, 2004; Hardingham, Fukunaga, & Bading, 2002), resulting in excess influx of calcium and activation of apoptotic pathways in neurons (Aarts et al., 2002; S. Liu et al., 2004; Manev, Favaron, Guidotti, & Costa, 1989). Current strategies for decreasing apoptotic neuronal loss involve blockade of glutamate receptors using receptor antagonists. However, these approaches interfere with normal brain function, thus limiting their therapeutic potential (Lees, 1998).

Therefore, a more promising approach may be to modulate glutamate receptor function rather than directly blocking their activity. One promising potential target is specifically inhibiting pathological changes in GluN2B-containing NMDARs, given their leading role in promoting neurotoxicity due to their high calcium permeability (Aarts et al., 2002; Goldberg & Choi, 1993; Hardingham et al., 2002; Wyllie et al., 2013). Indeed, blockade of GluN2B containing NMDARs protects neurons against ischemic-dependent cell death (Vieira et al., 2016). As a result, regulating NMDAR activity may allow for some control over NMDAR-dependent ischemic cell death. NMDAR subunit composition, localization, and surface expression affect channel activity and these properties are regulated by NMDAR subunit phosphorylation (Chung et al., 2004; Manabe et al., 2000; Swope et al., 1999; Tavalin & Colbran, 2017). As a result, the role of differential phosphorylation of NMDAR subunits, such as GluN2B, in neurotoxicity/neuroprotection associated with ischemia is critical. However, specific signaling mechanisms by which GluN2B-containing NMDARs are modulated basally and during ischemic neurotoxicity are unknown. While many studies of alterations in NMDAR phosphorylation promoting ischemic pathology have focused on protein kinases (Cheung, Teves, Wallace, & Gurd, 2001; S. Lee & Zhou, 2006; Y. Liu, Zhang, Gao, & Hou, 2001; Vieira et al., 2016; J. Wang, Liu, Fu, Wang, & Lu, 2003), less attention has been paid to the specific roles of serine/threonine phosphatases. Serine/threonine phosphatases are highly promiscuous and utilize targeting and inhibitory proteins to modulate NMDAR phosphorylation. Spinophilin is the major dendritic spine-enriched, scaffolding and

protein phosphatase 1 (PP1) targeting protein and is known to decrease NMDAR channel activity. Spinophilin interacts with multiple subunits of the NMDAR in mouse brain and decreases NMDAR function via PP1 targeting (Allen et al., 2006; Feng et al., 2000; S. Liu et al., 2004; Salek et al., 2019). We have recently shown that spinophilin specifically regulates phosphorylation of Ser-1284 on GluN2B. Others have shown that this site is hypo-phosphorylated in ischemia, but becomes hyperphosphorylated upon reperfusion (W. Lu et al., 2015). However, the functional and pathological consequences of altered GluN2B phosphorylation at Ser-1284 are unclear. In addition, Ser-1284 phosphorylation-dependent and phosphorylation-independent mechanisms by which spinophilin regulates GluN2B function are unclear.

Herein, we detail the spinophilin-dependent changes that modulate the function of GluN2B-containing NMDARs, such as subcellular localization, surface expression, and calcium influx. Furthermore, we explore spinophilin-dependent changes in neurotoxicity and cell death under conditions of excess glutamate. These studies will significantly contribute to our understanding of the role of spinophilin in modulating GluN2B phosphorylation and function and how these changes regulate NMDAR-dependent ischemic cell death and will assist in the identification of novel therapeutic targets to help treat ischemia.

3.3 Materials and Methods

3.3.1 Reagents

All custom materials will be shared upon reasonable request. Experiments were approved by the institutional biosafety committee (IBC-1594 and IN-1000).

cDNAs: Templates used for generation of expression vectors were: human spinophilin , human GluN2B (BC113618; Transomic Technologies, Huntsville, AL, USA), mouse GluN1 (BC039157; Transomic Techologies), GCaMP6s (40753, Addgene, Watertown, MA, USA), F451A mutant was generated from the full-length construct. Mutagenesis was performed by site-directed mutagenesis kit (QuickChange II, Agilent Technologies, Santa Clara, CA) (Morris et al., 2018; Salek et al., 2019). Transfection Reagent: Polyjet (SignaGen Laboratories, Rockville, MD, USA) was used for transfections.

Antibodies: Antibodies used for IPs and/or primary blotting: goat polyclonal spinophilin (A-20, SC14774, RRID: AB_2169477; Santa Cruz Biotechnology, Dallas, TX, USA), sheep

polyclonal Spinophilin Antibody (PA5-48102, RRID: AB_2605900, ThermoFisher Scientific, Waltham, MA, USA), rabbit monoclonal anti-NMDAR2B (GluN2B) (D15B3, RRID: AB_2112463 or D8E10, RRID: AB_2798506, 4212 or 14544; Cell Signaling Technology, Beverly, MA, USA), rabbit monoclonal anti-NMDAR1 (GluN1) (D65B7, RRID: AB_1904067, 5704, Cell Signaling Technology), rabbit polyclonal anti-NMDAR2A (GluN2A) (RRID: AB_2112295, 4205, Cell Signaling Technology), rabbit monoclonal anti-AMPAR2 (GluA2) (E1L8U, RRID: AB_2650557, 13607, Cell Signaling Technology), rabbit polyclonal anti-Caspase 3 (RRID: AB_331439, 9662, Cell Signaling Technology), rabbit polyclonal anti-Cleaved Caspase 3 (Asp175) (RRID: AB_2341188, 9661, Cell Signaling Technology), rabbit monoclonal anti-GFP (D5.1, RRID: AB_1196615, 2956, Cell Signaling Technology), Secondary antibodies used were: Alexa Fluor 790-conjugated AffiniPure Donkey Anti-Rabbit IgG (711-655-152, RRID: AB_2340628; Jackson ImmunoResearch Laboratories), Alexa Fluor 680-conjugated AffiniPure Donkey Anti-Sheep IgG (RRID: AB_2340753; Jackson ImmunoResearch Laboratories).

Other reagents: D-AP5 (D-145, Alomone, Jerusalem, Israel) or (14539, Cayman Chemicals, Ann Arbor, MI, USA), BSA (A9647-100G, Sigma-Aldrich, St Louis, MO, USA), Leibovitz's L-15 media (21083027, Gibco by Life Technologies, ThermoFisher Scientific, Waltham, MA, USA), Papain (P4762-500MG, Sigma-Aldrich), Modified Eagle's Medium (MEM) (51200038, Gibco by Life Technologies, ThermoFisher Scientific), Fetal Bovine Serum (FBS) (16140063, Gibco by Life Technologies, ThermoFisher Scientific), Horse serum (26050070, Gibco by Life Technologies, ThermoFisher Scientific), L-Glutamine (35050-061, Gibco by Life Technologies, ThermoFisher Scientific), Penicillin/Streptomycin (Pen/Strep) (15140-122, Gibco by Life Technologies, ThermoFisher Scientific), Glucose (G5767-500G, Sigma Aldrich), Insulin/Selenite/Transferrin (IST) (I1884-1VL, Sigma-Aldrich), Neurobasal Media (12349015, Gibco by Life Technologies, ThermoFisher Scientific), B27 Supplement (17504044, Gibco by Life Technologies, ThermoFisher Scientific), Gentamycin reagent (15750-060, Gibco by Life Technologies, ThermoFisher Scientific). Sulfo-NHS-SS-Biotin (325143-98-4, A8005, APExBIO Technology LLC, Houston, Texas, USA), NeutrAvidin beads (29201, ThermoFisher Scientific), Protease inhibitor cocktail (Thermo-Fisher Scientific or Bimake, Houston, TX, USA), Glutamate (G2834-100G, L-Glutamic acid, monosodium, Salt monohydrate, 98%, Molecular weight:187.13 (GA)), 12 mm coverslips (1254582, ThermoFisher Scientific), Cytosine β-D-arabinofuranoside (Ara-C) (C1768-100MG, Sigma-Aldrich).

All other utilized reagents were of highest purity obtained from ThermoFisher Scientific, Sigma-Aldrich, or Gibco.

3.3.2 Animals

Experiments were approved by the School of Science Institutional Animal Care and Use Committee (SC270R, SC310R) and performed in accordance with the Guide for the Care and Use of Laboratory Animals and under the oversight of the Indiana University-Purdue University, Indianapolis (IUPUI). Animals were provided food and water ad libitum. Mice were maintained on a normal 12 hour light (7am-7pm)/dark (7pm-7am) cycle. Spinophilin KO mice were initially purchased from Jackson Laboratories (Bar Harbor, ME, USA; Stock #018609; RRID: MMRRC_049172-UCD) and a breeding colony has been maintained at IUPUI. Male or female, WT, C57Bl6, (Jackson laboratories) or spinophilin knockout mouse brains were dissected at Postnatal day 28–32 (P28). Animals were group housed and WT and KO littermates were used (WT and KO animals were from heterozygote x heterozygote breeding pairs). Animals were weaned ~ P21. For generation of neuronal cultures, mice were weaned at P0. For biochemical analyses and generation of neuronal cultures, animals were euthanized by decapitation without anesthesia.

3.3.3 Mutagenesis

Mutagenesis was performed as described before (Salek et al., 2019). Briefly, reactions were performed using the site-directed mutagenesis kit (Agilent Technologies, Santa Clara, CA, USA) using Q5 DNA polymerase in Q5 DNA buffer in the presence of DNTPs and template DNA followed by a mutagenesis PCR protocol. The PCR products were later transformed into DH5α E. coli. Vectors were then sequence verified (Genewiz Inc, South Plainfield, NJ, USA) for the mutations.

3.3.4 Mammalian Protein Expression

Neuro2a cells were used for mammalian protein expression. Cells were purchased and split into passage 9 and frozen down. The cells were used up to passage 22. After thawing, cells were incubated with MEM recovery media containing 20% FBS, 1% Pen/strep and 1% Sodium

Pyruvate. The cell culture and incubation after recovery was performed in MEM containing: 10% FBS, 1% Pen/Strep and 1% Sodium Pyruvate. 6- and 12-well plates were placed in a tissue culture incubator (Panasonic Healthcare; Secaucus, NJ, USA) at 37ºC and 5% CO2. Cells were counted and the density was adjusted to 70,000-100,000/mL. 6-well and 12-well plates received 2 mL or 1 mL, respectively, of cell containing media. Cells were transfected the next day at about 50-60% confluency. Confluency was measured by estimating cell coverage on the bottom of the flask. For 6-well plates, DNA (0.5–2 μg per DNA vector) was added to 250 μL of serum-free MEM in a 1.7 mL microcentrifuge tube. In a separate microfuge tube, transfection reagent was added to 250 μL of serum-free MEM. Polyjet was used in a 3: 1 volume: mass ratio (e.g. 9 μL of Polyjet was used with 3 μg DNA). For each well, DNA concentrations were equalized using an empty DNA vector, so that each condition in the same experiment had an equal mass of DNA and transfection reagent (all the volumes were cut in half for 12-well plate studies). The Polyjet containing MEM was then added to the tube containing DNA and incubated at room temperature for 15 min. The DNA-Polyjet mixture was then added to each well very slowly as the plate was being gently shaken on a horizontal axis to mix the DNA mixture with the media. The wells transfected with full-length GluN1 and full-length GluN2B expression vectors were then treated with 0.25 μg/mL of APV. 3 μg of APV was dissolved in 600 μL of MEM. 100 μL of this mixture was then added to each well of a 6-well plate containing 2 mL of cell media. The cells were then placed in the incubator overnight and were processed the next day. If the cells were cultured for imaging, they were imaged the next day prior to lysis. If not, the cells were processed the next day as follows: MEM was removed, and cells were washed with 2 mL of cold phosphate-buffered saline (PBS). PBS was aspirated off and cells were lysed in 0.75 mL KCl lysis buffer (150 mM KCl, 1 mM dithiothreitol (DTT), 2 mM EDTA, 50 mM Tris-HCl pH 7.5, 1% (v/v) Triton X-100, 20 mM β-glycerophosphate, 20 mM sodium fluoride, 10 mM sodium pyrophosphate, 20 mM sodium orthovanadate, 1X protease inhibitor cocktail) then transferred into 2 mL microcentrifuge tubes. Cells were sonicated at 25% amplitude for 15 s at 4°C using a probe sonicator (Thermo-Fisher Scientific) and centrifuged (4°C for 10 min at 16,900 x g).

3.3.5 Calcium Imaging In Neuro2a Cells

To image the changes in intracellular calcium levels, Neuor2a cells were plated in 12-well plates and were transfected with 0.5 μg each of V5-GluN1, Myc-GluN2B, GCaMP6s and/or 1 μg WT or F451A mutant HA-spinophilin. Each well received a final concentration of 2.5 μg/mL APV after the transfection. A detailed description of the mammalian protein expression protocol can be found above. The next day, APV containing MEM was aspirated off and replaced with 1 mL of calcium-free 1X PBS in room temperature. The cells were immediately placed in the Cytation 3 (Biotek, Winooski, Vermont, U.S.A.) cell imaging multi-mode reader. The reader was temperature and gas controlled and was set at 35-37ºC and 5% CO2. Changes in fluorescence were measured for 5 minutes at 9 s intervals, resulting in a total of 34 readings. To measure fluorescence, the excitation and emission wavelengths were set at 488 and 528 nm, respectively, reading from the bottom of the plate. This 5-minute incubation with calcium-free PBS, was used to minimize background fluorescence by decreasing intracellular calcium and concomitant GCaMP6s fluorescence. After the incubation, each well received CaCl2 (3-6 mM final concentration) via a built-in dispenser and briefly received an orbital shake for 2 s to uniformly mix the CaCl2 with the media. The plate was read at the same wavelengths mentioned above for another 5 minutes. After the reading was completed, the media was aspirated off the cells. The cells were then lysed and processed as above in 350 μL RIPA/PI lysis buffer. All the fluorescence reading values at each time point were normalized back to the baseline by subtracting each value from the fluorescence value at the 0-time point of the corresponding well. The data was then used to plot a graph and the area under the curve (AUC) was quantified and compared across different conditions using an ordinary One-way ANOVA or Two-way ANOVA depending on the experimental design. Multiple comparisons assays were performed using Tukey or Bonferroni posthoc tests depending on the experimental design.

3.3.6 Biotinylation In Neuro2a Cells

Neuro2a cell biotinylation was based on the protocol from Cao et. al., (Cao et al., 2007) and optimized for a 6-well cell culture plate. Neuro2a cells were washed 3 times in 1 mL of B buffer (0.5mM CaCl2, 0.5mM MgCl2-6H2O in 1X PBS). Following the wash, 1 mL of 0.5 mg/mL Sulfo-NHS-SS-Biotin in B buffer was added to each well and allowed to incubate at room

temperature for 5 minutes. The free biotin was then quenched by washing the cells twice with 1 mL of biotin quenching buffer (100 mM Glycine in B buffer). Following the quenching step, the cells were lysed in 750 µL of RIPA/PI buffer (1 mM EDTA, 150 mM NaCl, 20mM Tris-HCl, 1X protease inhibitor, 0.01% NP-40, 0.01% deoxycholate, 20mM Phosphatase inhibitor). The samples were then centrifugated at 14,000 x g at 4ºC for 15 minutes. To create the input, 150 µL of the lysate supernatant was mixed with 50 µL of 4X SDS containing sample buffer with DTT. 500 µL of the supernatant was mixed with 40 µL of a 50% slurry of NeutrAvidin beads and incubated with rotating at 4ºC overnight. The next day, the beads were washed 3X by centrifuging the samples at 2000 x g for 1 minute and replacing the supernatant with 500 µL RIPA/PI buffer and allowing to rock for 5 minutes at 4ºC. Following the last wash, 60 µL of 2X SDS containing sample buffer with DTT was added to the beads. The beads were thoroughly vortexed and placed at -20ºC for western blotting.

3.3.7 Biotinylation In Brain Slices

The protocol used for brain slice biotinylation is modified from Gabriel et. al., (Gabriel, Wu, & Melikian, 2014). Room temperature, 1X artificial cerebrospinal fluid (aCSF; 125 mM NaCl, 2.5 mM KCl, 1.2 mM NaH2PO4, 1.2 mM MgCl2-6H2O, 2.4 mM CaCl2, 26 mM NaHCO3, 11 mM Glucose) and ice-cold high sucrose solution (HSS) (250 mM Sucrose, 2.5 mM KCl, 1.2 mM NaH2PO4, 2.4 mM CaCl2, 26 mM NaHCO3, 11mM Glucose) were prepared and bubbled with carbogen (95% O2 and 5% CO2) for a minimum of 20 minutes. Animals were decapitated and the brains were dissected on ice. The brains were quickly transferred to ice-cold HSS and 300 µM slices were generated using a VT1200-S vibrating microtome (Leica Biosystems, Buffalo Grove, IL). Four hippocampi containing whole brain slices were generated from each brain. The slices were then transferred into a slice chamber and were incubated with 31ºC, circulating, carbogenated 1x aCSF for 40 minutes to recover. The following procedures were performed on ice unless otherwise stated. After the 40-minute recovery, the slices were transferred into an ice-cold, 24-well plate and were incubated with 750 µL of 1 mg/mL of Sulfo-NHS-SS-Biotin dissolved in ice-cold carbogenated 1X aCSF for 45 minutes followed by a 3X wash with 750 µL of ice-cold 1X aCSF. After the last wash, the slices were incubated with 750 µL of ice-cold 1X aCSF for 10 minutes followed by 3 washes with 750 µL of ice-cold biotin quenching buffer (100 mM Glycine

in 1X aCSF). Following the last wash, the slices were incubated with 750 µL of ice-cold biotin quenching buffer for 25 mins. The slices were then washed 3X with ice-cold 1X aCSF. After the last wash, the hippocampi were dissected from the slices and were transferred into a homogenizer containing 1200 µL of RIPA/PI buffer. The slices were homogenized using 18-20 up-and-down movements of a pestle in a 2-mL tight-fitting glass homogenizer. The homogenate was then sonicated once for 15 seconds at 25% amplitude followed by centrifugation for 15 minutes at 14,000 x g at 4ºC. 150 µL of the lysate supernatant was mixed with 50 µL of 4X SDS sample buffer and used as the input. 500 µL of the supernatant was mixed with 60 µL of pre-washed Neutravidin beads and rotated at 4ºC overnight to pulldown (PD) biotinylated proteins. The next day, the PD samples were washed three times using 500 µL of ice-cold RIPA/PI buffer. The samples were centrifugated for 1 minute at 2,000 x g, then the supernatant was aspirated off and replaced with 500 µL of ice-cold RIPA/PI. The tubes were then replaced on the rotator and were allowed to rotate at 4ºC for 5 minutes. This wash procedure was repeated 3 times. Following the last wash, the supernatant was removed and 60 µL of 2X SDS sample buffer+DTT was added to the beads, the tubes were briefly vortexed and placed at -20ºC.

3.3.8 Subcellular Fractionation

Male and female P28-P32 Spinophilin WT and KO mice were decapitated without anesthesia, brains were removed, the hippocampi were rapidly dissected, frozen in liquid nitrogen, and stored at −80 °C. Two whole frozen mouse hippocampi (one from each hemisphere) were pooled and homogenized in 2 ml of a detergent-free isotonic (150 mm KCl, 50 mm Tris-HCl, 1 mm DTT, 1X protease cocktail, 2mM EDTA, 20mM NaF, 20mM NaVO4, 20mM Beta-20mM Na-Pyrophosphate) buffer homogenized using 18-20 up-and-down movements of a pestle in a 2-mL tight-fitting glass homogenizer. Samples were then centrifuged at 100,000 × g at 4 °C for 1 hour. Supernatants (S1) were saved for SDS-PAGE. The pellet (P1) was resuspended in 1 ml of isotonic buffer containing 0.5% Triton X-100 in a microcentrifuge tube. Samples were then centrifuged at 14,000 × g at 4°C for 10 min. Supernatants (S2) were saved, and the P2 pellets were resuspended in 1 ml of isotonic buffer containing 1% Triton X-100 and 1% sodium deoxycholate and sonicated. Following incubation at 4 °C for 15 seconds. samples were then centrifuged at 14,000 × g for 10 min, and the supernatants (S3) were saved for SDS-PAGE. The 150 µL of lysate

samples from S1, S2, and S3 fractions were mixed with 4XSDS sample buffer containing DTT and the same amount of each sample from WT and KO brains was loaded on the gel. After the transfer of the proteins to nitrocellulose membrane, the membranes were stained with 1X Ponceau S stain for 5 minutes to stain for total proteins. After western blotting, the intensity of the band of the protein of interest was divided by the total amount of protein in the sample measured by Ponceau S stain using ImageJ. This value in the KOs was divided by that of the WT in the same trial. The normalized data were then analyzed by a One-column student t-test compared to a theoretical ratio of 1.

3.3.9 Hippocampal Primary Neuronal Cultures

Hippocampal primary neurons were dissociated and cultured using a previously published protocol (Bansal et al., 2019). In short, hippocampi were dissected from P0 mice in harvest media (0.02% BSA in Leibovitz's L-15 media). The hippocampi were then transferred to a 15 mL conical containing 0.5 mL dissociation media (0.038% papain in previously made 0.02% BSA/L15), carbogenated, recovered in a 37ºC water bath for 10 minutes, incubated in M5-5 media (5% FBS, 5% Horse serum, 0.2% L-Glutamine, 1% Pen/Strep, 1% Glucose, 0.25% IST in MEM), and dissociated by pipetting 30X using three different sizes of sterile, fire-polished, pasture pipets. After each round of pipetting the supernatant containing the dissociated cells was collected and pooled in a sterile 15 mL conical centrifuge tube. After the last round, the supernatant was centrifuged at 800 x g for 5 minutes at room temperature. The supernatant was removed, and the pellet was dissolved in 3 mL of M5-5 media. Then, 1 mL of the cell mixture was added to each well of a 24-well plate containing a 12 mm coverslip previously coated with 0.5 mg/mL Poly-Lysine and placed in 5% CO2, 37ºC cell culture incubator. After 48 hours, 0.5 mL of the M5-5 media was replaced with 1 mL of B27 supplement media (2% B27 Supplement, 0.25% L-Glutamine, 0.25% IST, 0.1% Gentamycin reagent, 15μL ARA-C in Neurobasal media, mixed and sterile filtered using 0.2 μm filter syringe). The plate was then placed back in the incubator until the day of the experiment (14-24 days in vitro; DIV).

3.3.10 Induction Of Glutamate Toxicity

Primary hippocampal cultures were assayed at 14-24 DIV. On the test day, the culture media was collected from the wells into a sterile 15 ml conical centrifuge tube to generate the conditioned Neurobasal (cNB) media. Each of the spinophilin WT and KO wells received 1 mL of fresh neurobasal media containing 100 μM glutamate. The cells were incubated with the media for 30 minutes to induce toxicity in 37ºC cell incubator. In the meantime, the conditioned Neurobasal media was sterile filtered using 0.2 μm filters and the volume was adjusted by adding fresh Neurobasal media (no more than 10% of the total media volume) and placed in a 37ºC water bath. After 30 minutes, the glutamate containing media was removed from the wells and replaced with 1.5 mL cNB media and incubated in a cell culture incubator for 90 minutes to recover. Following the recovery, the neurons were lysed and processed as follows: the media was removed from the wells and 300 μL of ice cold low ionic lysis buffer (2 mM Tris pH 7.5, 2 mM EDTA, 1 mM DTT, 1x Protease Inhibitor, 20 mM NaF, 20 mM Na orthovanadate, 10 mM Na pyrophosphate, 20 mM β-glycerophosphate, 1% Triton) was added to the cells. The cells were lysed by trituration until all the cells were detached from bottom of the wells. The lysate was then transferred into 1.7 mL microcentrifuge tubes and sonicated with a probe sonicator for 15 seconds at 25% amplitude followed by centrifugation at 4ºC for 15 minutes at 14,000 x g. 150 μL of the lysate supernatant was transferred into a new tube and mixed with 4X SDS sample buffer containing DTT. The samples were then placed at -20ºC until processed.

3.3.11 Immunoprecipitations And Western Blotting

Cell lysate inputs and/or PD samples were used for western blotting. All samples were heated at 70°C for 10 min prior to loading on the gel. PD samples were briefly vortexed and centrifuged at 1000 x g for 2 minutes to precipitate the NeutrAvidin agarose beads and separate them from the suspension prior to loading on the gel. 10-35 μL of input or 20-30 μL of PD sample were loaded onto a 1.00 mm hand-cast 10% polyacrylamide gel. The gels were electrophoresed at 75 V for 15 min and 175 V for approximately 1 h. Proteins were transferred to a nitrocellulose membrane using a wet transfer in an N-cyclohexyl-3-aminopropanesulfonic acid transfer buffer (10% MeOH, 0.01 M N-cyclohexyl-3-aminopropanesulfonic acid pH 11). The transfer was performed in a transfer tank attached to a cooling unit set at 4°C and transfer was operated at a

constant 1.0 Amps for 1.5 h. Membranes were stained with a 2 mg/mL Ponceau S stain dissolved in 10% Trichloroacetic acid for 5 min to normalize inputs for equal loading where applicable. Following Ponceau staining, membranes were scanned and subsequently washed with deionized water. Membranes were blocked in Tris-buffered saline with Tween (TBST; 50 mM Tris pH 7.5, 150 mM NaCl, 0.1% (v/v) Tween-20) containing 5% (w/v) nonfat dry milk. Blocking was performed three times, 10 min each, for a total of 30 min. Membrane was incubated with primary antibodies diluted in 5% milk in TBST overnight at 4°C with gentle shaking. After incubation, membranes were washed three times for 10 min per wash with TBST containing 5% milk. Appropriate secondary antibodies in TBST containing 5% milk were added to the membranes following the washes. Jackson ImmunoResearch antibodies were typically diluted 1 : 50,000 and Invitrogen antibodies were generally diluted 1 : 10000. Secondary antibodies were incubated with membranes for 1 h at 22ºC shaking in darkness. Membranes were washed three times with TBS without Tween for 10 min for each wash. Fluorescence scans were performed using the Odyssey imaging system (LiCor, Lincoln, NE, USA) and data analysis was done using Image Studio software (LiCor). We have previously shown linearity of fluorescence intensity using these conditions for multiple proteins and antibody pairs.

3.3.12 Statistical Inference And Data Plotting

The tests used for statistical analysis were One-sample t test/Wilcoxon test, One-way and Two-way ANOVA. For multiple comparison analysis, Bonferroni, Tukey, or Sidak tests were used depending on the experimental design. A detailed statistical analysis methodology is included in each result subsection. The mean and standard deviation (SD) of each condition in all the figures is summarized in Table 1. In the experiments with $n \leq 12$, individual data points were indicated in the graph with mean and standard error of the mean (SEM). The experiments with 12 or more data points were plotted as a bar graph with indication of mean and SEM.

The graphs generated from data obtained from Neuro2A cells or cultured neurons are in color while the graphs generated from data obtained from brain tissue are in black and white.

3.4 Results

3.4.1 Spinophilin Decreases NMDAR-Dependent Calcium Influx In Neuro2a Cells Independent Of Ser-1284 Phosphorylation

We have previously shown that spinophilin decreases the association of PP1 with the GluN2B subunit of NMDARs and increases the phosphorylation of Ser-1284 on this subunit (Salek et al., 2019). In this same study, we observed alterations in the GluN2B interactome in the hippocampus of P28 spinophilin KO mouse. Alterations in the phosphorylation of either NMDARs or spinophilin modulate their respective functions, protein interactions, and/or localization. As a result, we investigated the spinophilin-dependent modulation of the function of GluN2B-containing NMDARs. As previous studies found that loss of spinophilin stabilizes NMDAR currents by preventing current rundown, we hypothesized that spinophilin limits calcium influx through GluN2B-containing NMDARs. To test this hypothesis, we co-expressed GluN1 and GluN2B subunits of the NMDAR in Neuro2a cells, along with the calcium reporter, GCaMP6s, in the presence or absence of overexpressed, WT spinophilin (**Figure 10A**). Studies show that co-expression of both GluN1 and GluN2B subunits are sufficient for formation of functional NMDARs which, if left unblocked, will lead to activation of the expressed receptors (Collett & Collingridge, 2004). Therefore, we maintained the competitive NMDAR antagonist, AP5, in the culture media. 16-24 hours post transfection, the plates were processed, and the cumulative fluorescence level was measured as explained in the methods section. After the reading was completed, the quantified fluorescence level at each time point was baseline subtracted to the fluorescence level at the corresponding 0 time point in order to account for different transfection levels of GCaMP6s across conditions. The acquired data were then analyzed using a one-way ANOVA and Tukey posthoc test for multiple comparisons. Results show a significant difference across all the conditions (***F (5, 58) = 18.61, ****P<0.0001***). Specifically, we observed a significant decrease in GCaMP6s fluorescence in the presence, compared to the absence, of overexpressed WT-spinophilin (****P<0.001***), suggesting that calcium influx through GluN2B containing NMDARs is decreased when spinophilin is overexpressed (**Figure 10B**). As a control, we transfected cells with only GCaMP6s in the presence or absence of spinophilin, but not NMDAR and we observed no significant increase in fluorescence upon addition of CaCl2 when the NMDAR was not transfected compared to the presence of the NMDAR. This suggests that our observation

in **Figure 10B** is NMDAR dependent. To ensure that the effect is not due to autofluorescence, NMDAR subunits were expressed with and without spinophilin in the absence of GCaMP6s overexpression. The results show no significant change in the fluorescence level in these conditions suggesting that the observed result is not due to changes in autofluorescence (**Figure 10B**). As an additional control, the cells were treated with CaCl2 or vehicle. Consistent with a specific effect of extracellular calcium, our results demonstrate that the changes in the fluorescence level is solely present upon addition of extracellular CaCl2 (**Figure 10C**); however, we cannot rule out that extracellular calcium influx via NMDARs is leading to subsequent calcium release from intracellular stores which may be enhancing the GCaMP6s signal. Together, these results indicate that WT spinophilin significantly decreases the calcium influx through GluN2B containing NMDARs.

Next, we investigated whether the observed effects of spinophilin in modulating calcium influx is due to its PP1 binding ability. To study this, we utilized a mutant spinophilin (F451A) that we and others have shown has reduced binding to PP1 (Guo et al., 2019; Hsieh-Wilson et al., 1999; Morris et al., 2018; Salek et al., 2019; Yan et al., 1999). Here, we transfected cells with GluN1, GluN2B, and GCaMP6s in the presence of WT or F451A mutant spinophilin. Our results show that overexpression of the mutant spinophilin displays no significant difference compared to the condition where no spinophilin was overexpressed in terms of the changes in the level of fluorescence upon addition of CaCl2 (**Figure 10D**).

This suggests that the spinophilin-dependent changes in calcium influx are partly due to PP1 binding because abrogating the PP1-spinophilin interaction abolishes the spinophilin-dependent decrease in the GluN2B containing NMDAR-dependent calcium influx.

We have previously shown that spinophilin enhances Ser-1284 phosphorylation on the GluN2B subunit of NMDARs by sequestering PP1 (Salek et al., 2019). As a result, we were interested in investigating whether spinophilin-dependent phosphorylation of Ser-1284 on GluN2B is responsible for the spinophilin-dependent decrease in calcium influx through the channel. For this purpose, we generated Ser-1284 phosphorylation-deficient (Ser to Ala) and phosphorylation-mimic (Ser to Asp) mutants of GluN2B and investigated the calcium influx through the mutant isoforms in the presence or absence of WT spinophilin. For this purpose, Neuro2a cells were transfected with these different Ser-1284 point mutants of GluN2B along with WT GluN1 and GCaMP6s in the presence or absence of WT spinophilin overexpression (**Figure**

10E). Calcium influx through the receptors was measured similar to the previous experiment; however, the calculated AUC in each trial was further normalized to the WT-GluN2B+GluN1+GCaMP6s condition in the same trial to limit inter-trial variability. Statistical analyses were done using a Two-way ANOVA. Interestingly, quantified data revealed a significant effect of spinophilin expression (***F (1, 111) = 25.92, ****P<0.0001)*** and a significant effect of GluN2B mutation (***F (2, 111) = 13.65, ****P<0.0001***), but no significant interaction (***F (2, 111) = 0.1553, P=0.8564***). Multiple comparisons of the GluN2B isoforms using Bonferroni correction revealed a significant increase in the calcium influx through S1284D (***P<0.05***) but no effect of S1284A on calcium influx (***P=0.4688***) compared to WT-GluN2B in the absence of spinophilin. This suggests that phosphorylation of GluN2B on Ser-1284 enhances calcium influx through the channel (**Figure 10F**). However, overexpression of spinophilin in all conditions, significantly decreased the calcium influx to almost the same extent (***WT-GluN2B *P<0.05; S1284A *P<0.05; S1284D **P<0.01***) (**Figure 10F**). While spinophilin-dependent increases in Ser-1284 phosphorylation would be predicted to increase calcium influx through the channel, our data show that spinophilin decreases calcium influx through a pathway independent of its ability to regulate Ser-1284 phosphorylation.

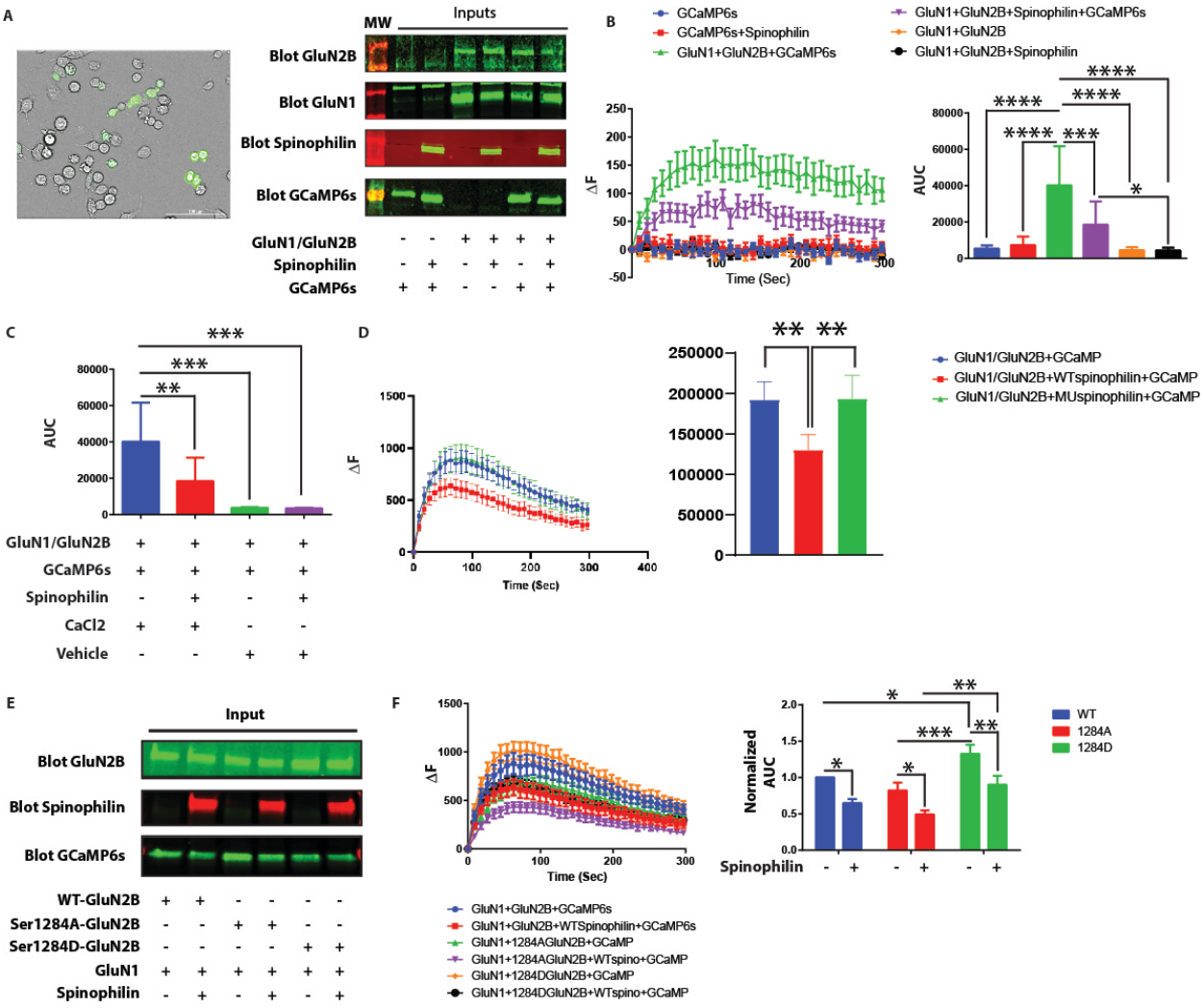

Figure 10 Spinophilin decreases NMDAR-dependent calcium influx in Neuro2a cells independent of Ser-1284 phosphorylation. 10A: Brightfield and fluorescence imaging of Neuro2a cells transfected with GCaMP6s along with GluN1 and GluN2B (Left). Representative western blotting results indicating the transfection conditions and efficiency in the Neuro2a cells (Right). **10B**: Normalized-to-baseline fluorescence values at each time point with 9 s intervals after addition of CaCl2 to the transfected Neuro2a cells (Left) and the quantified AUC of the figure indicating the total changes in the fluorescence level in each condition (Right). n=12 sets of transfections. **10C**: Quantified AUC of the GluN1+GluN2B with/without WT-spinophilin overexpression treated with CaCl2 or vehicle. n=12 sets of transfections **10D**: Normalized-to-baseline fluorescence values at each time point with 9 s intervals after addition of CaCl2 to the GluN1+GluN2B transfected Neuro2a cells in the absence and presence of WT and/or F451A MU spinophilin (Left) and the quantified AUC of the figure indicating the total changes in the fluorescence level in each condition (Right). The blue and green columns represent the same data as the blue columns in 9F (Right). n=20 sets of transfections. **10E**: Representative western blot indicating the transfection conditions and efficiency in the Neuro2a cells transfected with different genotypes of GluN2B in the presence and absence of WT-spinophilin overexpression. **10F**: Normalized-to-baseline fluorescence values at each time point with 9 s intervals after addition of CaCl2 to the Neuro2a cells transfected with different genotypes of GluN2B along with GluN1 in the absence and presence of WT-spinophilin (Left) and the quantified AUC of the figure indicating the total changes in the fluorescence level in each condition (Right) n=20 sets of transfections. *P<0.05. **P<0.01, ***P<0.001, ****P<0.0001, All the other comparisons are not significant.

3.4.2 Spinophilin-Dependent Changes In Calcium Influx Through GluN2B Containing NMDARS Is Partly Due To Changes In NMDAR Trafficking And Surface Expression

As stated above, overexpression of spinophilin along with GluN1 and GluN2B significantly decreased NMDAR-dependent calcium influx independent of Ser-1284 phosphorylation status. However, whether this effect of spinophilin is due to modulating NMDAR surface expression is unclear. To begin to investigate this question, surface biotinylation was used to quantify the surface expression of the GluN1 and GluN2B subunits in presence and absence of spinophilin (**Figure 11A**). Overexpression of spinophilin significantly decreased surface expression of the GluN2B subunit (**Figure 11C**) (***P<0.05***) but had no significant effect on the surface expression of the GluN1 subunit (**Figure 11B**). These experiments were performed without GCaMP6s overexpression. However, since the spinophilin dependent decrease in calcium influx though GluN2B containing NMDARs was performed in the presence of GCaMP6s overexpression, the biotinylation experiment was repeated with GCaMP6s overexpression to ensure that these changes were not due to potential buffering or modulation of calcium binding to the fluorescent protein. Again, the results reveal a significant reduction in the surface expression of GluN2B (**Figure 11E**) (****P<0.01***) but not GluN1 (**Figure 11D**) in the presence of overexpressed spinophilin in Neuro2a cells. These results suggest that the spinophilin dependent reduction in calcium influx is in part driven by enhanced internalization of GluN2B-containing NMDARs, but not GluN1 homomers, as there was no effect of total GluN1 surface expression (see Discussion).

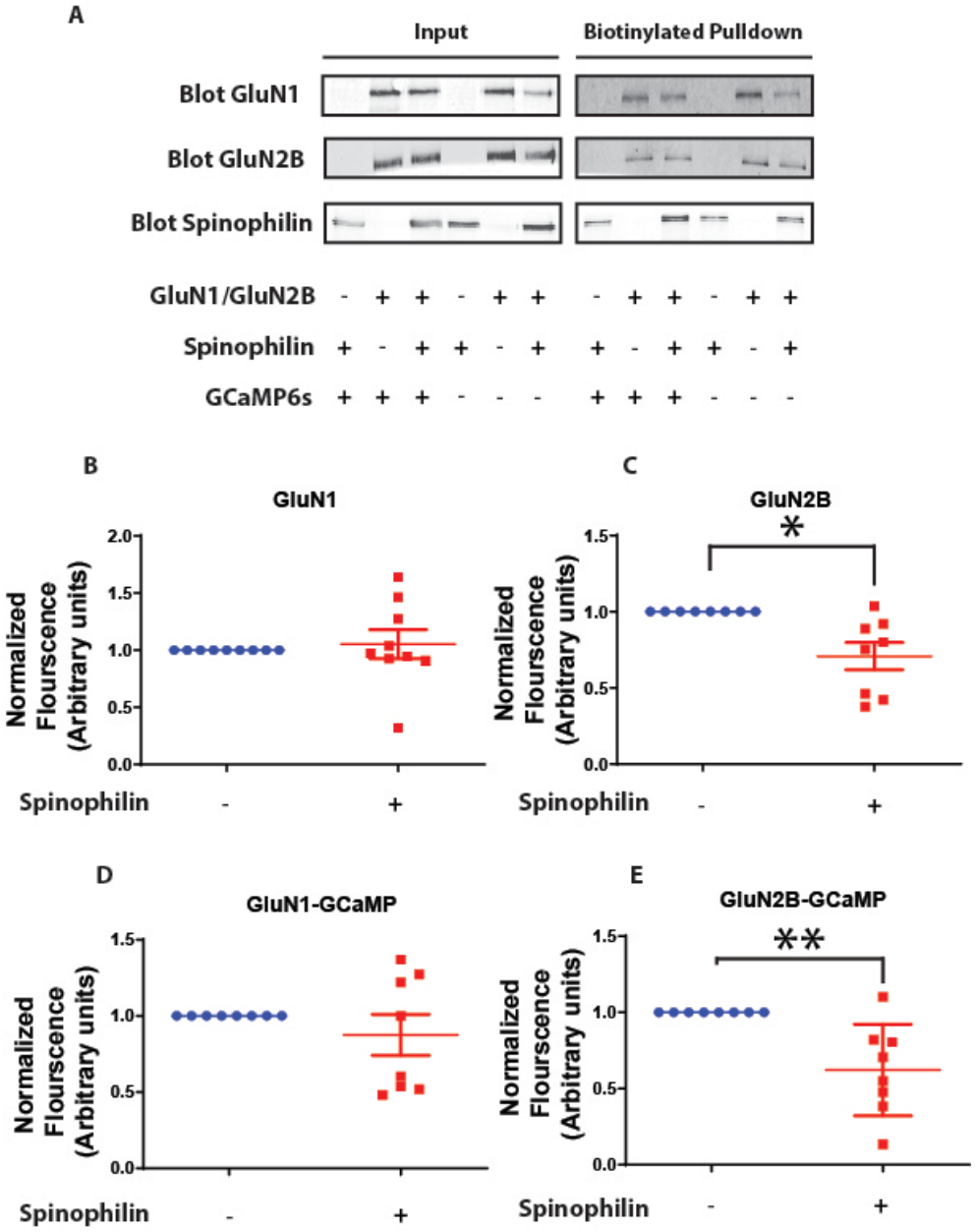

Figure 11. Spinophilin-dependent changes in GluN1 and GluN2B surface expression. 11A: Representative western blots indicting the transfection conditions and biotinylation efficiency in the Neuro2a cells. **11B**: Quantified data of GluN1 surface expression in the presence or absence of WT-spinophilin overexpression with no GCaMP6s overexpression throughout the conditions. **11C**: Quantified data of GluN2B subunit surface expression in the presence or absence of WT-spinophilin overexpression with no GCaMP6s overexpression throughout the conditions. **11D**: Quantified data of GluN1 surface expression in the presence or absence of WT-spinophilin overexpression with GCaMP6s overexpression throughout the conditions. **11E**: Quantified data of GluN2B subunit surface expression in the presence or absence of WT-spinophilin overexpression while GCaMP6s was overexpressed throughout the conditions. n=8-9 sets of transfection. *P<0.05, **P<0.01, all the other comparisons are not significant.

3.4.3 Ser-1284 Phosphorylation Regulates GluN2B Surface Expression In An Activity-Dependent Manner

As we showed above, spinophilin decreases surface expression of the GluN2B subunit of NMDARs (**Figure 11C**) which could explain the spinophilin-dependent decrease in the GCaMP6s signaling in Neuro2a cells (**Figure 10B**). We also showed that the Ser-1284 phosphorylation-mimic mutant, S1284D, has an enhanced calcium influx compared to WT (**Figure 10F**). However, it is not clear whether Ser-1284 phosphorylation modulates GluN2B surface expression or is altering channel activity *per se*. To investigate this, Neuro2a cells were transfected with WT, S1284A and S1284D mutant GluN2B DNA constructs along with WT GluN1 in the presence or absence of WT-spinophilin overexpression (**Figure 12A**).

After transfection, the cells were incubated for 16-24 hours in the presence of AP5. The next day, AP5 was washed off and surface biotinylation was performed. After biotinylation, the samples were separated by SDS-PAGE and the intensity of GluN1 or GluN2B in the biotinylated pulldown (PD) was normalized to input intensity. The quantified ratios were then analyzed using a Two-way ANOVA and a Sidak posthoc test for multiple comparisons. The results reveal a very significant effect of spinophilin expression (***F (1, 51) = 22.36, ****P<0.0001***) and a trend for a significant effect of GluN2B mutation (***F (2, 51) = 3.034, P=0.0569***) with no significant interaction (***F (2, 51) = 0.5628, P=0.5731***). Furthermore, Two-way ANOVA test revealed no significant effect of spinophilin expression (***F (1, 54) = 0.005796, P=0.9396***) on GluN1 surface expression. While the Two-way ANOVA results shows a significant effect of GluN2B mutation on GluN1 surface expression (***F (2, 54) = 3.372, P=0.0417***), the multiple comparisons test using Tukey's test, reveal no significant difference in the GluN1 surface expression across the different GluN2B mutations (**Figure 12C**). By post-hoc analysis, we did not detect any significant changes in the surface expression of S1284A compared to the WT-GluN2B (**Figure 12B**). However, there was a significant decrease in the surface expression of S1284D mutant (**Figure 12B**) (***P<0.05***). Our previous data investigating the changes in GCaMP6s fluorescence in S1284D containing NMDARs (**Figure 10F**) showed a significant increase in the calcium influx compared to the WT-GluN2B. Consequently, we hypothesize that reduction in the surface expression of S1284D is an activity-dependent, compensatory mechanism against enhanced calcium influx though S1284D containing channels. To test this hypothesis, we transfected the Neuro2a cells with WT or S1284D GluN2B with AP5 to block the channels (**Figure 12D**) as before. However, the next day, we

performed all the biotinylation procedures with media containing AP5 to block the NMDAR activity during the biotinylation process unlike our previous biotinylation experiments. The quantified data demonstrate no change in the surface expression of S1284D compared to WT GluN2B when AP5 is present throughout the experiment (**Figure 12E**). Together, these results suggest that Ser-1284 phosphorylation can decrease the surface expression of the GluN2B containing NMDARs in an activity dependent manner.

Furthermore, our results indicate that overexpression of spinophilin can decrease the surface expression of the GluN2B-containing NMDA receptors independent of Ser-1284 phosphorylation status suggesting that spinophilin driven decreases in surface expression are independent of Ser-1284 phosphorylation (**WT-GluN2B **$P<0.01$; Ser-1284A GluN2B *$P<0.05$**).

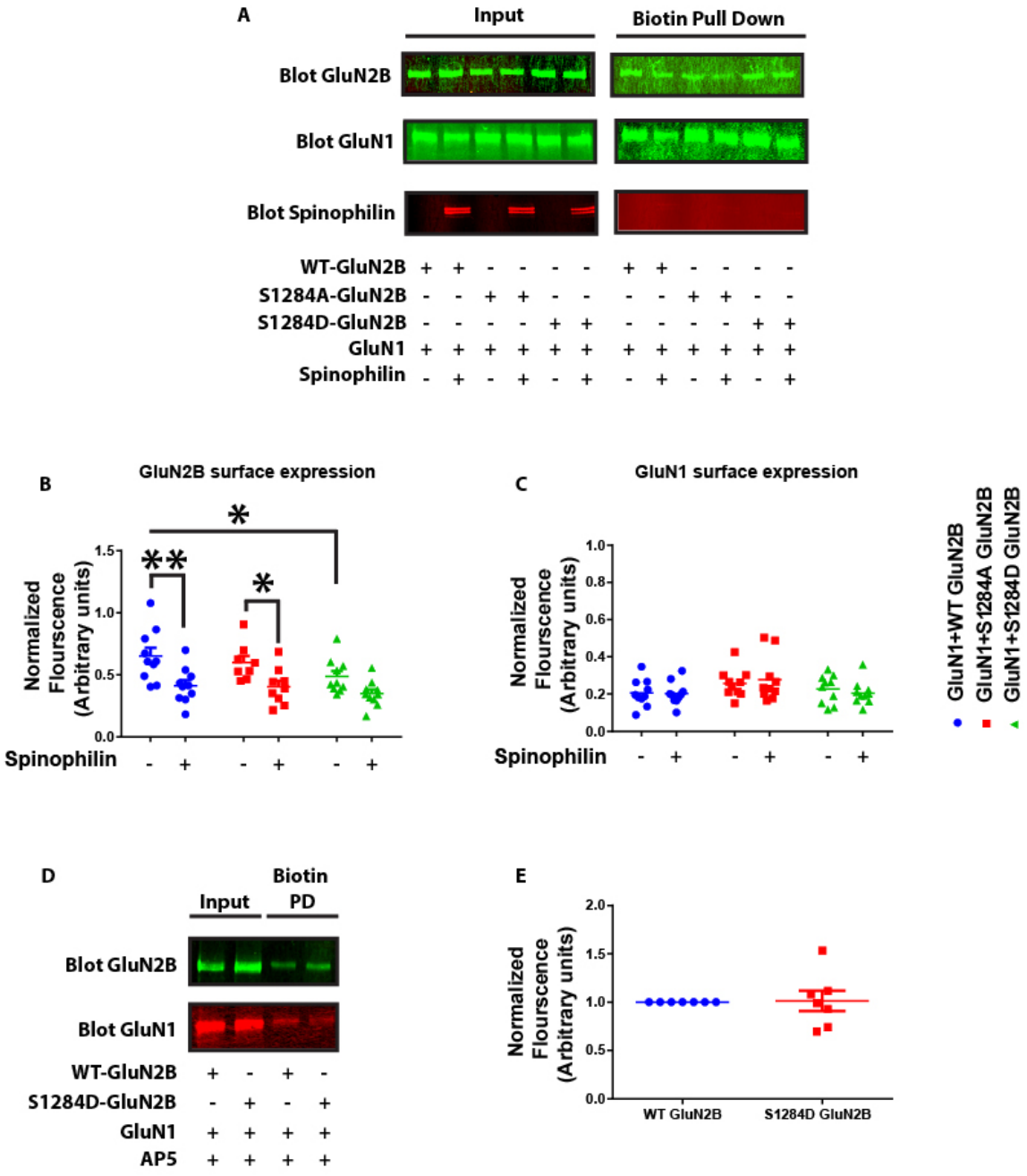

Figure 12. Surface expression of WT, S1284A and S1284D mutant GluN2B containing NMDA receptors. 12A: Representative western blots indicating the transfections and biotinylation conditions and efficiency. **12B**: Quantified data indicating the surface expression of WT, S1284A, and S1284D mutant GluN2B, in the presence or absence of overexpressed WT-spinophilin. n=10 sets of transfections. **12C**: Quantified data indicating the surface expression of GluN1 when co-expressed with WT, S1284A and S1284D mutant GluN2B, in the presence and absence of overexpressed WT-spinophilin. n=10 sets of transfections. **12D**: Representative western blots indicating the transfection and biotinylation efficiency of WT and/or S1284D GluN2B in the presence and absence of AP5 application throughout the biotinylation procedure. n=7 sets of transfections. **12E**: Quantified data of the surface expression of WT and S1284D mutant GluN2B, in the presence of AP5 application during biotinylation n=7. *P<0.05, **P<0.01, All the other comparisons are not significant.

3.4.4 Surface Expression Of GluN2B Subunit Of NMDARs And GluA2 Subunit Of AMPARs Is Altered In The Hippocampus Of P28 Spinophilin KO Animals

Our data demonstrate modulation of NMDAR surface expression by spinophilin in a heterologous cell system; however, to explore the effects of spinophilin on NMDAR surface expression in brain tissue, we investigated surface expression of NMDAR subunits in the hippocampus of WT and spinophilin KO mice. Hippocampal slices were generated from WT and global spinophilin KO animals. Surface biotinylation was performed on these slices (**Figure 13A**). The results show a significant increase in the surface expression of the GluN2B subunit of the NMDAR (**Figure 13D**) (***P<0.05***) but no significant change in the surface expression of GluN1 (**Figure 13B**) or GluN2A (**Figure 13C**). An increased surface expression of GluN2B in spinophilin KO mice is consistent with the decreased surface expression of GluN2B upon overexpression of spinophilin in the Neuro2a cells.

We also investigated surface expression of the calcium-impermeable GluA2 subunit of the AMPAR (Man, 2011) given its role in regulating calcium permeability and trafficking of AMPARs. Interestingly, our results show a significant increase in the surface expression of GluA2 in the spinophilin KO hippocampi (**Figure 13E**) (***P<0.05***) suggesting a potential role of spinophilin in regulating both AMPAR and NMDAR trafficking.

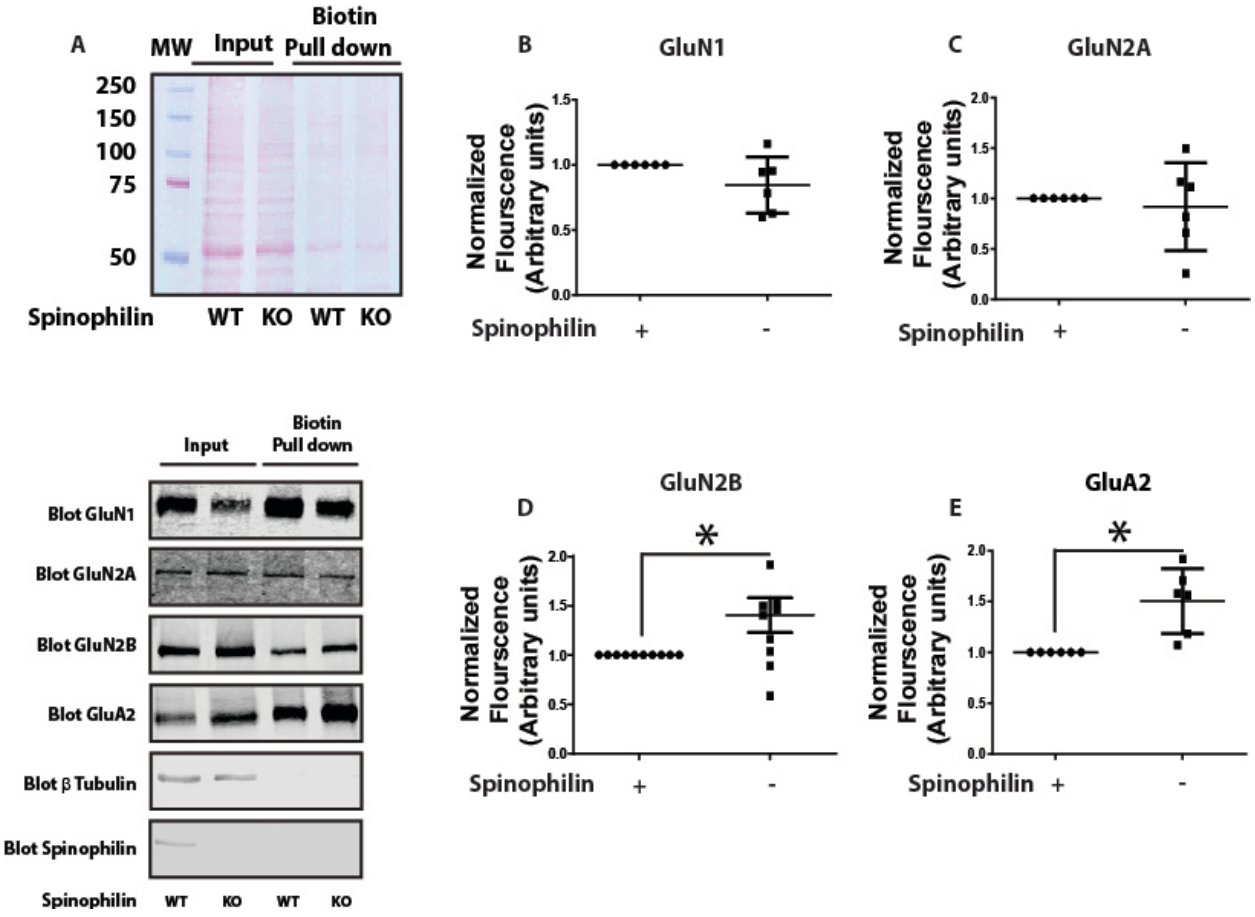

Figure 13 Surface expression of GluN2B subunit of NMDARs and GluA2 of AMPARs is altered in the hippocampus of spinophilin KO mouse brain. **13A**: Ponceau staining of the biotinylated inputs and pulldowns (Top). Western blotting of proteins of interest in the inputs and biotinylated pull downs. **13B**: Quantified data indicating a no significant change in the surface expression of GluN1 subunit. n=6. **13C**: Quantified data indicating a no significant change in the surface expression of GluN2A subunit. n=6. **13D**: Quantified data indicating a significant increase in the surface expression of GluN2B subunit. n=9. **13E**: Quantified data indicating a significant increase in the surface expression of GluA2 subunit of AMPARs. n=6. *P<0.05, All the other comparisons are not significant

3.4.5 The Subcellular Localization Of NMDAR Subunits Is Modified In P28 Spinophilin Global KO Mouse Hippocampus

Above, we found that spinophilin KO mice have enhanced GluN2B expression at the membrane; however, if this enhanced expression is due to decreased localization in non-synaptic membranes, is unclear. To detail if loss of spinophilin impacts NMDAR subcellular localization, we used a crude fractionation protocol (**Figure 14A**) to evaluate the levels of GluN1, GluN2A, GluN2B subunit of NMDARs in S2 (membrane-associated non-postsynaptic density (PSD)) and S3 (Synaptic, PSD) fraction of postnatal day (P) 28 hippocampus of spinophilin WT and KO mice (**Figure 14C**). To validate this crude fractionation, we also blotted our samples for GAPDH, an S1 (cytosolic) marker, mGluR5, an S2 marker, and PSD95, an S3 marker (**Figure 14B**). Our lab has previously shown that vesicle trafficking proteins, such as myosin Va, are observed in the S2 and S3 fraction, suggesting that both of these fractions may contain different vesicle pools in addition to plasma membrane proteins. Our results show a significant decrease of GluN1 in the S2 fraction (***P<0.05***) but no significant change in the S3 fraction (**Figure 14D**). GluN2A results show no significant change in the S2 fraction with a significant increase in the S3 fraction (***P<0.05***) (**Figure 14E**). Like GluN1, GluN2B expression was decreased in the S2 fraction (***P<0.05**) but had no significant change in S3 fraction (**Figure 14F**). These results show that global knockout of spinophilin alters subcellular localization of NMDA receptor subunits in P28 mouse hippocampus. Furthermore, GluN2B-containing NMDARs are less associated with the S2, potentially internalized fraction, whereas GluN2A-containing NMDARs are more associated with a synaptic fraction. Taken together with data in Figure 4, this suggests a more total expression of GluN2B-containing NMDARs on the surface, and equal GluN2A-containing NMDARs on the surface, but a redistribution of those receptors to the synaptic fraction.

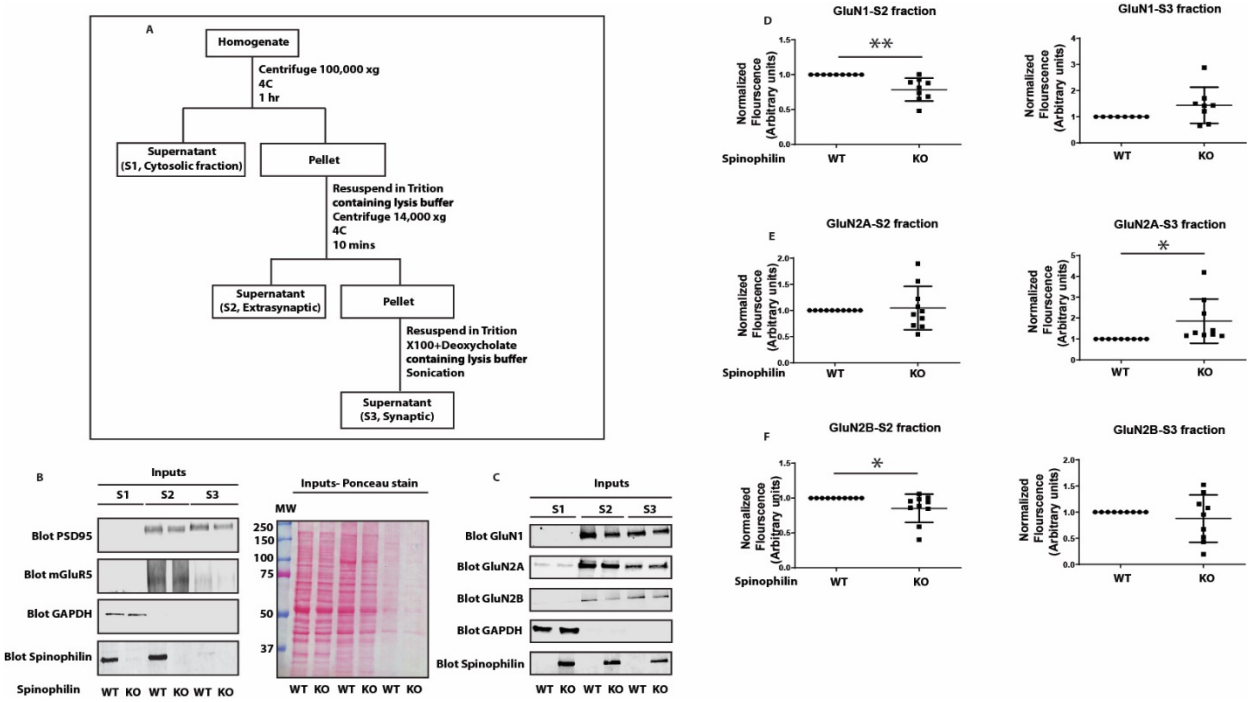

Figure 14. The subcellular localization of NMDAR subunits is modified in P28 spinophilin global KO mouse hippocampus. 14A: Crude fractionation protocol used to assess subcellular localization. **14B**: western blot indicating the control proteins in S1, S2 and S3 fraction (Left) and the total protein level in the ponceau staining (Right). **14C**: Western blot indicating the qualitative levels of luN1, GluN2A and GluN2B in the S1, S2 and S3 fraction. **14D**: Quantified data showing the level of subcellular localization of GluN1 in S2 (left) and S3 (Right) fraction. The results show a significant decrease of GluN1 in S2 fraction. n=9 . **14E**: Quantified data showing the level of subcellular localization of GluN2A in S2 (left) and S3 (Right) fraction. The results show a significant increase of GluN2A in S2 fraction. n=9. **14F**: Quantified data showing the level of subcellular localization of GluN2B in S2 (left) and S3 (Right) fraction. The results show a significant decrease of GluN2B in S2 fraction. n=9. *P<0.05. **P<0.01, All the other comparisons are not significant

3.4.6 Spinophilin KO Hippocampal Cultures Are More Susceptible To Activation Of Apoptotic Pathways

Overactivation of glutamate receptors, such as NMDARs by high levels of glutamate in the extracellular space can lead to neurotoxicity (Y. Liu et al., 2007; Rothman & Olney, 1995; Wu, Chen, Yang, Jiao, & Qiu, 2017). The subcellular localization of NMDAR subunits, specifically the GluN2B subunit, plays an important role in defining the downstream signaling pathways upon activation of NMDA receptor. Specifically, activation of synaptic GluN2B-containing NMDARs is tied to pro-survival pathways while activation of extrasynaptic GluN2B NMDARs is more linked to pro-death pathways (Forder & Tymianski, 2009; Hardingham & Bading, 2002, 2010; Hardingham et al., 2002). GluN2B-containing NMDARs, due to their high calcium permeability, have a pronounced role in promoting neurotoxicity (Aarts et al., 2002; Goldberg & Choi, 1993; Hardingham et al., 2002; Wyllie et al., 2013). Given our previous results showing the spinophilin-dependent decrease in the calcium influx of GluN2B containing NMDARs, as well as increased surface levels of the NMDAR in spinophilin KO mice, we hypothesized a neuroprotective role for spinophilin in excitotoxic conditions. To test this hypothesis, we cultured hippocampal primary neurons from global spinophilin WT and KO P0 (day of birth) mouse pups. These cells were then treated with bath application of 100 μM glutamate for 30 minutes to mimic glutamate toxicity and re-perfused with the original media for 90 minutes (**Figure 15A**). The cells were then lysed and separated by SDS-PAGE (**Figure 15B**). We found that the cleaved caspase 3 (CC3) to caspase 3 (C3) ratio is three times higher in the spinophilin KO cells compared to the WT cells (**Figure 15C**) (***P<0.05***). These results suggest that spinophilin KO neurons have more CC3 compared to WT neurons which can be due to more susceptibility to glutamate toxicity or basal increases in CC3 production. This suggests a potential neuro-protective role for spinophilin.

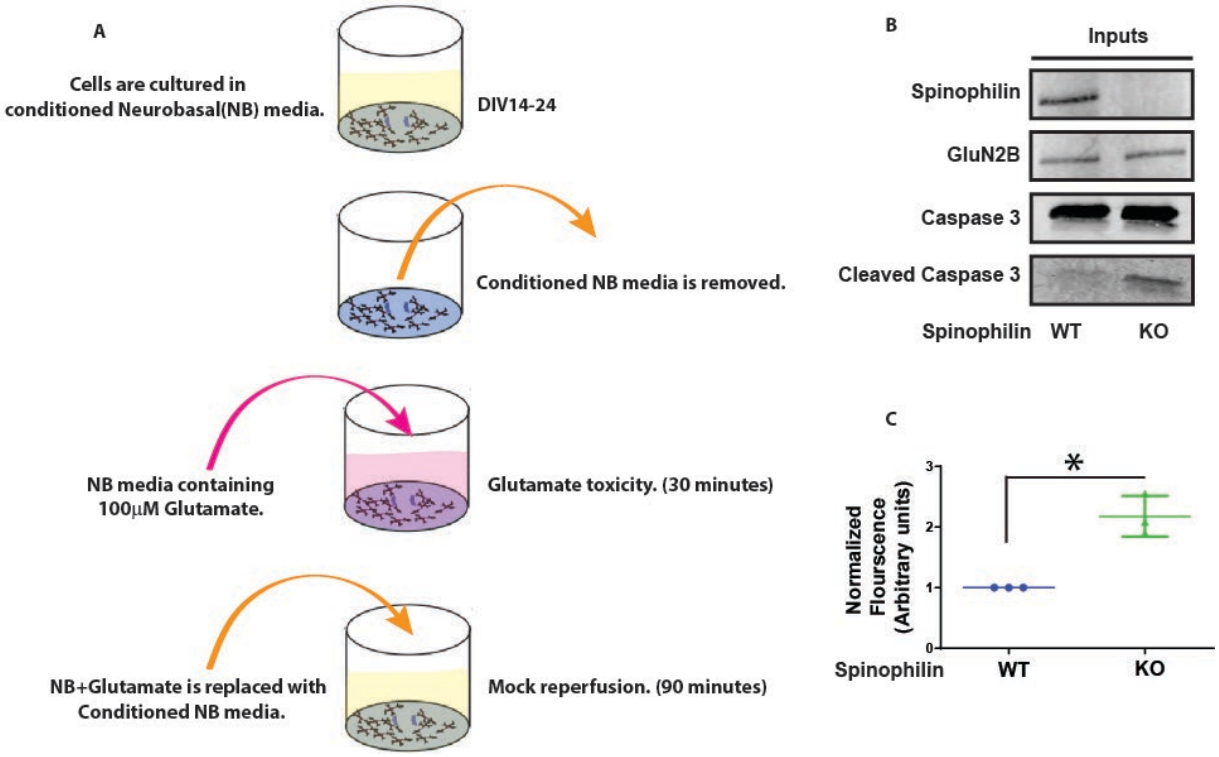

Figure 15. Spinophilin KO hippocampal cultures are more susceptible to activation of apoptotic pathways. 15A: The glutamate toxicity procedure. **15B**: Western blot data showing C3 and CC3 bands in the spinophilin WT and KO hippocampal cultures. **15C**: Quantified data indicating a significant increase in the CC3/C3 ratio in the KOs compared to the WT cells. n=3. *P<0.05

3.5 Discussion

Spinophilin is the most abundant PP1 binding protein in the PSD (Allen et al., 1997; Colbran et al., 1997). Through this interaction, spinophilin can modulate the phosphorylation state of various proteins by either targeting PP1 activity towards or inhibiting PP1 activity at various substrates. Spinophilin has been identified in NMDA receptor complexes and we have previously demonstrated that spinophilin interacts with the intracellular tail region of the GluN2B subunit (Salek et al., 2019). Spinophilin has been shown to modulate the activity of NMDARs such that inhibition of PP1 in the presence, but not absence, of spinophilin increases NMDAR currents (Feng et al., 2000). Previous studies investigating the effect of spinophilin on NMDAR function, have not evaluated the mechanisms by which spinophilin impacts channel function. Therefore, how spinophilin regulates calcium influx through the NMDA receptor is not clear. Here, we investigated the spinophilin-dependent changes in calcium influx through GluN2B-containing NMDA receptors in heterologous cell system. Our data indicate that the total amount of intracellular calcium upon addition of CaCl2 is decreased when spinophilin is co-transfected with GluN2B-containing NMDARs in Neuro2a cells compared to transfection with the NMDARs alone. This observation can be explained in two possible ways: 1) Spinophilin is decreasing the channel conductance to calcium and/or 2) spinophilin is decreasing surface expression of the receptor. The receptor surface expression was tested by quantification of surface expressed GluN2B subunits in presence and absence of spinophilin. Surface biotinylation reveals that spinophilin overexpression significantly decreases the surface expression of GluN2B but not GluN1, in Neuro2A cells. As GluN1 and GluN2B form a functional tetramer, it may be surprising that GluN1 was unchanged. While GluN1 homomeric channels may exist at the membrane , they lack the glutamate binding site that is present in the heteromeric channel (Furukawa et al., 2005). Therefore, our data suggest that spinophilin does not regulate GluN1 membrane trafficking but does regulate the trafficking of the heteromeric GluN1/GluN2B channel. Future studies will need to evaluate if spinophilin can regulate GluN1/GluN2A or other functional NMDA receptor subunits or if these effects are specific to GluN2B-containing NMDA receptors.

In addition to the in vitro effects of spinophilin, we observed increased surface expression of GluN2B in hippocampal slices isolated from global spinophilin KO animals compared to their WT control littermates. Moreover, consistent with a specific role for spinophilin on GluN2B-containing NMDAR surface expression, we observed no significant difference in GluN1 or

GluN2A surface expression. Together, these data suggest that the spinophilin-dependent decrease in the GluN2B-containing NMDAR calcium influx is in part due to spinophilin-dependent decreases in surface expression. However, as stated above, we cannot rule out the possibility of spinophilin modifying channel conductance to calcium.

We have previously shown that spinophilin modulates the phosphorylation state of Ser-1284 on GluN2B *in vitro* and *in vivo* (Salek et al., 2019). As a result, it is possible that the spinophilin-dependent decrease in calcium influx is due to spinophilin-dependent increases in Ser-1284 phosphorylation. While the non-phosphorylateable mutant S1284A, had no impact on calcium influx via the NMDA receptor, we found that the S1284D phosphorylation mutant enhanced calcium influx in the GluN2B-containing NMDAR transfected cells. Moreover, this increased calcium influx was not due to greater surface expression as this mutant had decreased surface expression compared to WT. These data suggest that our previously reported spinophilin-dependent increases in Ser-1284 phosphorylation, are not responsible for the spinophilin-dependent decreases in GluN2B surface expression. Consistent with this, overexpression of spinophilin decreases calcium influx to the same extent across the WT, S1284A, and S1284D GluN2B genotypes. Moreover, as S1284D enhances calcium influx concurrent with decreased GluN2B surface expression, these data suggest that 1284 phosphorylation enhances the calcium influx through the receptor. However, decrease in the surface expressed receptors is probably due to the greater channel function driving an activity-dependent internalization. Together, these data suggest that spinophilin can bidirectionally modulate calcium influx through NMDARs by 1) Enhancing the Ser-1284 phosphorylation which increases calcium influx through GluN2B-containing NMDARs and 2) Decreasing the GluN2B-NMDAR dependent calcium influx by decreasing surface expression of the channel through an unknown, activity- and Ser-1284 phosphorylation-independent pathway.

As stated above, our data suggest that spinophilin decreases surface expression of the receptor independent of Ser-1284 phosphorylation and possibly independent of NMDA receptor activity. This mechanism could involve clathrin-mediated endocytosis given that we have previously observed clathrin in spinophilin co-IPs (Watkins, True, Mosley, & Baucum, 2019) and GluN2B-containing NMDA receptors undergo clathrin-mediated endocytosis (Y. Wu et al., 2017). Moreover, alterations in vesicle trafficking could involve the motor protein, Myosin Va, since we have previously found that spinophilin and GluN2B interact with Myosin Va and others have

shown that myosin-Va associates with vesicles and is critical in AMPA receptor trafficking and function (Correia et al., 2008; Rudolf, Bittins, & Gerdes, 2011). Furthermore, in our previous study, we observed a decreased interaction of GluN2B with myosin Va in spinophilin KO mice (Salek et al., 2019), which when taken together with decreases in GluN2B in non-PSD membranes may suggest decreased association of GluN2B with synaptic vesicle membranes in spinophilin KO mice. Mechanistically, how spinophilin may promote association with proteins such as myosin Va, clathrin, or others to enhance GluN2B internalization is unclear. While we found spinophilin regulates Ser-1284 phosphorylation, it appears as if changes in GluN2B internalization is not through modulation of GluN2B at this site. Moreover, we previously found that other sites on GluN2B, such as Ser-929/930, Ser-1050, and Ser-1303 were not regulated by PP1 and spinophilin (Salek et al., 2019). However, additional sites on GluN2B could modulate interactions with vesicle trafficking proteins. For instance, previous studies have found that phosphorylation at Ser-1323 on GluN2B can enhance NMDA currents; however, if it modulates NMDA receptor trafficking is unclear (Liao et al., 2001). Additionally, Ser-1480 which is a PP1 site within the PDZ ligand and maintains GluN2B at extrasynaptic sites in the membrane, may modulate interactions with vesicle trafficking proteins. However, if spinophilin modulates Ser-1323 or Ser-1480 phosphorylation is unknown. In addition to GluN2B, spinophilin may impact vesicle trafficking protein phosphorylation which could modulate how these proteins interact with GluN2B. Therefore, future studies need to delineate if spinophilin specifically modulates GluN2B targeting to endocytic vesicles and the mechanisms by which it does this.

Excessive calcium influx specifically through NMDA receptors and more specifically through GluN2B-containing NMDARs during glutamate toxicity plays an important role in activation of apoptotic pathways. Here, we observed that spinophilin can increase GluN2B activity via increasing Ser-1284 phosphorylation. Of note, excessive activation of GluN2B containing NMDA receptors led to a rapid activity-dependent internalization of the receptor. Moreover, spinophilin overexpression also decreased GluN2B surface expression independent of Ser-1284 phosphorylation. Moreover, spinophilin KO mice had greater GluN2B surface expression, which would be predicted to increase calcium influx through GluN2B containing NMDARs. Given that excessive calcium influx is neurotoxic and that spinophilin can decrease the calcium influx through GluN2B containing NMDARs, we hypothesized that spinophilin may play a neuroprotective role during conditions of excessive glutamate release. In addition, other groups have reported that the

phosphorylation of Ser-1284 is decreased by ischemia but increased during reperfusion. This observation taken together with our results showing that Ser-1284 phosphorylation enhances the calcium influx in the GluN2B expressing cells suggests a greater activity of the receptor during reperfusion (Ai et al., 2017; W. Lu et al., 2015). Consistent with this, reperfusion is associated with greater NMDA receptor activity and toxicity (D. Li, Shao, Vanden Hoek, & Brorson, 2007; Wei, Fiskum, Rosenthal, & Perry, 1997; Werling, Jacocks, Rosenthal, & Fiskum, 1993). To test this hypothesis, we simulated glutamate toxicity in primary hippocampal cultures obtained from spinophilin WT and KO mouse pups. Following exposure to glutamate, we quantified the level of CC3 to C3 ratio across WT and KO neurons. Interestingly, we observed a three-fold increase in the CC3/C3 ratio in the KOs compared to the WTs. These data suggest that cultured spinophilin KO hippocampal neurons are more susceptible to caspase cleavage (**Figure 16**), potentially because of greater GluN2B-containing NMDA receptor surface expression and activity. One important question to answer here is to investigate whether spinophilin KOs basally have more CC3 or this enhanced CC3 level is solely due to high glutamate conditions. If the former is the case, it may suggest that the spinophilin KOs are more susceptible to apoptosis in general. This may explain the fact that spinophilin KO mice have smaller hippocampi compared to WT animals (Allen et al., 1997). However, whether this susceptibility in the KOs is due to excessive GluN2B activity, is not known. Future studies delineating the specific mechanism of increased caspase production in spinophilin KO mice as well as studies performing ex-vivo and in-vivo models of OGD and ischemia need to detail the mechanistic and functional roles of spinophilin on apoptosis.

In addition to membrane expression of GluN2B-containing NMDA receptors, previous studies have shown that channel localization is important in determining whether GluN2B is neuroprotective or neurotoxic during ischemic insult. Specifically, activation of synaptic GluN2B containing NMDARs triggers pro-survival pathways whilst activation of extrasynaptic receptors activates more pro-death pathways (Hardingham & Bading, 2002, 2010; Hardingham et al., 2002). In our crude subcellular fractionation results, we found that there is a decrease in the localization of GluN2B in the extrasynaptic fraction with no significant change in the synaptic fraction. Activation of extrasynaptic GluN2B receptors is associated with pro-survival pathways, which is the opposite of our observations with the caspase data which show that the spinophilin KO hippocampal cultures are more susceptible to caspase 3 cleavage, a marker of apoptosis. However, as we performed a crude fractionation, this fraction also includes synaptic vesicle membranes and

therefore, this decrease may be due to decreases in glutamate receptors on internalized vesicles rather than extrasynaptic GluN2B receptors. Future studies will require more sensitive high-resolution microscopy or biochemical analyses to detail how spinophilin regulates GluN2B localization in specific subcellular fractions.

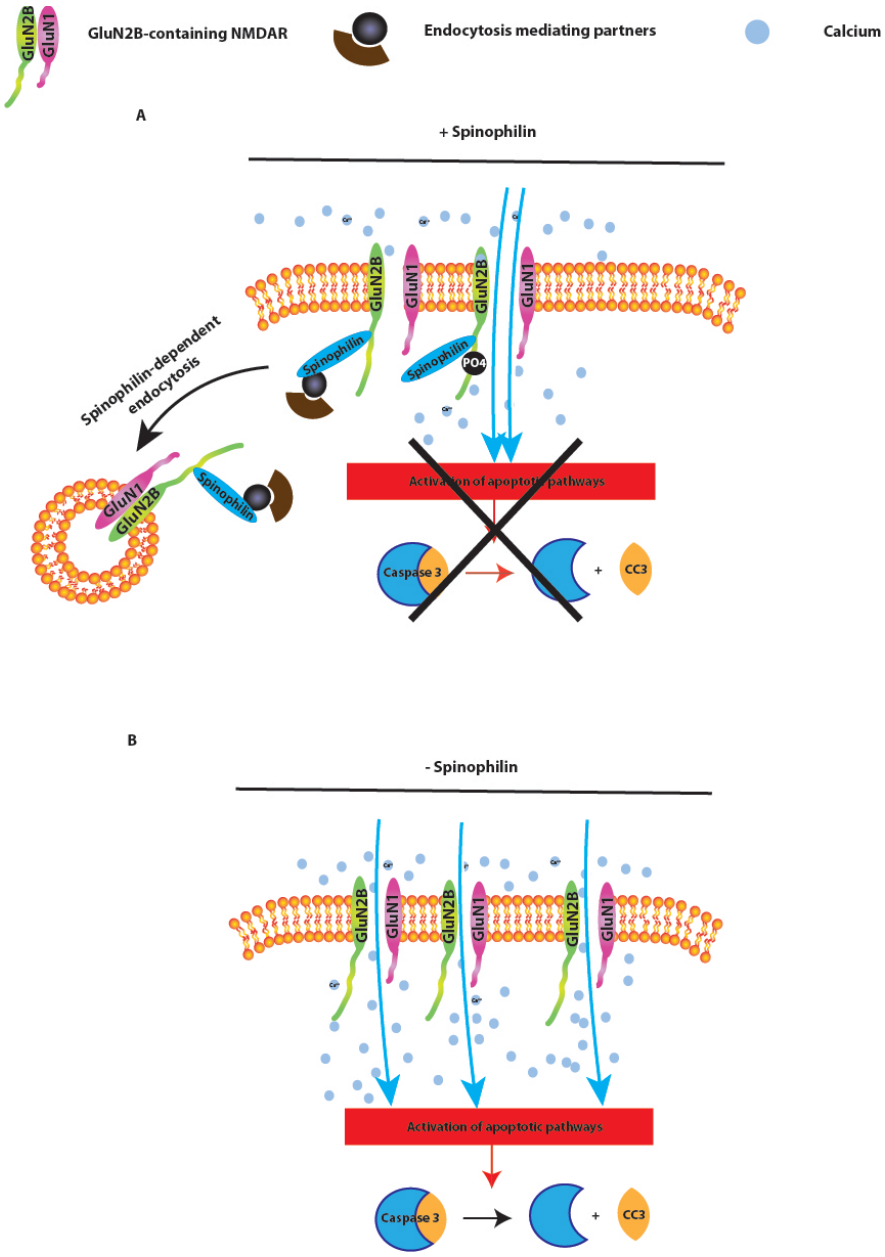

Figure 16. Schema indicating proposed model of spinophilin-dependent regulation of GluN2B-containing NMDA receptor-dependent calcium influx. 16A: Spinophilin increases the phosphorylation of Ser-1284 on GluN2B, thereby enhancing calcium influx through the GluN2B containing NMDARs. In contrast, spinophilin limits GluN2B-containing surface expression putatively due to modulation of GluN2B interactions with endocytotic proteins. Since the second effect of spinophilin occurs independent of the first, we observe an overall decrease in calcium influx through GluN2B containing NMDARs when spinophilin is present. This low, basal calcium influx is less likely to be promote calcium-dependent activation of caspase and downstream apoptotic pathways. **16B**: In the absence of spinophilin, the spinophilin-driven internalization of the receptors is decreased, more receptors are expressed on the surface and calcium influx into the cell is increased. This high levels of intracellular calcium triggers apoptotic pathways leading to cell death. This impact may be more dramatic in cells with high expression of GluN2B-containing NMDA receptors.

3.6 Summary

Together, our data demonstrate that spinophilin can biphasically regulate calcium influx through GluN2B containing NMDARs, by increasing Ser-1284 phosphorylation and also decreasing GluN2B surface expression independent of Ser-1284 phosphorylation. Spinophilin-dependent regulation of GluN2B surface expression may be responsible for increases in cleaved caspase 3 observed in the spinophilin KO hippocampal primary neurons subjected to glutamate toxicity compare to WT neurons. Therefore, spinophilin may be neuroprotective in excitotoxic conditions such as ischemic stroke (**Figure 16**).

CHAPTER 4. THE IMPACT OF LOSS OF SPINOPHILIN ON HIPPOCAMPAL-DEPENDENT LEARNING AND MEMORY

4.1 Abstract

Neuronal plasticity, which includes modifications in dendritic spine morphology and density, is a key mechanism underlying learning and memory. Spinophilin is an actin- and PP1-binding and scaffolding protein present in the PSD and is required for coordination of spine dynamics by modulating F-actin bundling in addition to anchoring PP1 to PSD members such as NMDARs and AMPARs. Given this background, and the important role of spine dynamics and AMPAR and NMDAR function in neuronal plasticity, spinophilin may be a prominent candidate in mediating hippocampal plasticity and behaviors associated with hippocampal-dependent learning and memory. Here, using spinophilin WT and global KO mice, we investigated the role of spinophilin in tasks involving learning and memory, such as novel object recognition (NOR), novel location recognition (NLR), Morris Water Maze (MWM), and reversal learning in the MWM (rMWM). Our results suggest that while the spinophilin WT and KO animals do not reveal any significant difference in NOR and NLR tests, spinophilin KOs actually have a non-significant deficit in the NOR task and increase in learning a MWM task. Moreover, spinophilin KOs have deficits in the rMWM, potentially suggesting perseveration on this spatial reversal learning task.

4.2 Introduction

Changes in the number or size and shape of dendritic spines are strongly associated with learning (Horn, Bradley, & McCabe, 1985; Moser, Trommald, & Andersen, 1994) as well as developmental (Boyer, Schikorski, & Stevens, 1998), electrophysiological, (Calverley & Jones, 1990; Lisman & Harris, 1993) and hormonal (D. D. Murphy & Segal, 1996) alterations. Since actin is the most important cytoskeletal component of spines (Schubert & Dotti, 2007), actin binding proteins are strong candidates in mediating actin crosslinking and thus spine morphology. Consequently, spinophilin, a major actin binding protein residing in the dendritic spines (Allen et al., 2006), is a putative key spine regulator linking learning/memory to alterations in spine properties. Moreover, spinophilin plays an important role in recruiting Rho family GTPases in

reorganizing the actin network (Ryan et al., 2005) which strengthens its candidacy to play a key role in defining spine morphology.

Previous studies investigating the role of spinophilin in brain morphology found that spinophilin KO mice have smaller hippocampi (Feng et al., 2000). Moreover, postnatal day (P) 15 spinophilin KO mice have been shown to have significantly higher spine density. In addition, filopodia and spine like protrusions in hippocampal primary cultures have been shown to start earlier in spinophilin KO cells and are much larger in number (Feng et al., 2000).

Furthermore, spinophilin recruits Asef2, an important mediator of spine density and morphology, to the spines following NMDAR activation (Evans et al., 2015) in hippocampal cultures. This recruitment eventually results in activation of Rac, a Rho-GTPase associated with actin reorganization. Interestingly, disruption of this Spinohpilin-Asef2-Rac pathway disrupts spine and synapse formation (Evans et al., 2015).

This background provides strong evidence for spinophilin candidacy in mediating spine morphology and thus neuronal plasticity and hippocampal-dependent behaviors associated with this plasticity. Besides mediating spine morphology by regulating actin dynamics, spinophilin can also mediate plasticity by anchoring PP1 to various PSD members important for plasticity such as AMPARs, NMDARs, and CaMKII (Blank et al., 1997; Strack, Choi, Lovinger, & Colbran, 1997; Y. T. Wang & Salter, 1994; Yan et al., 1999).

Besides spinophilin, NMDARs have been long implicated in neuronal plasticity. For example, LTP strongly depends on calcium influx through NMDARs at specific synapses and the subsequent activation of CaMKII (Stein et al., 2014). Specifically, GluN2B containing NMDARs have been shown to be important in mediating learning and memory, such that selective blockade of GluN2B-containing NMDARs after acute stress promotes memory as measured in novel object and novel object-place recognition tests (Howland & Cazakoff, 2010; Wong et al., 2007; Yang, Huang, & Hsu, 2005) and that mutation in the GluN2B subunit of NMDARs can cause deficits in the Morris Water Maze (MWM) spatial learning task (Stein et al., 2014).

We have shown in the previous chapters that spinophilin interacts with GluN2B subunit of NMDARs and can modulate its phosphorylation, calcium influx, surface expression and interactome (Baucum et al., 2013; Salek et al., 2019). Given this background and that both spinophilin and GluN2B-containing NMDARs are implicated in learning and memory, here we investigate the effect of spinophilin global KO on learning and memory tasks that require GluN2B-

containing NMDAR activity such as novel object recognition (NOR), novel location recognition (NLR) and MWM.

4.3 Material and Methods

The following equipment/materials were used: Phenotyper cages (Noldus Information Technology, Wageningen, Netherlands), Ethovision XT video tracking software (Noldus Information Technology), Toys (Spark Create Imagine), 120 cm MWM pool (Maze engineers, Cambridge, MA), Heater (Maze engineers), Platform (30cm, Maze engineers), Gantry (Maze engineers), Color camera (Noldus Information Technology), Crayola washable paint powder (white, nontoxic).

4.3.1 Animals

Experiments were approved by the School of Science Institutional Animal Care and Use Committee (SC270R, SC310R) and performed in accordance with the Guide for the Care and Use of Laboratory Animals and under the oversight of Indiana University-Purdue University, Indianapolis (IUPUI). Animals were provided food and water ad libitum and were housed on a 12-hour light/dark cycle. Spinophilin KO mice on a C57Bl/6J backround were initially purchased from Jackson Laboratories (Bar Harbor, ME, USA; Stock #018609; RRID: MMRRC_049172-UCD) and a breeding colony has been maintained at IUPUI. This colony is backcrossed ~every 6 months with WT C57Bl/6J mice. WT and knockout (KO) littermates were used (WT and KO animals were from heterozygote x heterozygote breeding pairs). Animals were weaned ~ P21. Animals were group housed until the genotyping was completed ~ P23. At ~P23, male or female, spinophilin KO mice or WT littermates were singly housed throughout the behavior studies. The habituation was initiated on ~P23 and the behavior studies were performed every day until P35. The cages were changed and cleaned once per week with caution in order to minimize stressing the animals. After the testing was completed, the animals were euthanized by decapitation without anesthesia and the brains were used for further analysis. All the experiments were performed between 11AM and 6PM.

4.3.2 Novel Object Recognition (NOR) And Novel Location Recognition (NLR) Tests

4.3.2.1 Object And Location Setting

The objects were odorless plastic baby toys. The toys had no sharp edges. The toys had different shapes and shades of color. Since the toys were lightweight, they were filled with cement and allowed to completely dry before use so they cannot be moved by the mice (**Figure 17A**). Testing arena is a square space (Phenotyper cages, dimensions: 30 x 30 cm) in which all the animal behavior is monitored by a built-in camera in the cage lid. The arena consists of the floor of the phenotyper cage (**Figure 17B**).

Testing zones are the rectangular space designated around each object. The locations of the zones are designed to have the same distance from the corners and the walls (**Figure 17C**). During the testing session, the software records the cumulative duration of time that the animal's nose point is in each zone or outside of the zones. After the test, the number of entrances (frequency) and the cumulative duration of the times that animal's nose point was in the zones are quantified using the software and are used as an index to study time and frequency of exploration of the novel and familiar object or location. After each use of the Phenotyper cage, the cage is sprayed and wiped down with 70% ethanol to eliminate any potential odor or residuals from the previous animal.

4.3.2.2 Habituation

The animals were habituated to the environment for three consecutive days, 15 minutes per day. During the habituation session, each animal was placed in the clean and empty Phenotyper cage and allowed to explore for 15 minutes (**Figure 17C**). After 15 minutes, the animal was gently removed from the cage and replaced in the home cage. The cage was sprayed and wiped down with 70% ethanol.

4.3.2.2 Familiarization

Two identical objects (parrots, hippos, or giraffes) were placed in the designated zones. The objects had the same distance from the walls and corners. The animals were then placed into the arena and were allowed to familiarize with the objects for 20 minutes (**Figure 17D**).

4.3.2.3 Acquisition

After acquisition, the animals were returned to their home cage. The testing was performed at two different time points: 30 mins post acquisition to explore short-term memory and 24 hours post acquisition to explore long-term memory.

4.3.2.4 Testing

Following the habituation and familiarization phase, two different testing paradigms were used: NLR and NOR

4.3.2.4.1 Novel Location Recognition-30 minutes

30 minutes post familiarization, the NLR test was performed. At the time of testing, the location of one of the familiar objects was changed. The animal was then placed in the Phenotyper cage and was allowed to explore for 5 minutes (**Figure 17E**). After the 5 minutes, the animal was returned to the home cage and allowed to recover for 5 minutes. After the test, the cumulative duration of the times in which the nose point was in the boundaries of familiar object and novel object zones and the frequency of entries to them was measured using Ethovision software.

4.3.2.4.2 Novel Object Recognition-30 minutes

While the animal was recovering in the home cage after the NLR test, the Phenotyper cage was set up for the NOR test. For NOR, one of the objects of the familiarization phase (**Figure 17D**) was replaced with a novel object (parrot, hippo, or giraffe) (**Figure 17F**). The animal was then placed in the cage and was allowed to explore for 5 minutes. After the test, the cumulative duration of the times in which the nose point was in the boundaries of the familiar object and novel object zones and the frequency of entries into each zone was measured using Ethovision software.

4.3.2.4.3 Novel Location Recognition-24 hours

24 hours post familiarization, the NLR and NOR tests were performed. The procedures used were the same as NLR performed at 30 minutes post familiarization. However, the novel

location used in this test was different than the previously set up novel location (**Figure 17G**). After the test, the animal was returned to the home cage and allowed to recover for 5 minutes to prepare for the long-term NOR test.

4.3.2.4.4 Novel Object Recognition-24 hours

While the animal was recovering in the home cage after the NLR test, the cage was set up for NOR test. Again, the procedures were performed similar to the post-familiarization NOR test; however, the novel object used (elephant) was different from the novel object used last time (**Figure 17H**). After the test, the animals were returned to the home cage and were placed back in the regular housing room.

.

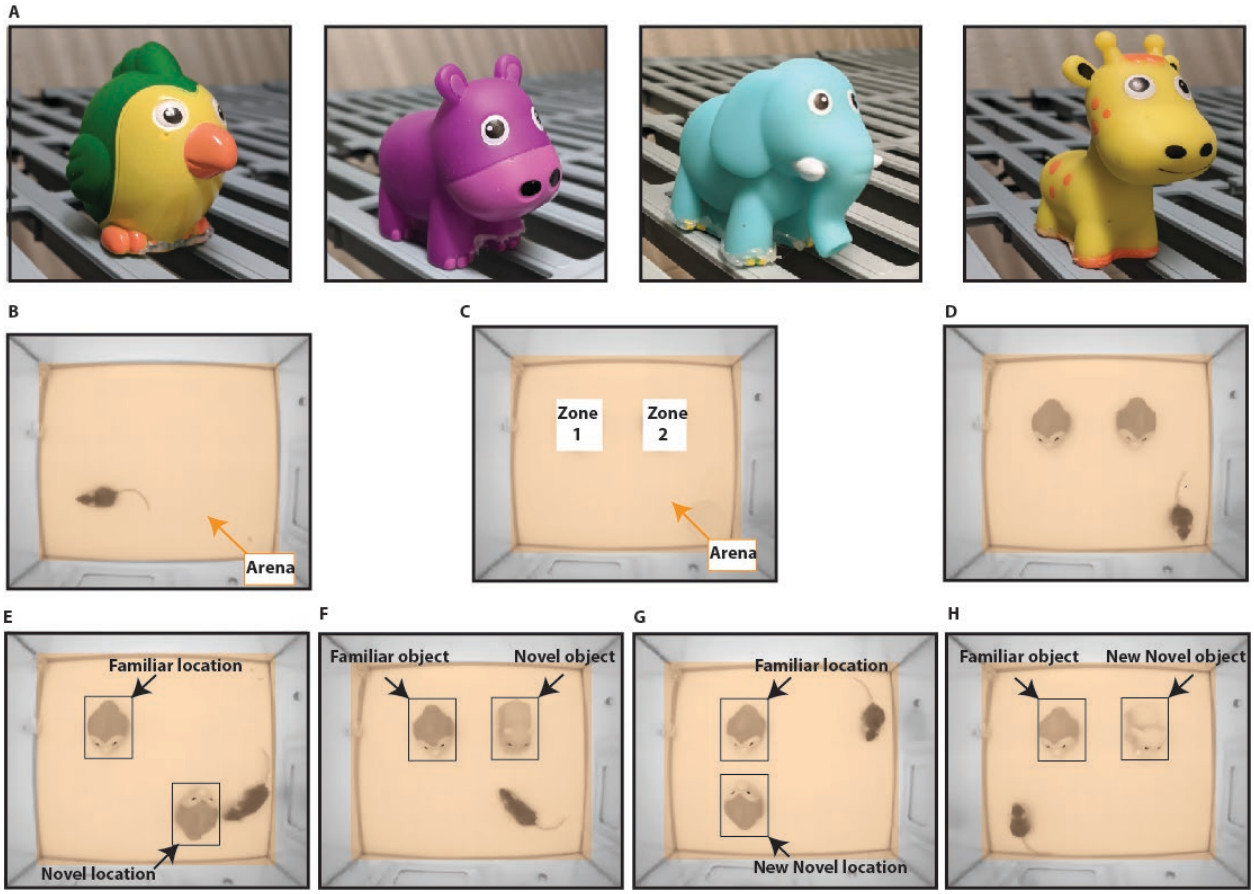

Figure 17 Phenotyper cage set up for NOR and NLR test. 17A: Objects used for the tests. **17B**: Phenotyper cage arena in habituation phase. **17C**: Phenotyper cage sample set up for software detection settings. **17D**: NOR and NLR test, Familiarization phase. **17E**: Arena setting in the NLR, short-term testing (30 minutes). **17F**: Arena setting in the NOR, short-term (30 minutes) testing. **17G**: Arena setting for NLR long-term (24 hr) testing. **17H**: Arena setting for NOR long-term (24hr) testing

4.3.3 Morris Water Maze (MWM) And Reversal Learning

4.3.3.1 Morris Water Maze

~ 2 hours after the end of the NOR and NLR tests, the first phase of MWM was initiated. MWM was done in three phases (Bromley-Brits, Deng, & Song, 2011). Phase 1: Day 0, Flag day. Phase 2: Days 1, 2, 3, 4 training. Phase three: Day 5, testing (**Figure 18A**). After the testing day, the reversal learning paradigm was performed (Explained later). Before initiation of the experiment, all cages in which the animals were singly housed were transferred to the experimental room and covered with a breathable sheet for ~30 minutes, to recover before start of the experiment. All animals were covered the whole time unless being tested. Moreover, during the experiments, the experimenter would be unobserveable to the animals to allow for more free behavior of the animal. Also, during all the phases, the animals were released into the pool facing the wall of the pool.

The pool was videotaped during all phases. The pool was divided into 4 quadrants: South-West (SW), South-East (SE), North-East (NE), North-West (NW). To provide visual cues, four different contrasting cues were placed on the pool wall at 90 degrees apart (**Figure 18B**). The water was temperature controlled (~70ºC) and was drained and the pool was cleaned with 70% ethanol once every other day.

Phase 1: The purpose of phase 1 is to familiarize the animals with the location of the platform in the pool and, as mice do not like to swim, it allows them to identify and learn the location of a place that allows them to stop swimming. For this phase, the pool was filled with water (temperature ~70ºC) and the platform was placed in the NE quadrant (Same quadrant where the platform was hidden in the MWM training days). The platform was placed ~1 cm above the water. The water was clear to allow visualization of the platform. The platform was labeled with a red flag for easier observation and finding. One mouse at a time was released gently in the water in the SW quadrant and was allowed to find the platform in 60 seconds. If the animal did not find the platform in 60 seconds, the animal was grabbed by base of the tail and was placed on the platform for 10 seconds.

Phase 2 (Training): The animals were trained for 4 consecutive days for 4 times each day. The trainings were all performed between 2-6 PM. The pool was filled with water (temperature ~70ºC). White Crayola paint was used to make the water opaque. The platform was placed in the

NE quadrant, 1 cm beneath water surface. During each training day, each animal was trained four times to find the platform. Each time, the animal was released into the pool in a different quadrant. The release quadrant order was SW, SE, NE, NW. After the animal was released in the assigned quadrant, it was allowed to investigate and find the platform within 60 seconds and stay on the platform for 5 seconds. If it could not find the platform after 60 seconds, the animal was grabbed by the base of the tail and placed on the platform and let sit for 10 seconds. After each training, the animal was dried with a towel and returned to the home cage and allowed to recover for 15 minutes before the next training on the same day.

Phase 3 (Testing): On the testing day, the platform was removed. During the testing, each animal was placed in the pool in the furthest point from the platform (Middle of SW and SE quadrant) and was allowed to swim for 60 seconds. The total time spent in each individual quadrant was measured. To ensure that the animals did not differ in motor function, the total distance traveled, and the velocity were quantified as well.

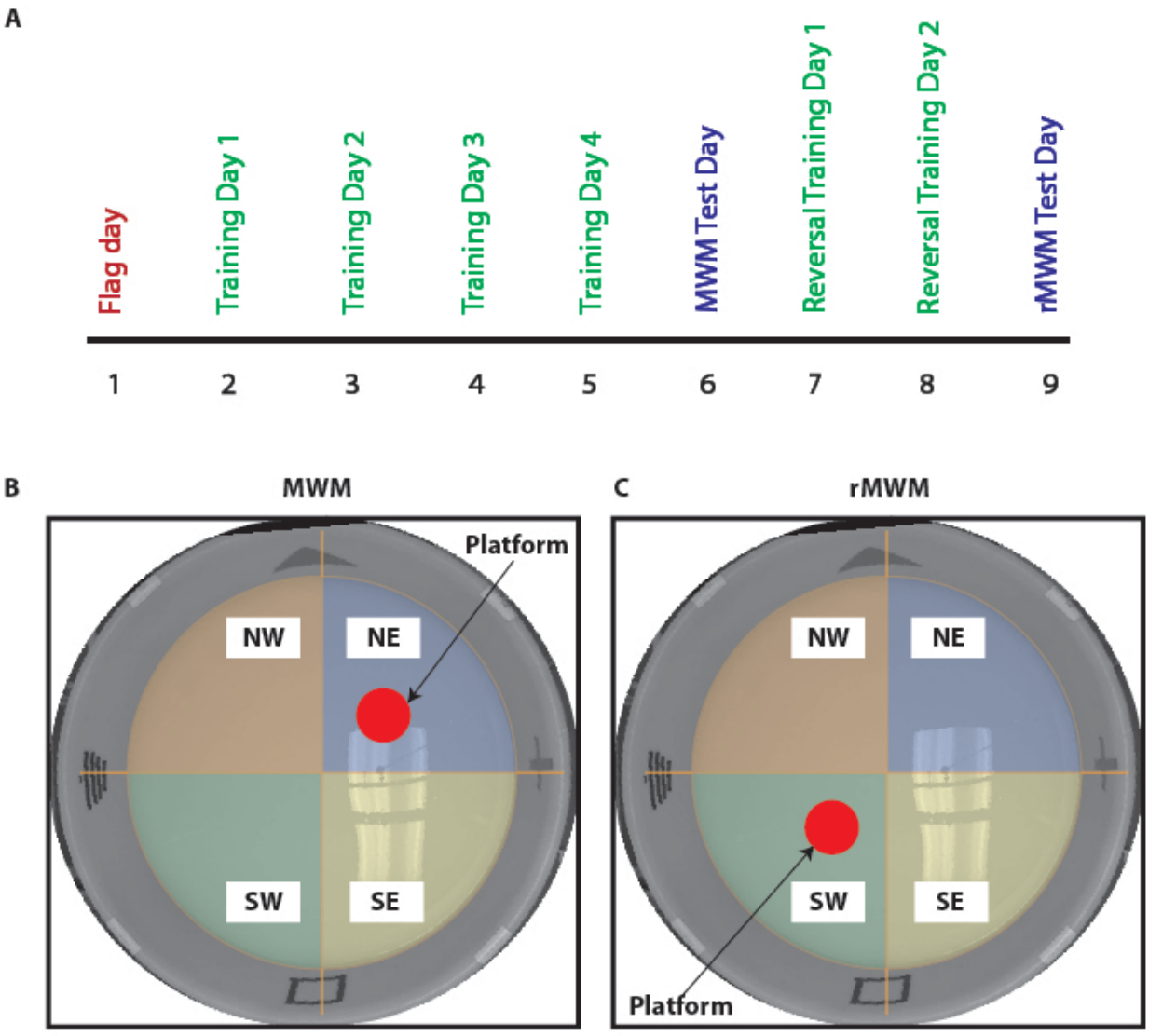

Figure 18 MWM and rMWM testing paradigm and arena setting. 18A: Testing paradigm schema for MWM and rMWM. **18B**: Arena setting for MWM. **18C**: Arena setting for rMWM.

4.3.3.2 Reversal Morris Water Maze Learning (rMWM)

~24 hours after the MWM testing day, the animals were retrained for two consecutive days, 4 times each day. In the rMWM training, the animals were trained to learn the new location of the platform (SW quadrant). The training was performed similar to the MWM training procedure; however, the platform was not submerged under the water and was 1cm above the water, visible to the animals.

On the test day, the platform was removed, and the animal was placed in a starting point furthest from the platform location (Between NE and NW). The animal was released into the pool and was allowed to swim for 60 seconds. The total time spent in each quadrant, the total distance traveled, and the velocity of the animal was measured and compared across all groups. After the testing, the animals were sacrificed.

4.4 Results

4.4.1 ~P26-P27 Spinophilin KO Mice Do Not Show Any Deficits In Novel Object Recognition Test Compared To The WT Animals After Short-Term And Long-Term Interval

The total amount of time spent exploring the familiar and novel object and the frequency of novel and familiar object visits were quantified in the testing session (**Figure 19A, 19F**). To ensure that the quantifications are not skewed due to animal motor deficits, the total distance traveled, and the velocity of the spinophilin WT and KO animals were quantified as well. The velocity and distance traveled were analyzed using a two-tailed, unpaired t-test and reveal no significant difference between WT and KO animals in the 30 minutes NOR test (***Velocity P=0.2986, Distance P=0.2385***) (**Figure 19B ,19C**) and 24 hours NOR test (***Velocity P=0.4148, Distance P=0.4248***) (**Figure 19G, 19H**). To analyze time spent with the familiar and the novel object, the quantified data were analyzed using Two-way ANOVA. The ANOVA analysis revealed no significant effect in the duration of time spent with the novel object following short-term (*Genotype*: ***F (1, 24) = 0.2808, P=0.6010***), *object novelty* (***F (1, 24) = 0.01298, P=0.9102***) or interaction (***F (1, 24) = 0.2668 , P= P=0.6102***) or long-term (*Genotype:* ***F (1, 20) = 0.2306 P=0.6363;*** *object novelty:* ***F (1, 20) = 0.4620 , P= P=0.5045;*** *interaction:* ***F (1, 20) = 1.676, P=0.2102***) NOR tests (**Figure 19D, E, I, J**). A lack of significance may, in part, be due to these

studies being underpowered, particularly in the KO groups. Therefore, we performed individual paired t-tests comparing exploration within the genotypes to ensure that our WT animals were responding appropriately. However, preliminary data suggest that the WT animals spend more time exploring the novel object compared to the familiar object both in short-term (familiar (6.34 s) versus novel (8.130 s); ***P=0.3118***) and long-term (familiar (5.47s) versus novel (11.5 s); ****P=0.0399***) NOR tests (**Figure 19D, 19I**). But, the KO animals do not seem to explore the novel object more than the familiar one in both short-term (9.303s versus 8.138 s; P=0.87) and long-term (10.89 s versus 9.017 s P=0.3777). We have observed the same trend in the frequency of the visit of the familiar and the novel object. The quantified data using Two-Way ANOVA shows no significant effects in the short-term (**Genotype:** (***F (1, 24) = 0.2314, P=0.6349***); **Object Novelty** (***F (1, 24) = 0.6575, P=0.4254***); or **Interaction** (***F (1, 24) = 0.9522, P=0.3389***) or long-term (***Genotype: F (1, 20) = 0.0006133, P=0.9805; object novelty: F (1, 20) = 2.135, P=0.1595; interaction: F (1, 20) = 0.2214, P=0.6431***) NOR tests (**Figure 19E, J**). However, similar to duration of visit, when individual two-tailed t-tests are used to compare the frequency of visit of the novel and familiar object, the WTs visit the novel object significantly more than the familiar object in the short-term test (*P<0.05) but not in the long-term test (P=0.13). On the other hand, the KOs don't show any significant difference in the frequency of visit in the short-term (P=0.9358) or long-term (P=0.12) tests. While these data are underpowered, they may suggest a genotype difference and ongoing studies are being performed to validate this effect.

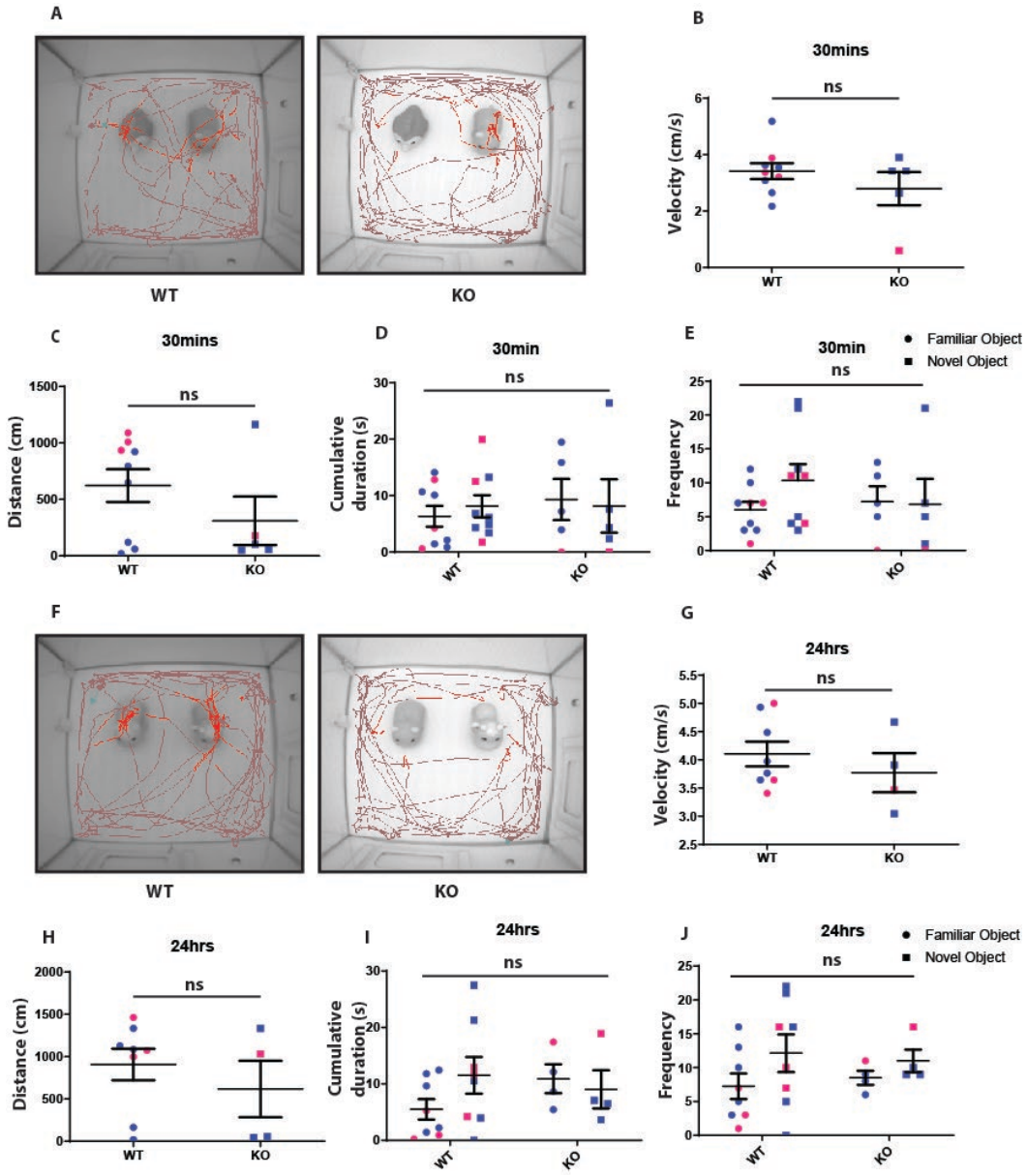

Figure 19. Preliminary data suggest that spinophilin WT animals may have different object exploration times or frequency in the short-term and long-term NOR test. 19A: Track visualization of spinophilin WT and KO animals at the end of the short-term NOR testing. **19B-C**: Spinophilin WT and KOs do not show any significant differences in the velocity and the distance traveled in the short-term NOR test. **19D-E**: Spinophilin WT (n=9) and KO animals (n=5) indicated no significant differences in the time spent (D) and the frequency of visit (E) of the familiar and the novel objects using Two-way ANOVA test. **19F**: Track visualization of spinophilin WT and KO animals at the end of the long-term NOR testing. **19G-H**: Spinophilin WT and KOs do not show any significant differences in the velocity and the distance traveled in the long-term NOR test. **19I-J**: Spinophilin WT (n=8) and KO animals (n=4) indicated no significant differences in the time spent (I) and the frequency of visit (J) of the familiar and the novel object using Two-way ANOVA test. The pink data points indicate female and blue indicate male animals. ns – not significant.

4.4.2 ~P26-P27 Spinophilin KO Mice Do Not Show Any Deficits In Novel Location Recognition Test Compared To The WT Animals After Short-Term And Long-Term Interval

The total amount of time spent exploring the familiar and novel location and the frequency of novel and familiar location visits were quantified in the testing session (**Figure 20A, F**). To ensure that there is no differences in the motor function between spinophilin WT and KO animals, similar to the NOR test, the total distance traveled, and the velocity of the spinophilin WT and KO animals were quantified. The velocity and distance traveled data were analyzed using a two-tailed, unpaired t-test and reveal no significant difference between WT and KO animals in the short-term (*Velocity:* ***P=0.1512,*** *Distance:* ***P=0.3820***) (**Figure 20B, C**) or long-term (*Velocity:* ***P=0.8600,*** *Distance:* ***P=0.4808***) NLR test (**Figure 20G, H**). To analyze time spent with the object in the familiar and the novel location, the quantified data was analyzed using Two-way ANOVA. The ANOVA analysis of the duration with the object in the short-term NLR test revealed no significant effect of *genotype* (**F (1, 24) = 0.03063, P=0.8625**), *location novelty* (**F (1, 24) = 0.6226, P=0.4378**) or *interaction* (**F (1, 24) = 3.718, P=0.0658**). The Two-Way ANOVA analysis of the duration with the object in the long-term NLR test revealed no significant effect of *genotype* (***F (1, 20) = 0.06896, P=0.7955),*** *location novelty* (***F (1, 20) = 0.1020, P=0.7527)*** or *interaction* (***F (1, 20) = 3.277, P=0.0853***) (**Figure 20D, I**). We have observed the same trend in the frequency of the visit of the familiar and the novel locations. The quantified data using Two-Way ANOVA analysis of the short-term frequency of interactions with the object shows no significant effect of *genotype* (**F (1, 24) = 1.038, P=0.3184**), *object novelty* (**F (1, 24) = 0.001729, P=0.9672**) or *interaction* (**F (1, 24) = 2.497, P=0.1271**). The quantified data using Two-Way ANOVA analysis of the long-term frequency of interactions with the object shows no significant effect of *genotype* (**F (1, 20) = 0.02002, P=0.8889*),*** *object novelty* **F (1, 20) = 0.2314, P=0.6357*)*** or *interaction* (**F (1, 20) = 2.083, P=0.1645**) (**Figure 20E, J**). As in the NOR test, additional animals will be required to validate these initial conclusions; however, in the NLR test, the KO data trend very similarly to the WT data, suggesting that loss of spinophilin has no impact on NLR, but may on NOR.

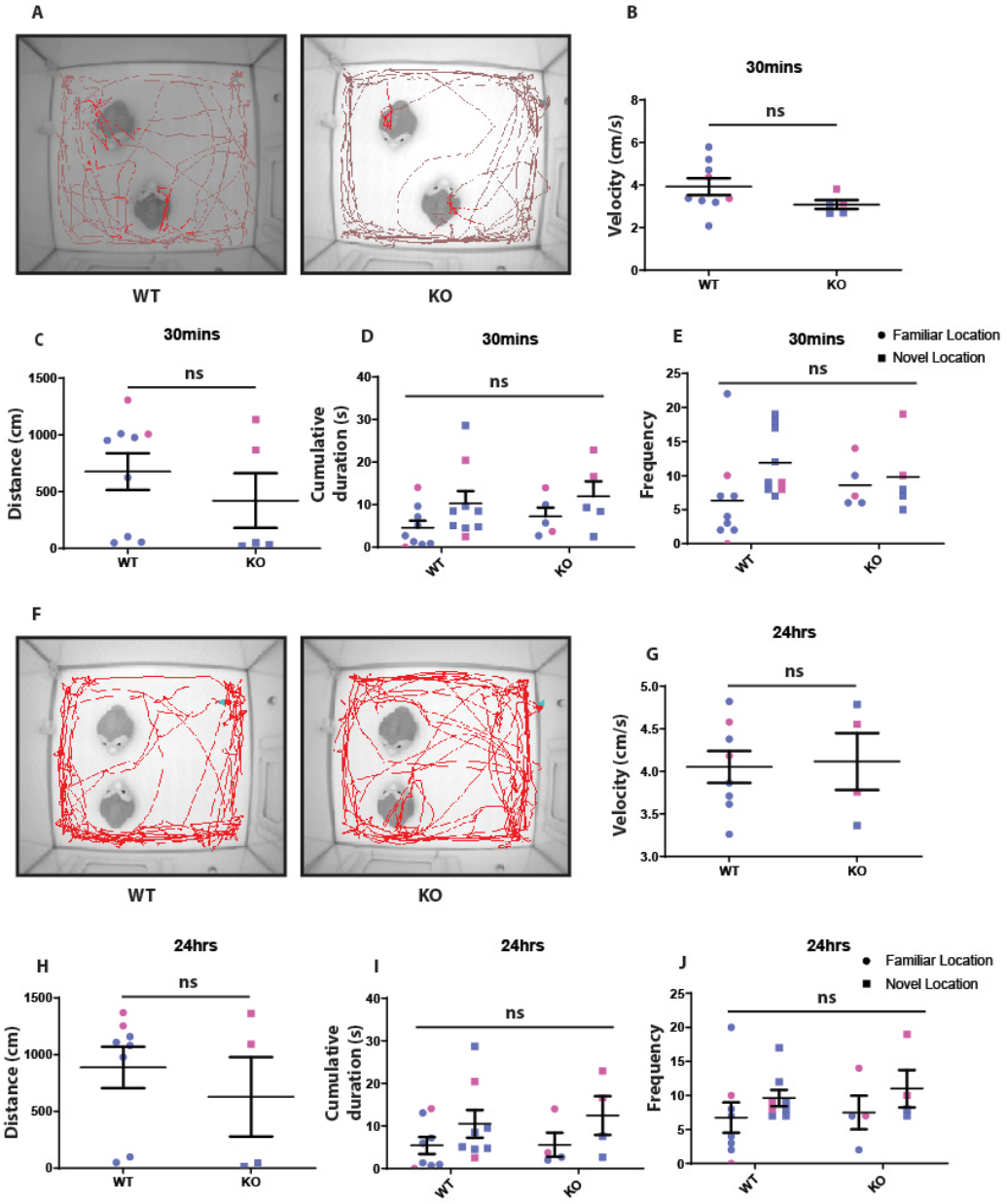

Figure 20. Spinophilin WT and KO animals had similar performance in the short-term and long-term NLR test. 20A: Track visualization of spinophilin WT and KO animals at the end of the short term NLR testing. **20B-C**: Spinophilin WT and KOs do not show any significant differences in the velocity and the distance traveled in the short-term NLR test. **20D-E**: Spinophilin WT (n=8) and KO animals (n=4) indicated no significant differences in the time spent (D) and the frequency of visit (E) of the familiar and the novel location. **20F**: Track visualization of spinophilin WT and KO animals at the end of the long-term NLR testing. **20G-H**: Spinophilin WT and KOs do not show any significant differences in the velocity and the distance traveled in the long-term NLR test. **20I-J**: Spinophilin WT (n=8) and KO animals (n=4) indicated no significant differences in the time spent (I) and the frequency of visit (J) of the familiar and the novel location. The pink data points indicate Female and blue indicate Male animals. ns – not significant

4.4.3 Spinophilin KO Animals Spend More Time In The Platform Quadrant In The MWM

To study the effect of spinophilin global KO on learning and reversal learning, a MWM task was performed. Animals were trained for four consecutive days, 4 times/day. Each time, the animals were released from a different quadrant and were given 1 minute to find the hidden platform placed in the NE quadrant. The latency to the platform was measured across 4 days (**Figure 21A, B, C, D**). After 4 days of training, the animals were placed in the arena and were allowed to swim for 1 minute (**Figure 21E-F**). The total amount of time spent in the NE quadrant (**Figure 21G**) was quantified and analyzed using a two-tailed, unpaired t-test. The results show a significant increase in the time spent in the NE quadrant in the KO compared to the WT mice (***P<0.05**). Furthermore, comparing the cumulative duration of time spent in all 4 quadrants (**Figure 21H**) across the WT and KO groups using a Two-way ANOVA, reveals a significant interaction (**F (3, 48) = 4.516, **P<0.01**) between the quadrant and the genotype. However, the sole effect of Genotype (**F (1, 48) = 4.517e-006, P=0.9983**) was not significant and the effect of quadrant was trending towards significance (**F (3, 48) = 2.445 P=0.0753**). Multiple comparison analysis using a Sidak posthoc test shows a significant difference between spinophilin WT and KO animals in their respective times spent in the NE quadrant (***P<0.05**) but not in the other quadrants. To ensure for normal motor function in both animal genotypes, the velocity of movement (**Figure 21I**) and total distance traveled (**Figure 21J**) was quantified and compared across WT and KO animals using a two-tailed, unpaired t-test. However, no significant difference was detected in the velocity (**P=0.7004**) and distance traveled (**P=0.6976**) across genotypes.

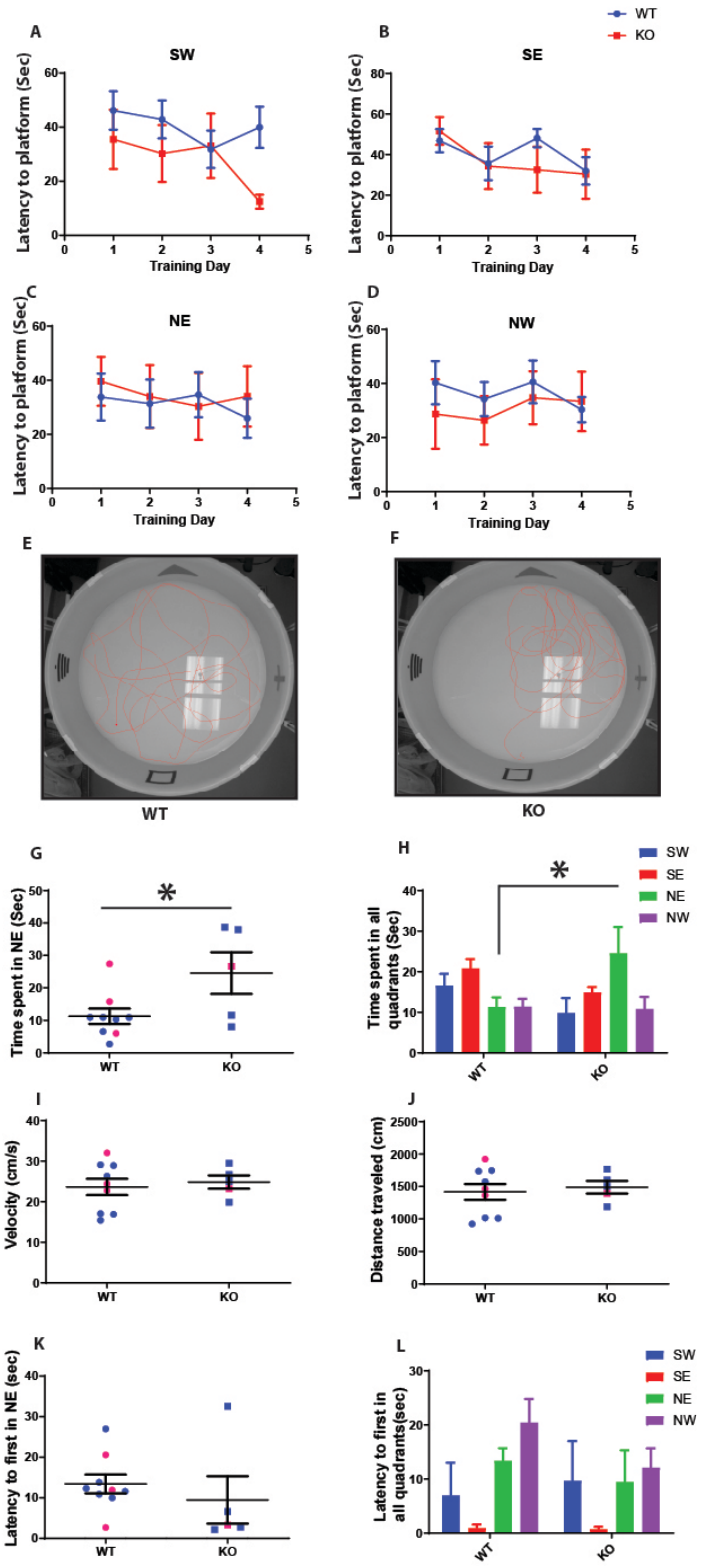

Figure 21 MWM test in spinophilin WT and KO animals. 21A-D: Latency to platform across 4 days of training when animal is released from SW (**A**), SE (**B**), NE(**C**) and NW (**D**) quadrant. **21E-F**: Swim track of the WT and KO animals in the testing day. **21G**: Time spent in NE quadrant by WT and KO animals. **21H**: Time spent in all quadrants by spinophilin WT and KO animals. **21I-J**: Velocity (**I**) and distance traveled (**J**) by spinophilin WT and KO animals during the testing session. **21K**: Latency to first entry to NE quadrant. **21L**: Latency to first entry to all quadrants. * $P<0.05$. All other comparisons are not significant

Figure 22

4.4.4 Spinophilin KO Animals Perseverate More In The Reversal Learning Task (Rmwm)

After the MWM testing, we were interested in investigating reversal learning behavior in the animals. Specifically, we wanted to ascertain how fast and flexible the animals were to switch to a new set of information. For this purpose, we retrained the animals for two consecutive days, with the platform being placed in the opposite quadrant (SW) than the MWM test (NE). Similar to MWM, each animal received 4 trainings per day and in each training the animal was released into the arena from a different quadrant (**Figure 22A-D**). On the testing day, the platform was removed, and the animal was released into the arena from the furthest point away from the platform location (Middle of NE and NW). The animals were allowed to swim for 60 seconds (**Figure 22E, F**) and after 60 seconds were placed back in their home cage. Similar to the MWM, the total amount of time spent in the platform quadrant (SW) was measured across WT and KO animals. The quantified results using a two-tailed, unpaired t-test reveals a trend for a significant difference across WT and KO groups (***P=0.06***). Specifically, the KO animals, spent less time in the SW quadrant (new platform quadrant) than the WT animals (**Figure 22G**) and spent most of their time in the NE (old platform) quadrant which suggests a resistance to switch and adjust their behavior. Furthermore, comparing the time spent in all four quadrants using a Two-way ANOVA, shows a significant interaction between the genotype and quadrant factors (**F (3, 48) = 3.640, *P=0.0191**) and a significant effect of the quadrant (**F (3, 48) = 4.694, **P=0.0059**) but not genotype (**F (1, 48) = 0.001187, P=0.9727**). Specifically, the WT animals spent more time in the SW quadrant compared to the KOs while the KOs spent significantly more time in the NE (Previous platform quadrant) than the SW (new platform quadrant) (**P<0.01). Again, to ensure that the observed changes are not due to motor deficits of the animals, the velocity (**Figure 22I**) and the total distance traveled (**Figure 22J**) were quantified and shows no significant difference across WT and KO groups. Together, these result suggest that the KO animals perseverate more in their spatial learning behavior compared to the WT mice.

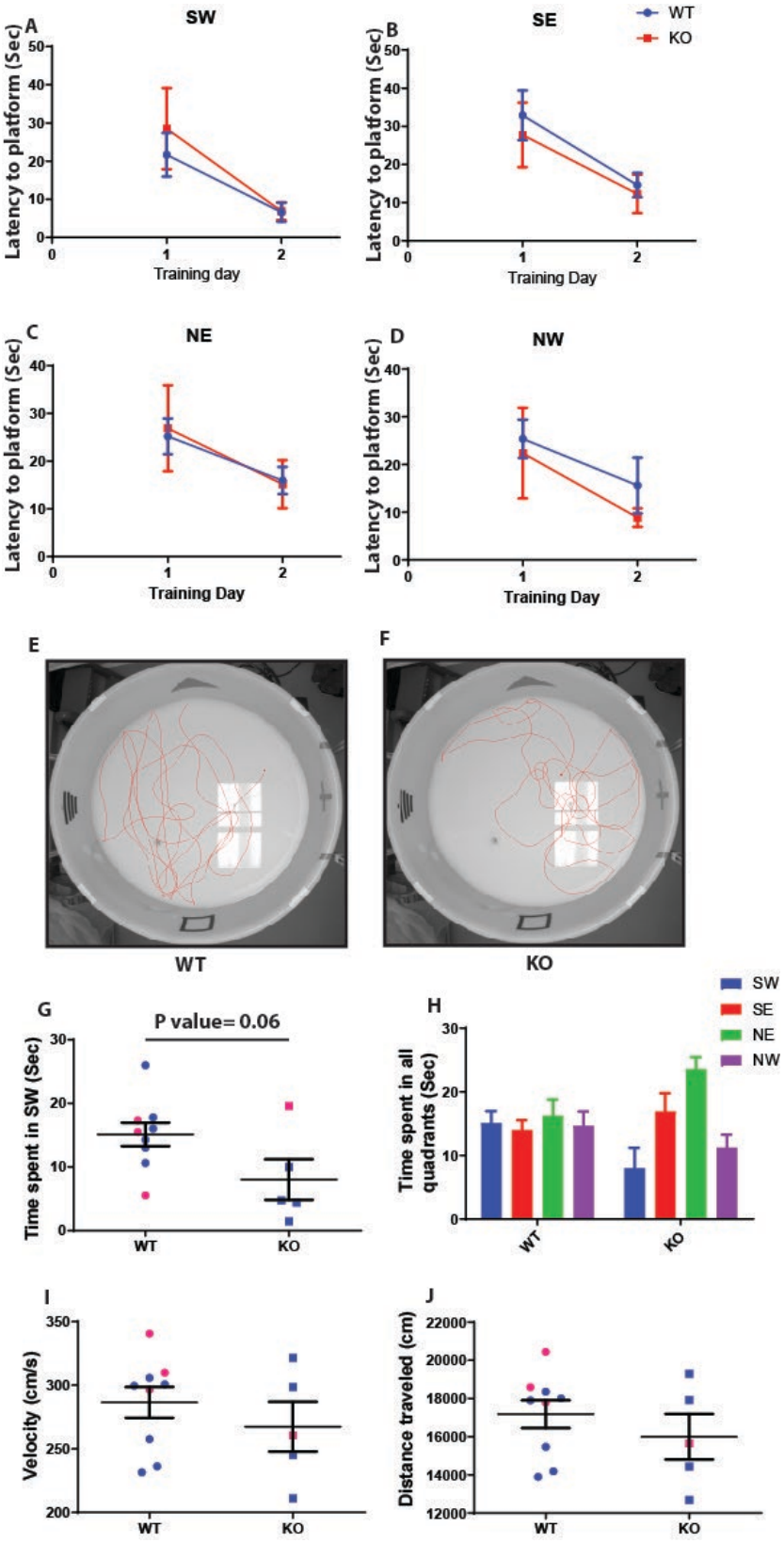

Figure 23 rMWM test in spinophilin WT and KO animals. **22A-D**: Latency to platform across 2 days of re-training when animal is released from SW (**A**), SE (**B**), NE(**C**) and NW (**D**) quadrant. **22E-F**: Swim track of the WT and KO animals in the testing day. **22G**: Time spent in SW quadrant by WT and KO animals. **22H**: Time spent in all quadrants by spinophilin WT and KO animals. **I-J**: Velocity (**I**) and distance traveled (**J**) by spinophilin WT and KO animals during the testing session. Comparisons are not significant.

4.5 Discussion

Dendritic spines change their morphology and density in response to various factors such as learning and memory formation and consolidation (Horn et al., 1985; Moser et al., 1994). Spinophilin, as a scaffolding and a PP1 binding protein, can potentially coordinate spine dynamics by anchoring PP1 to various PSD members important for plasticity such as AMPA and NMDA receptors (Blank et al., 1997; Y. T. Wang & Salter, 1994; Yan et al., 1999), CaMKII (Strack et al., 1997), and actin (Hsieh-Wilson et al., 1999) which suggest a potential role for spinophilin in mediating synaptic plasticity and plasticity-dependent behaviors such as learning and memory. Some studies have investigated the role that protein spinophilin plays in modulating behavioral output. For instance, an investigation of Conditioned Taste Aversion (CTA) learning in the spinophilin WT and KO animals reveal that spinophilin KOs were unable to learn CTA when a stimulus was paired with a moderate dose of LiCl2. In the higher dose of LiCl2, spinophilin KOs acquired CTA learning; however, extinguished faster than the WTs. Interestingly, when a more salient (taste+odor) stimulus was paired with LiCl2, the spinophilin KOs acquired and extinguished CTA learning similar to WTs (Stafstrom-Davis et al., 2001). These studies suggest an important role for spinophilin in learning normal CTA. One other study investigated the effects of spinophilin KO in response to cocaine or amphetamine and found out that knocking out spinophilin blocks the sensitization to cocaine or amphetamine (Morris et al., 2018) while maintaining the normal conditioned place preference to cocaine at a high-dose of cocaine(Areal et al., 2019), but not a lower dose of cocaine(Allen et al., 2006).

NMDA receptors and subsequent activation of CaMKII have been strongly implicated in neuronal plasticity (Bear & Malenka, 1994; Halt et al., 2012; Malenka & Bear, 2004; Stein et al., 2014). Specifically, GluN2B-containing NMDA receptors have been implicated in mediating learning and memory such that their selective blockade after acute stress promotes memory in novel object and novel object-place recognition tests (Howland & Cazakoff, 2010; Wong et al., 2007; Yang et al., 2005). Moreover, NMDA receptors play an important role in spatial memory. When NMDARs are blocked by injection of NMDAR antagonists to the hippocampus, the animal can find the non-hidden platform (when the platform is above the water surface) but cannot remember the location of hidden platform. However blockade of NMDARs after the animal has learned the task, does not interfere with normal memory recall (Kandel, 2013). Specifically, GluN2B is important in spatial learning such that its mutation to disrupt GluN2B and CaMKII

interaction causes deficits in acquiring MWM task (Stein et al., 2014). Furthermore, overexpression of GluN2B in shown to improve performance in MWM acquisition in the adult mice (Shipton & Paulsen, 2014; Tang et al., 1999)

Given this background, both spinophilin and the GluN2B subunit of NMDARs are potential candidates in mediating plasticity underlying learning and memory. Moreover, spinophilin interacts with multiple subunits of the NMDAR (Baucum et al., 2013; Salek et al., 2019). Moreover, we have previously shown that spinophilin can reduce the targeting of PP1 to GluN2B thus changing the phosphorylation of Ser-1284 on the receptor (Salek et al., 2019). Functionally, we have shown that spinophilin decreases surface expression of GluN2B-containing NMDARs, independent of Ser-1284 phosphorylation. These results suggest a potential role of spinophilin-dependent regulation of GluN2B-containing NMDARs in learning and memory. Given this background, we used young (~P25-P35) WT and global spinophilin KO mice to assess their behavior in NOR, NLR, MWM and rMWM tests. NMDAR subunit composition is developmentally regulated such that GluN2B-containing NMDARs are more highly expressed compared to other subtypes of NMDAR in early stages of development and are critical for synapse formation (S. Cull-Candy et al., 2001; Tovar & Westbrook, 1999). As development continues, GluN2B subunits are substituted with GluN2A subunits specifically in the synaptic fraction. Previous studies have shown this shift occurs during postnatal weeks 2-5 in which exclusively GluN2B-containing NMDARs shift to NMDARs containing a significant GluN2A contribution, e.g., 2GluN1/2GluN2A diheteromeric receptors or 2GluN1/1GluN2A/1GluN2B triheteromeric receptors (McKay et al., 2018; Wyllie et al., 2013). Spinophilin expression is known to peak around P21-P26 and decline slightly in adult mice (Allen et al., 1997). For that reason, we utilized P28-P35 mice since we wanted to investigate the effect of spinophilin on behaviors rooted in NMDAR function. While our data are preliminary, they suggest that WT animals spend more time with either novel objects or known objects in a novel location. However, while KO animals appeared to have a similar response as WT animals in the NLR test, they may have had deficits in the NOR test. This suggests potential memory deficits in spinophilin KOs compared to the WTs in the NOR, but not NLR tests in ~P25-P26 animals. Future studies will be performed to validate these initial findings.

One concern is the differences in the velocity and the total distance traveled by WT and KO animals. While the statistical analysis did not detect any significant difference between WT

and KOs, it still is a valid concern since it the KO mice appear to have decreases in their total distance traveled in all the tests (NOR and NLR both in the short-term and long-term (30 minutes and 24 hours)). If future studies observe a significant difference between the WT and KO velocity and distance traveled, this might be due to motor deficits or differences in the anxiety in the KO mice. Wu et. al have shown previously that loss of spinophilin decreases anxiety-like behavior in middle-age mice but not young mice using elevated plus maze task (H. Wu et al., 2017). This suggests a potential role for spinophilin in mediating anxiety-related pathways. Normalizing the cumulative duration of exploration of the novel and familiar object or location back to the total distance traveled, seems to be an alternative approach to mitigate changes in motor output. One other potential concern would be to ensure that the animals are not biased to a certain side or corner of the cage due to parameters such as lighting differences. For this, the animals in the habituation phase (in which the phenotyper cage is empty), were videotaped and the amount of time spent in 4 quadrant of the cage was compared (Data not shown) and no significant differences were detected.

To further investigate the effect of global loss of spinophilin in plasticity-dependent behaviors, MWM and rMWM tests were performed. Similar to NOR and NLR tests, one concern was the performance being affected by the differences in motor coordination and ability. To test for this concern, the velocity and the total distance traveled was quantified and no significant differences or trends for differences were observed across WT and KO animals in MWM and rMWM.

In the MWM test, our preliminary data indicate a non-significant difference in the acquisition of MWM throughout 4 days of training across WT and KO animals. In the testing session, the latency to first enter the platform quadrant was not significantly different across WT and KO animals (**Figure 21K, *P=0.46***) meaning that both groups reached the same quadrant at the same time. However, KO animals were less likely to adjust their behavior once they could not find the platform. In other words, while they spend significantly more time in the platform quadrant, once they could not find the platform, they would still explore the same quadrant while the WTs would readjust and start exploring the other quadrants.

In order to further investigate this perseveration, after the MWM testing, the animals were re-trained for two consecutive days to find the platform in the opposite quadrant. Both WT and KO animals showed the same trend for the latency to reach the platform during the training days.

However, on the testing day, the KOs spent more time in the previous platform quadrant while the WTs spent the most time in the new platform quadrant. This could mean that similar to MWM test, the KO animals have a tendency to perseverate rather than adjusting their behavior. One potential explanation would be potential deficits in spinophilin KO animals in shifting attention which is, in-part, rooted in neurogenesis. Other groups have previously indicated that hippocampal neurogenesis (Gross, 2000) is important in shifting attention such that reduction in the adult neurogenesis in rodents causes deficits in shifting attention to a second stimuli (Hendrickson, Kimble, & Kimble, 1969; Weeden, Mercurio, & Cameron, 2019). Hippocampal adult neurogenesis that occurs in the dentate gyrus has been found to be important in pattern discrimination and episodic memory, depression, and anxiety and attention (Gross, 2000). No specific research has studied the role of spinophilin in hippocampal adult neurogenesis; however, there is strong evidence indicating the importance and potential contribution of spinophilin in normal adult neurogenesis. For example, spinophilin KO animals have been shown to have a smaller hippocampus compared to the WT animals. Specifically, the thickness of multiple layers of hippocampus are reduced in the KO animals such as stratum radiatum, stratum pyramidale, statum lacunosum and relevant to neurogenesis, the dentate gyrus (Feng et al., 2000). One potential explanation for this would be a higher rate of neuronal death in the spinophilin KO animals compared to the WTs. Our previous findings showing a higher level of CC3/C3 ratio in the KO compared to the WT hippocampal cultures, supports this hypothesis. Furthermore, spinophilin has been shown to interact with doublecortin (Dcx), a microtubule-associated protein, which in known to bundle microtubules in the growth cone and also is a marker of newly born neurons (Friocourt et al., 2003; Tsukada, Prokscha, Oldekamp, & Eichele, 2003). Furthermore, spinophilin and Dcx interaction is important in long-distance axonal growth in corpus collasum (Agarwal-Mawal & Paudel, 2001). Given this background, spinophilin might be one of the key players in hippocampal adult neurogenesis through which it can mediate focus and attention shifting behavior. For this reason, global loss of spinophilin might yield deficits in attention shifting. Future studies would focus on investigating the specific effect of spinophilin in mediating hippocampal adult neurogenesis and in these new-born neurons and the functional consequences of this event.

CHAPTER 5. SUMMARY AND FUTURE DIRECTIONS

5.1 Conclusion

Normal brain function requires proper connectivity between neurons. To achieve this connectivity, the pre- and post-synaptic cells need proper protein machinery and protein-protein interactions in axon terminals and dendritic spines. Spinophilin is one of the most abundant proteins residing in the dendritic spines. This protein is an actin-, PP1-binding, and scaffolding protein that is enriched in the PSD. Spinophilin is required for regulating spine dynamics by modulating F-actin bundling. Moreover, spinophilin can anchor PP1 to PSD members such as NMDA and AMPA receptors. Given this background and the important role of spine dynamics and AMPA and NMDA receptor function in neuronal connectivity, spinophilin may be a prominent candidate in mediating hippocampal circuitry, plasticity, and behaviors associated with hippocampal-dependent learning and memory. NMDA receptors have been identified as key players in modulating neuronal function and their proper activity is important in normal brain function. Specifically, hyperactivation of NMDA receptors causes enhanced calcium influx into the cell which eventually leads to activation of apoptotic pathways. Strong evidence suggests that differential subunit phosphorylation of NMDA receptors define their activity and ability to activate downstream signaling pathways. NMDA receptor subunits are phosphorylated by multiple kinases and dephosphorylated by different phosphatases. Besides phosphatases and kinases, per se, phosphorylation of synaptic proteins that regulate kinase or phosphatase targeting and activity also mediate NMDA receptor phosphorylation. Spinophilin is known to alter substrate phosphorylation via its ability to target PP1 to these substrates. Our data demonstrate that spinophilin attenuates PP1 binding to GluN2B and that this decreased binding enhances Ser-1284 phosphorylation on GluN2B. We have identified that spinophilin binds to amino acids 839-1088 on GluN2B. However, we observed that spinophilin modulates Ser-1284 phosphorylation, a site outside of the spinophilin binding domain on GluN2B. This observation suggests that the spinophilin-dependent reduction in PP1 binding to GluN2B could be due to spinophilin having a higher affinity for PP1 and actually displacing PP1 from GluN2B. This is consistent with the idea that PP1 does not exist alone and requires a binding partner, such that when spinophilin is absent, PP1 associates with it as it is a higher affinity targeting protein; however, PP1 can also associate with GluN2B in the absence of

spinophilin, either directly or indirectly, it is currently unclear. Moreover, loss of spinophilin enhances GluN2B interactions with PSD-enriched proteins such as PSD-95 and CaMKII. It is not clear if these changes are due to changes in Ser-1284 phosphorylation. Mutagenesis studies using viral transfection of WT spinophilin hippocampal cultures by the phospho-mimic and phospho-deficient mutant residues in Ser-1284 site with concomitant knock down of endogenous GluN2B would help us better answer this questions.

Furthermore, our data demonstrate that spinophilin can regulate calcium influx through GluN2B containing NMDARs, by increasing Ser-1284 phosphorylation and also decreasing GluN2B surface expression, independent of Ser-1284 phosphorylation. However, it is not clear whether spinophilin-dependent changes in the calcium influx of GluN2B expressing Neuro2a cells is limited to these cell lines. Moreover, we do not know how Ser-1284 phosphorylation modulates calcium influx through the channels. It could be through changing the channel open time, or conductance to calcium. Furthermore, whether spinophilin-dependent changes in receptor surface expression is due to limiting the receptor surface expression or enhancing the receptor internalization is not known. Spinophilin-dependent regulation of GluN2B surface expression may be responsible for increases in CC3 observed in the spinophilin KO, compared to WT, hippocampal primary neurons that were subjected to glutamate toxicity. Here, while we have utilized a methodology to expose the cells to glutamate toxicity, we do not have any evidence whether this toxicity has really insulted the cells and whether altered CC3 levels is due to glutamate toxicity. Regardless, the higher levels of CC3/C3 in the spinophilin KO cells suggests a higher susceptibility of the KO cells to caspase 3 cleavage, a marker of apoptosis. Therefore, spinophilin may be neuroprotective in excitotoxic conditions that are associated with excessive glutamate, such as ischemic stroke. Moreover, given the importance of NMDARs in regulation of hippocampal behaviors and that spinophilin modulates the function of GluN2B-containing NMDARs, we investigated the role of spinophilin in tasks involving learning and memory such as NOR, NLR, MWM and rMWM. Our results suggest that while the spinophilin WT and KO animals do not reveal any difference in the NLR tests, spinophilin KOs have a non-significant deficit in the NOR task and enhanced learning in a MWM task. Moreover, spinophilin KOs have deficits in the rMWM, suggesting perseveration on this spatial reversal learning task. Taken together, our studies demonstrate a spinophilin-dependent regulation of NMDAR phosphorylation and function as well as NMDAR-dependent behaviors.

5.2 Future Directions

Our future studies will mostly revolve around understating the underlying mechanisms by which spinophilin decreases GluN2B-containing NMDAR surface expression and the concomitant decreases in calcium influx. As stated before, we hypothesized that this effect of spinophilin involves enhancing the association of endocytic proteins, such as clathrin and myosin-Va, with GluN2B. Identifying the spinophilin interacting proteins through which spinophilin mediates the receptor surface expression is yet to be known. Moreover, whether this effect of spinophilin is through modulation of phosphorylation sites other than Ser-1284 on GluN2B or on phosphorylation sites on endocytic proteins will be studied.

In addition to trafficking, identifying spinophilin-dependent changes in GluN2B-containing NMDAR channel currents is of great importance. To study this, future experiments will utilize cells transfected with GluN1, GluN2B, in the presence or absence of spinophilin and perform single channel, cell attached patch clamp, to measure how spinophilin can modulate specific channel properties. Future studies should also focus on generating the necessary techniques such as FRET to be able to visualize colocalization of these proteins in live cells. Measuring the field potential in the primary hippocampal cultures generated from spinophilin WT and KO animals in the presence and absence of AP5, would also reveal spinophilin-dependent changes in NMDAR channel currents.

In addition to understanding spinophilin-dependent regulation of NMDAR trafficking and channel properties, the idea of spinophilin playing a neuroprotective role in excitotoxic conditions needs to be further investigated. Future studies will investigate the level of CC3 in ex-vivo and in-vivo models of ischemia. For example, the level of CC3 in the spinophilin WT and KO hippocampal cultures exposed to oxygen-glucose deprived conditions will be investigated, Moreover, the quantification of CC3 using staining or western blotting in spinophilin WT and KO brain slices exposed to oxygen-glucose deprivation models of ischemia would detail how spinophilin modulates response to a specific model of ischemia. Furthermore, quantifying the level of cell death using cell viability kits and staining for propidium iodide (dead cells) and calcein-AM (live cells) would help us visualize the rate of cell death in the absence compared to presence of spinophilin.

To further investigate the role of spinophilin in mediating hippocampal-dependent behaviors, we need to increase the number of tested animals to come to a reliable conclusion.

However, given the important role of spinophilin in spine formation and dynamics, and its interaction with doublecortin, a neurogenesis marker, we hypothesize that spinophilin may be important in mediating adult neurogenesis. Furthermore, the fact that adult neurogenesis is important in mediating attention shift, and that the spinophilin KOs seem to have difficulty in shifting attention and tend to perseverate more in rMWM, strengthens our hypothesis on the importance of spinophilin in mediating hippocampal adult neurogenesis. Future studies will focus on assessing the rate of neurogenesis in conditional spinophilin KOs using BrdU staining. Furthermore, viral transduction of spinophilin into hippocampi of global spinophilin KO animals would inform us whether spinophilin expression in the hippocampus can reverse the perseverating behavior observed in the KOs.

All in all, our future experiments will try to uncover spinophilin dependent changes in NMDAR trafficking and channel currents, NMDAR-dependent pathology observed in ischemia-like conditions, and hippocampal behavior and adult neurogenesis.

PUBLICATIONS

Asma B. Salek, Ruchi Bansal, Nicolas F. Berbari, Anthony J. Baucum II. Spinophilin decreases GluN2B containing NMDA receptor surface expression and limits glutamate-induced toxicity in hippocampal neurons. In Preparation (2020).

Asma B. Salek, Michael C. Edler, Jonathon P. McBride, Anthony J. Baucum II**.** Spinophilin regulates phosphorylation and interactions of the GluN2B subunit of the N-Methyl-D-Aspartate Receptor. *J. Neurochem* 2019. Oct; 151(2):185-203.

Cameron W. Morris, Darryl S. Watkins, **Asma B. Salek**, Michael C. Edler, Anthony J. Baucum II. The association of spinophilin with disks large-associated protein 3 (SAPAP3) is regulated by metabotropic glutamate receptor (mGluR) 5. *Mol Cell Neuro*. 2018 Jun 14;90:60-69. Underlines are co-1st authorship.

Michael C. Edler, **Asma B. Salek**, Darryl S. Watkins, Harjot Kaur, Cameron W. Morris, Bryan K. Yamamoto, Anthony J. Baucum II. Mechanisms regulating the association of protein phosphatase 1 with spinophilin and neurabin. *ACS Chem Neuro. 2018 Nov 21;9(11):2701-2712.* Underlines are co-1st authorship.

REFERENCES

Aarts, M., Liu, Y., Liu, L., Besshoh, S., Arundine, M., Gurd, J. W., . . . Tymianski, M. (2002). Treatment of ischemic brain damage by perturbing NMDA receptor- PSD-95 protein interactions. *Science, 298*(5594), 846-850. doi:10.1126/science.1072873

Agarwal-Mawal, A., & Paudel, H. K. (2001). Neuronal Cdc2-like protein kinase (Cdk5/p25) is associated with protein phosphatase 1 and phosphorylates inhibitor-2. *J Biol Chem, 276*(26), 23712-23718. doi:10.1074/jbc.M010002200

Ai, H., Shi, X. F., Hu, X. P., Fang, W. Q., Zhang, B., & Lu, W. (2017). Acute stress regulates phosphorylation of N-methyl-d-aspartate receptor GluN2B at S1284 in hippocampus. *Neuroscience, 351*, 24-35. doi:10.1016/j.neuroscience.2017.03.029

Allen, P. B., Ouimet, C. C., & Greengard, P. (1997). Spinophilin, a novel protein phosphatase 1 binding protein localized to dendritic spines. *Proc Natl Acad Sci U S A, 94*(18), 9956-9961. Retrieved from http://www.ncbi.nlm.nih.gov/entrez/query.fcgi?cmd=Retrieve&db=PubMed&dopt=Citation&list_uids=9275233

Allen, P. B., Zachariou, V., Svenningsson, P., Lepore, A. C., Centonze, D., Costa, C., . . . Greengard, P. (2006). Distinct roles for spinophilin and neurabin in dopamine-mediated plasticity. *Neuroscience, 140*(3), 897-911. Retrieved from http://www.ncbi.nlm.nih.gov/entrez/query.fcgi?cmd=Retrieve&db=PubMed&dopt=Citation&list_uids=16600521

Andersen, P. (2007). *The hippocampus book*. Oxford ; New York: Oxford University Press.

Areal, L. B., Hamilton, A., Martins-Silva, C., Pires, R. G. W., & Ferguson, S. S. G. (2019). Neuronal scaffolding protein spinophilin is integral for cocaine-induced behavioral sensitization and ERK1/2 activation. *Mol Brain, 12*(1), 15. doi:10.1186/s13041-019-0434-7

Arundine, M., & Tymianski, M. (2004). Molecular mechanisms of glutamate-dependent neurodegeneration in ischemia and traumatic brain injury. *Cell Mol Life Sci, 61*(6), 657-668. doi:10.1007/s00018-003-3319-x

Bansal, R., Engle, S. E., Antonellis, P. J., Whitehouse, L. S., Baucum, A. J., 2nd, Cummins, T. R., . . . Berbari, N. F. (2019). Hedgehog Pathway Activation Alters Ciliary Signaling in Primary Hypothalamic Cultures. *Front Cell Neurosci, 13*, 266. doi:10.3389/fncel.2019.00266

Barria, A., & Malinow, R. (2005). NMDA receptor subunit composition controls synaptic plasticity by regulating binding to CaMKII. *Neuron, 48*(2), 289-301. doi:10.1016/j.neuron.2005.08.034

Baucum, A. J., 2nd, Brown, A. M., & Colbran, R. J. (2013). Differential association of postsynaptic signaling protein complexes in striatum and hippocampus. *J Neurochem, 124*(4), 490-501. doi:10.1111/jnc.12101

Baucum, A. J., 2nd, Jalan-Sakrikar, N., Jiao, Y., Gustin, R. M., Carmody, L. C., Tabb, D. L., . . . Colbran, R. J. (2010). Identification and validation of novel spinophilin-associated proteins in rodent striatum using an enhanced ex vivo shotgun proteomics approach. *Mol Cell Proteomics, 9*(6), 1243-1259. doi:10.1074/mcp.M900387-MCP200

Baucum, A. J., 2nd, Shonesy, B. C., Rose, K. L., & Colbran, R. J. (2015). Quantitative proteomics analysis of CaMKII phosphorylation and the CaMKII interactome in the mouse forebrain. *ACS Chem Neurosci, 6*(4), 615-631. doi:10.1021/cn500337u

Baucum, A. J., 2nd, Strack, S., & Colbran, R. J. (2012). Age-dependent targeting of protein phosphatase 1 to Ca2+/calmodulin-dependent protein kinase II by spinophilin in mouse striatum. *PLoS One, 7*(2), e31554. doi:10.1371/journal.pone.0031554

Baumann, K., Mandelkow, E. M., Biernat, J., Piwnica-Worms, H., & Mandelkow, E. (1993). Abnormal Alzheimer-like phosphorylation of tau-protein by cyclin-dependent kinases cdk2 and cdk5. *FEBS Lett, 336*(3), 417-424.

Bear, M. F., & Malenka, R. C. (1994). Synaptic plasticity: LTP and LTD. *Curr Opin Neurobiol, 4*(3), 389-399. Retrieved from http://www.ncbi.nlm.nih.gov/entrez/query.fcgi?cmd=Retrieve&db=PubMed&dopt=Citation&list_uids=7919934

Benjamin, E. J., Blaha, M. J., Chiuve, S. E., Cushman, M., Das, S. R., Deo, R., . . . Stroke Statistics, S. (2017). Heart Disease and Stroke Statistics-2017 Update: A Report From the American Heart Association. *Circulation, 135*(10), e146-e603. doi:10.1161/CIR.0000000000000485

Bibb, J. A., Nishi, A., O'Callaghan, J. P., Ule, J., Lan, M., Snyder, G. L., . . . Greengard, P. (2001). Phosphorylation of protein phosphatase inhibitor-1 by Cdk5. *J Biol Chem, 276*(17), 14490-14497. doi:10.1074/jbc.M007197200

Bielas, S. L., Serneo, F. F., Chechlacz, M., Deerinck, T. J., Perkins, G. A., Allen, P. B., . . . Gleeson, J. G. (2007). Spinophilin facilitates dephosphorylation of doublecortin by PP1 to mediate microtubule bundling at the axonal wrist. *Cell, 129*(3), 579-591. Retrieved from http://www.ncbi.nlm.nih.gov/entrez/query.fcgi?cmd=Retrieve&db=PubMed&dopt=Citation&list_uids=17482550

Blank, T., Nijholt, I., Teichert, U., Kugler, H., Behrsing, H., Fienberg, A., . . . Spiess, J. (1997). The phosphoprotein DARPP-32 mediates cAMP-dependent potentiation of striatal N-methyl-D-aspartate responses. *Proc Natl Acad Sci U S A, 94*(26), 14859-14864. Retrieved from https://www.ncbi.nlm.nih.gov/pubmed/9405704

Bliss, T. V., & Lomo, T. (1973). Long-lasting potentiation of synaptic transmission in the dentate area of the anaesthetized rabbit following stimulation of the perforant path. *J Physiol, 232*(2), 331-356. doi:10.1113/jphysiol.1973.sp010273

Blom, N., Gammeltoft, S., & Brunak, S. (1999). Sequence and structure-based prediction of eukaryotic protein phosphorylation sites. *J Mol Biol, 294*(5), 1351-1362. doi:10.1006/jmbi.1999.3310

Blom, N., Sicheritz-Ponten, T., Gupta, R., Gammeltoft, S., & Brunak, S. (2004). Prediction of post-translational glycosylation and phosphorylation of proteins from the amino acid sequence. *Proteomics, 4*(6), 1633-1649. doi:10.1002/pmic.200300771

Bollen, M. (2001). Combinatorial control of protein phosphatase-1. *Trends Biochem Sci, 26*(7), 426-431.

Bollen, M., Peti, W., Ragusa, M. J., & Beullens, M. (2010). The extended PP1 toolkit: designed to create specificity. *Trends Biochem Sci, 35*(8), 450-458. doi:S0968-0004(10)00046-0 [pii]
10.1016/j.tibs.2010.03.002

Bollen, M., Peti, W., Ragusa, M. J., & Beullens, M. (2010). The extended PP1 toolkit: designed to create specificity. *Trends in biochemical sciences, 35*(8), 450-458. doi:10.1016/j.tibs.2010.03.002

Bolshakov, V. Y., Golan, H., Kandel, E. R., & Siegelbaum, S. A. (1997). Recruitment of new sites of synaptic transmission during the cAMP-dependent late phase of LTP at CA3-CA1 synapses in the hippocampus. *Neuron, 19*(3), 635-651. doi:10.1016/s0896-6273(00)80377-3

Boyer, C., Schikorski, T., & Stevens, C. F. (1998). Comparison of hippocampal dendritic spines in culture and in brain. *J Neurosci, 18*(14), 5294-5300. Retrieved from https://www.ncbi.nlm.nih.gov/pubmed/9651212

Brinkworth, R. I., Breinl, R. A., & Kobe, B. (2003). Structural basis and prediction of substrate specificity in protein serine/threonine kinases. *Proc Natl Acad Sci U S A, 100*(1), 74-79. doi:10.1073/pnas.0134224100

Bromley-Brits, K., Deng, Y., & Song, W. (2011). Morris water maze test for learning and memory deficits in Alzheimer's disease model mice. *J Vis Exp*(53). doi:10.3791/2920

Calverley, R. K., & Jones, D. G. (1990). Contributions of dendritic spines and perforated synapses to synaptic plasticity. *Brain Res Brain Res Rev, 15*(3), 215-249. Retrieved from https://www.ncbi.nlm.nih.gov/pubmed/2289086

Cao, M., Xu, J., Shen, C., Kam, C., Huganir, R. L., & Xia, J. (2007). PICK1-ICA69 heteromeric BAR domain complex regulates synaptic targeting and surface expression of AMPA receptors. *J Neurosci, 27*(47), 12945-12956. doi:10.1523/JNEUROSCI.2040-07.2007

Carmody, L. C., Baucum, A. J., Bass, M. A., & Colbran, R. J. (2008). Selective targeting of the γ1 isoform of protein phosphatase 1 to F-actin in intact cells requires multiple domains in spinophilin and neurabin. *The FASEB journal : official publication of the Federation of American Societies for Experimental Biology, 22*(6), 1660. doi:10.1096/fj.07-092841

Cercato, M. C., Vazquez, C. A., Kornisiuk, E., Aguirre, A. I., Colettis, N., Snitcofsky, M., . . . Baez, M. V. (2016). GluN1 and GluN2A NMDA Receptor Subunits Increase in the Hippocampus during Memory Consolidation in the Rat. *Front Behav Neurosci, 10*, 242. doi:10.3389/fnbeh.2016.00242

Ceulemans, H., & Bollen, M. (2006). A tighter RVxF motif makes a finer Sift. *Chem Biol, 13*(1), 6-8. doi:10.1016/j.chembiol.2005.12.004

Cheung, H. H., Teves, L., Wallace, M. C., & Gurd, J. W. (2001). Increased phosphorylation of the NR1 subunit of the NMDA receptor following cerebral ischemia. *J Neurochem, 78*(5), 1179-1182. doi:10.1046/j.1471-4159.2001.0780051179.x

Chiu, A. M., Wang, J., Fiske, M. P., Hubalkova, P., Barse, L., Gray, J. A., & Sanz-Clemente, A. (2019). NMDAR-Activated PP1 Dephosphorylates GluN2B to Modulate NMDAR Synaptic Content. *Cell Rep, 28*(2), 332-341 e335. doi:10.1016/j.celrep.2019.06.030

Chung, H. J., Huang, Y. H., Lau, L. F., & Huganir, R. L. (2004). Regulation of the NMDA receptor complex and trafficking by activity-dependent phosphorylation of the NR2B subunit PDZ ligand. *J Neurosci, 24*(45), 10248-10259. doi:10.1523/JNEUROSCI.0546-04.2004

Cohen, P. T. (2002). Protein phosphatase 1--targeted in many directions. *J Cell Sci, 115*(Pt 2), 241-256.

Colbran, R. J., Bass, M. A., McNeill, R. B., Bollen, M., Zhao, S., Wadzinski, B. E., & Strack, S. (1997). Association of brain protein phosphatase 1 with cytoskeletal targeting/regulatory subunits. *J Neurochem, 69*(3), 920-929. Retrieved from http://www.ncbi.nlm.nih.gov/entrez/query.fcgi?cmd=Retrieve&db=PubMed&dopt=Citation&list_uids=9282913

Collett, V. J., & Collingridge, G. L. (2004). Interactions between NMDA receptors and mGlu5 receptors expressed in HEK293 cells. *Br J Pharmacol, 142*(6), 991-1001. doi:10.1038/sj.bjp.0705861

Correia, S. S., Bassani, S., Brown, T. C., Lise, M. F., Backos, D. S., El-Husseini, A., . . . Esteban, J. A. (2008). Motor protein-dependent transport of AMPA receptors into spines during long-term potentiation. *Nat Neurosci, 11*(4), 457-466. doi:10.1038/nn2063

Crump, F. T., Dillman, K. S., & Craig, A. M. (2001). cAMP-dependent protein kinase mediates activity-regulated synaptic targeting of NMDA receptors. *J Neurosci, 21*(14), 5079-5088.

Cull-Candy, S., Brickley, S., & Farrant, M. (2001). NMDA receptor subunits: diversity, development and disease. *Curr Opin Neurobiol, 11*(3), 327-335. doi:10.1016/s0959-4388(00)00215-4

Cull-Candy, S. G., & Leszkiewicz, D. N. (2004). Role of distinct NMDA receptor subtypes at central synapses. *Sci STKE, 2004*(255), re16. doi:10.1126/stke.2552004re16

Das, S., Sasaki, Y. F., Rothe, T., Premkumar, L. S., Takasu, M., Crandall, J. E., . . . Nakanishi, N. (1998). Increased NMDA current and spine density in mice lacking the NMDA receptor subunit NR3A. *Nature, 393*(6683), 377-381. doi:10.1038/30748

Dhavan, R., & Tsai, L. H. (2001). A decade of CDK5. *Nat Rev Mol Cell Biol, 2*(10), 749-759. doi:10.1038/35096019

Di Sebastiano, A. R., Fahim, S., Dunn, H. A., Walther, C., Ribeiro, F. M., Cregan, S. P., . . . Ferguson, S. S. (2016). Role of Spinophilin in Group I Metabotropic Glutamate Receptor Endocytosis, Signaling, and Synaptic Plasticity. *J Biol Chem, 291*(34), 17602-17615. doi:10.1074/jbc.M116.722355

Dingledine, R., Borges, K., Bowie, D., & Traynelis, S. F. (1999). The glutamate receptor ion channels. *Pharmacol Rev, 51*(1), 7-61.

Dudek, S. M., & Bear, M. F. (1992). Homosynaptic long-term depression in area CA1 of hippocampus and effects of N-methyl-D-aspartate receptor blockade. *Proc Natl Acad Sci U S A, 89*(10), 4363-4367. doi:10.1073/pnas.89.10.4363

Edler, M. C., Salek, A. B., Watkins, D. S., Kaur, H., Morris, C. W., Yamamoto, B. K., & Baucum, A. J., 2nd. (2018). Mechanisms Regulating the Association of Protein Phosphatase 1 with Spinophilin and Neurabin. *ACS Chem Neurosci, 9*(11), 2701-2712. doi:10.1021/acschemneuro.8b00144

Egloff, M. P., Johnson, D. F., Moorhead, G., Cohen, P. T., Cohen, P., & Barford, D. (1997). Structural basis for the recognition of regulatory subunits by the catalytic subunit of protein phosphatase 1. *Embo j, 16*(8), 1876-1887. doi:10.1093/emboj/16.8.1876

Erreger, K., Chen, P. E., Wyllie, D. J., & Traynelis, S. F. (2004). Glutamate receptor gating. *Crit Rev Neurobiol, 16*(3), 187-224.

Esteves, S. L., Domingues, S. C., da Cruz e Silva, O. A., Fardilha, M., & da Cruz e Silva, E. F. (2012). Protein phosphatase 1alpha interacting proteins in the human brain. *OMICS, 16*(1-2), 3-17. doi:10.1089/omi.2011.0041

Evans, J. C., Robinson, C. M., Shi, M., & Webb, D. J. (2015). The guanine nucleotide exchange factor (GEF) Asef2 promotes dendritic spine formation via Rac activation and spinophilin-dependent targeting. *J Biol Chem, 290*(16), 10295-10308. doi:10.1074/jbc.M114.605543

Feng, J., Yan, Z., Ferreira, A., Tomizawa, K., Liauw, J. A., Zhuo, M., . . . Greengard, P. (2000). Spinophilin regulates the formation and function of dendritic spines. *Proc Natl Acad Sci U S A, 97*(16), 9287-9292. Retrieved from http://www.ncbi.nlm.nih.gov/entrez/query.fcgi?cmd=Retrieve&db=PubMed&dopt=Citation&list_uids=10922077

Forder, J. P., & Tymianski, M. (2009). Postsynaptic mechanisms of excitotoxicity: Involvement of postsynaptic density proteins, radicals, and oxidant molecules. *Neuroscience, 158*(1), 293-300. doi:10.1016/j.neuroscience.2008.10.021

Fosang, A. J., & Colbran, R. J. (2015). Transparency Is the Key to Quality. *J Biol Chem, 290*(50), 29692-29694. doi:10.1074/jbc.E115.000002

Francis, S. H., Turko, I. V., & Corbin, J. D. (2001). Cyclic nucleotide phosphodiesterases: relating structure and function. *Prog Nucleic Acid Res Mol Biol, 65*, 1-52.

Friocourt, G., Koulakoff, A., Chafey, P., Boucher, D., Fauchereau, F., Chelly, J., & Francis, F. (2003). Doublecortin functions at the extremities of growing neuronal processes. *Cereb Cortex, 13*(6), 620-626. Retrieved from https://www.ncbi.nlm.nih.gov/pubmed/12764037

Furukawa, H., Singh, S. K., Mancusso, R., & Gouaux, E. (2005). Subunit arrangement and function in NMDA receptors. *Nature, 438*(7065), 185-192. doi:10.1038/nature04089

Futter, M., Uematsu, K., Bullock, S. A., Kim, Y., Hemmings, H. C., Jr., Nishi, A., . . . Nairn, A. C. (2005). Phosphorylation of spinophilin by ERK and cyclin-dependent PK 5 (Cdk5). *Proc Natl Acad Sci U S A, 102*(9), 3489-3494. Retrieved from http://www.ncbi.nlm.nih.gov/entrez/query.fcgi?cmd=Retrieve&db=PubMed&dopt=Citation&list_uids=15728359

Gabriel, L. R., Wu, S., & Melikian, H. E. (2014). Brain slice biotinylation: an ex vivo approach to measure region-specific plasma membrane protein trafficking in adult neurons. *J Vis Exp*(86). doi:10.3791/51240

Gardoni, F., Bellone, C., Cattabeni, F., & Di Luca, M. (2001). Protein kinase C activation modulates alpha-calmodulin kinase II binding to NR2A subunit of N-methyl-D-aspartate receptor complex. *J Biol Chem, 276*(10), 7609-7613. doi:10.1074/jbc.M009922200

Goldberg, M. P., & Choi, D. W. (1993). Combined oxygen and glucose deprivation in cortical cell culture: calcium-dependent and calcium-independent mechanisms of neuronal injury. *J Neurosci, 13*(8), 3510-3524. Retrieved from https://www.ncbi.nlm.nih.gov/pubmed/8101871

Gomperts, S. N. (1996). Clustering membrane proteins: It's all coming together with the PSD-95/SAP90 protein family. *Cell, 84*(5), 659-662. Retrieved from https://www.ncbi.nlm.nih.gov/pubmed/8625403

Gorter, J. A., Petrozzino, J. J., Aronica, E. M., Rosenbaum, D. M., Opitz, T., Bennett, M. V., . . . Zukin, R. S. (1997). Global ischemia induces downregulation of Glur2 mRNA and increases AMPA receptor-mediated Ca2+ influx in hippocampal CA1 neurons of gerbil. *J Neurosci, 17*(16), 6179-6188. Retrieved from https://www.ncbi.nlm.nih.gov/pubmed/9236229

Graham, S. H., Shiraishi, K., Panter, S. S., Simon, R. P., & Faden, A. I. (1990). Changes in extracellular amino acid neurotransmitters produced by focal cerebral ischemia. *Neurosci Lett, 110*(1-2), 124-130. doi:10.1016/0304-3940(90)90799-f

Grant, E. R., Guttmann, R. P., Seifert, K. M., & Lynch, D. R. (2001). A region of the rat N-methyl-D-aspartate receptor 2A subunit that is sufficient for potentiation by phorbol esters. *Neurosci Lett, 310*(1), 9-12.

Groc, L., Heine, M., Cousins, S. L., Stephenson, F. A., Lounis, B., Cognet, L., & Choquet, D. (2006). NMDA receptor surface mobility depends on NR2A-2B subunits. *Proc Natl Acad Sci U S A, 103*(49), 18769-18774. doi:10.1073/pnas.0605238103

Gross, C. G. (2000). Neurogenesis in the adult brain: death of a dogma. *Nat Rev Neurosci, 1*(1), 67-73. doi:10.1038/35036235

Grossman, S. D., Futter, M., Snyder, G. L., Allen, P. B., Nairn, A. C., Greengard, P., & Hsieh-Wilson, L. C. (2004). Spinophilin is phosphorylated by Ca2+/calmodulin-dependent protein kinase II resulting in regulation of its binding to F-actin. *J Neurochem, 90*(2), 317-324. Retrieved from http://www.ncbi.nlm.nih.gov/entrez/query.fcgi?cmd=Retrieve&db=PubMed&dopt=Citation&list_uids=15228588

Guo, Z., Li, H. L., Cao, Z., Suo, Z. W., Yang, X., & Hu, X. D. (2019). Spinophilin negatively controlled the function of transient receptor potential vanilloid 1 in dorsal root ganglia neurons of mice. *Eur J Pharmacol, 863*, 172700. doi:10.1016/j.ejphar.2019.172700

Halt, A. R., Dallapiazza, R. F., Zhou, Y., Stein, I. S., Qian, H., Juntti, S., . . . Hell, J. W. (2012). CaMKII binding to GluN2B is critical during memory consolidation. *EMBO J, 31*(5), 1203-1216. doi:emboj2011482 [pii]

10.1038/emboj.2011.482

Hardingham, G. E., & Bading, H. (2002). Coupling of extrasynaptic NMDA receptors to a CREB shut-off pathway is developmentally regulated. *Biochim Biophys Acta, 1600*(1-2), 148-153. doi:10.1016/s1570-9639(02)00455-7

Hardingham, G. E., & Bading, H. (2010). Synaptic versus extrasynaptic NMDA receptor signalling: implications for neurodegenerative disorders. *Nat Rev Neurosci, 11*(10), 682-696. doi:10.1038/nrn2911

Hardingham, G. E., Fukunaga, Y., & Bading, H. (2002). Extrasynaptic NMDARs oppose synaptic NMDARs by triggering CREB shut-off and cell death pathways. *Nat Neurosci, 5*(5), 405-414. doi:10.1038/nn835

Hendrickson, C. W., Kimble, R. J., & Kimble, D. P. (1969). Hippocampal lesions and the orienting response. *J Comp Physiol Psychol, 67*(2), 220-227. doi:10.1037/h0026757

Heroes, E., Lesage, B., Gornemann, J., Beullens, M., Van Meervelt, L., & Bollen, M. (2013). The PP1 binding code: a molecular-lego strategy that governs specificity. *FEBS J, 280*(2), 584-595. doi:10.1111/j.1742-4658.2012.08547.x

Hiday, A. C., Edler, M. C., Salek, A. B., Morris, C. W., Thang, M., Rentz, T. J., . . . Baucum, A. J., 2nd. (2017). Mechanisms and Consequences of Dopamine Depletion-Induced Attenuation of the Spinophilin/Neurofilament Medium Interaction. *Neural Plast, 2017*, 4153076. doi:10.1155/2017/4153076

Hollmann, M., & Heinemann, S. (1994). Cloned glutamate receptors. *Annu Rev Neurosci, 17*, 31-108. doi:10.1146/annurev.ne.17.030194.000335

Horn, G., Bradley, P., & McCabe, B. J. (1985). Changes in the structure of synapses associated with learning. *J Neurosci, 5*(12), 3161-3168. Retrieved from https://www.ncbi.nlm.nih.gov/pubmed/4078621

Howland, J. G., & Cazakoff, B. N. (2010). Effects of acute stress and GluN2B-containing NMDA receptor antagonism on object and object-place recognition memory. *Neurobiol Learn Mem, 93*(2), 261-267. doi:10.1016/j.nlm.2009.10.006

Hsieh-Wilson, L. C., Allen, P. B., Watanabe, T., Nairn, A. C., & Greengard, P. (1999). Characterization of the neuronal targeting protein spinophilin and its interactions with protein phosphatase-1. *Biochemistry, 38*(14), 4365-4373. doi:10.1021/bi982900m

Hsieh-Wilson, L. C., Benfenati, F., Snyder, G. L., Allen, P. B., Nairn, A. C., & Greengard, P. (2003). Phosphorylation of spinophilin modulates its interaction with actin filaments. *J Biol Chem, 278*(2), 1186-1194. Retrieved from http://www.ncbi.nlm.nih.gov/entrez/query.fcgi?cmd=Retrieve&db=PubMed&dopt=Citation&list_uids=12417592

Janssens, V., Longin, S., & Goris, J. (2008). PP2A holoenzyme assembly: in cauda venenum (the sting is in the tail). *Trends Biochem Sci, 33*(3), 113-121. doi:10.1016/j.tibs.2007.12.004

Johannessen, C. M., Boehm, J. S., Kim, S. Y., Thomas, S. R., Wardwell, L., Johnson, L. A., . . . Garraway, L. A. (2010). COT drives resistance to RAF inhibition through MAP kinase pathway reactivation. *Nature, 468*(7326), 968-972. doi:10.1038/nature09627

Jones, M. L., & Leonard, J. P. (2005). PKC site mutations reveal differential modulation by insulin of NMDA receptors containing NR2A or NR2B subunits. *J Neurochem, 92*(6), 1431-1438. doi:10.1111/j.1471-4159.2004.02985.x

Kandel, E. R. (2013). *Principles of neural science* (5th ed ed.). New York: McGraw-Hill Medical.

Karakas, E., Simorowski, N., & Furukawa, H. (2011). Subunit arrangement and phenylethanolamine binding in GluN1/GluN2B NMDA receptors. *Nature, 475*(7355), 249-253. doi:10.1038/nature10180

Kelker, M. S., Dancheck, B., Ju, T., Kessler, R. P., Hudak, J., Nairn, A. C., & Peti, W. (2007). Structural basis for spinophilin-neurabin receptor interaction. *Biochemistry, 46*(9), 2333-2344. Retrieved from http://www.ncbi.nlm.nih.gov/entrez/query.fcgi?cmd=Retrieve&db=PubMed&dopt=Citation&list_uids=17279777

Kim, M. J., Dunah, A. W., Wang, Y. T., & Sheng, M. (2005). Differential roles of NR2A- and NR2B-containing NMDA receptors in Ras-ERK signaling and AMPA receptor trafficking. *Neuron, 46*(5), 745-760. doi:10.1016/j.neuron.2005.04.031

Kindler, S., Rehbein, M., Classen, B., Richter, D., & Bockers, T. M. (2004). Distinct spatiotemporal expression of SAPAP transcripts in the developing rat brain: a novel dendritically localized mRNA. *Brain Res Mol Brain Res, 126*(1), 14-21. doi:10.1016/j.molbrainres.2004.03.014

Kirino, T. (1982). Delayed neuronal death in the gerbil hippocampus following ischemia. *Brain Res, 239*(1), 57-69. doi:10.1016/0006-8993(82)90833-2

Lan, J. Y., Skeberdis, V. A., Jover, T., Grooms, S. Y., Lin, Y., Araneda, R. C., . . . Zukin, R. S. (2001). Protein kinase C modulates NMDA receptor trafficking and gating. *Nat Neurosci, 4*(4), 382-390. doi:10.1038/86028

Lee, H.-K. (2006). Synaptic plasticity and phosphorylation. *Pharmacology & therapeutics, 112*(3), 810-832. doi:10.1016/j.pharmthera.2006.06.003

Lee, H. K., Barbarosie, M., Kameyama, K., Bear, M. F., & Huganir, R. L. (2000). Regulation of distinct AMPA receptor phosphorylation sites during bidirectional synaptic plasticity. *Nature, 405*(6789), 955-959. doi:10.1038/35016089

Lee, S., & Zhou, Z. J. (2006). The synaptic mechanism of direction selectivity in distal processes of starburst amacrine cells. *Neuron, 51*(6), 787-799. doi:10.1016/j.neuron.2006.08.007

Lees, K. R. (1998). Does neuroprotection improve stroke outcome? *Lancet, 351*(9114), 1447-1448. doi:10.1016/S0140-6736(05)78865-6

Li, B., Chen, N., Luo, T., Otsu, Y., Murphy, T. H., & Raymond, L. A. (2002). Differential regulation of synaptic and extra-synaptic NMDA receptors. *Nat Neurosci, 5*(9), 833-834. doi:10.1038/nn912

Li, B. S., Sun, M. K., Zhang, L., Takahashi, S., Ma, W., Vinade, L., . . . Pant, H. C. (2001). Regulation of NMDA receptors by cyclin-dependent kinase-5. *Proc Natl Acad Sci U S A, 98*(22), 12742-12747. doi:10.1073/pnas.211428098

Li, D., Shao, Z., Vanden Hoek, T. L., & Brorson, J. R. (2007). Reperfusion accelerates acute neuronal death induced by simulated ischemia. *Exp Neurol, 206*(2), 280-287. doi:10.1016/j.expneurol.2007.05.017

Liao, G. Y., Wagner, D. A., Hsu, M. H., & Leonard, J. P. (2001). Evidence for direct protein kinase-C mediated modulation of N-methyl-D-aspartate receptor current. *Mol Pharmacol, 59*(5), 960-964. doi:10.1124/mol.59.5.960

Lisman, J. E., & Harris, K. M. (1993). Quantal analysis and synaptic anatomy--integrating two views of hippocampal plasticity. *Trends Neurosci, 16*(4), 141-147. Retrieved from https://www.ncbi.nlm.nih.gov/pubmed/7682347

Liu, H., Wang, H., Peterson, M., Zhang, W., Hou, G., & Zhang, Z. W. (2019). N-terminal alternative splicing of GluN1 regulates the maturation of excitatory synapses and seizure susceptibility. *Proc Natl Acad Sci U S A, 116*(42), 21207-21212. doi:10.1073/pnas.1905721116

Liu, S., Lau, L., Wei, J., Zhu, D., Zou, S., Sun, H. S., . . . Lu, Y. (2004). Expression of Ca(2+)-permeable AMPA receptor channels primes cell death in transient forebrain ischemia. *Neuron, 43*(1), 43-55. doi:10.1016/j.neuron.2004.06.017

Liu, Y., Sun, Q. A., Chen, Q., Lee, T. H., Huang, Y., Wetsel, W. C., . . . Zhang, X. (2009). Targeting inhibition of GluR1 Ser845 phosphorylation with an RNA aptamer that blocks AMPA receptor trafficking. *J Neurochem, 108*(1), 147-157. doi:10.1111/j.1471-4159.2008.05748.x

Liu, Y., Wong, T. P., Aarts, M., Rooyakkers, A., Liu, L., Lai, T. W., . . . Wang, Y. T. (2007). NMDA receptor subunits have differential roles in mediating excitotoxic neuronal death both in vitro and in vivo. *J Neurosci, 27*(11), 2846-2857. doi:10.1523/JNEUROSCI.0116-07.2007

Liu, Y., Zhang, G., Gao, C., & Hou, X. (2001). NMDA receptor activation results in tyrosine phosphorylation of NMDA receptor subunit 2A(NR2A) and interaction of Pyk2 and Src with NR2A after transient cerebral ischemia and reperfusion. *Brain Res, 909*(1-2), 51-58. doi:10.1016/s0006-8993(01)02619-1

Lu, F., Shao, G., Wang, Y., Guan, S., Burlingame, A. L., Liu, X., . . . Jiang, X. (2018). Hypoxia-ischemia modifies postsynaptic GluN2B-containing NMDA receptor complexes in the neonatal mouse brain. *Exp Neurol, 299*(Pt A), 65-74. doi:10.1016/j.expneurol.2017.10.005

Lu, W., Ai, H., Peng, L., Wang, J. J., Zhang, B., Liu, X., & Luo, J. H. (2015). A novel phosphorylation site of N-methyl-D-aspartate receptor GluN2B at S1284 is regulated by Cdk5 in neuronal ischemia. *Exp Neurol, 271*, 251-258. doi:10.1016/j.expneurol.2015.06.016

Lu, W. Y., Xiong, Z. G., Lei, S., Orser, B. A., Dudek, E., Browning, M. D., & MacDonald, J. F. (1999). G-protein-coupled receptors act via protein kinase C and Src to regulate NMDA receptors. *Nat Neurosci, 2*(4), 331-338. doi:10.1038/7243

Luo, X., Popov, S., Bera, A. K., Wilkie, T. M., & Muallem, S. (2001). RGS proteins provide biochemical control of agonist-evoked [Ca2+]i oscillations. *Mol Cell, 7*(3), 651-660. Retrieved from https://www.ncbi.nlm.nih.gov/pubmed/11463389

MacMillan, L. B., Bass, M. A., Cheng, N., Howard, E. F., Tamura, M., Strack, S., . . . Colbran, R. J. (1999). Brain actin-associated protein phosphatase 1 holoenzymes containing spinophilin, neurabin, and selected catalytic subunit isoforms. *J Biol Chem, 274*(50), 35845-35854. Retrieved from http://www.ncbi.nlm.nih.gov/entrez/query.fcgi?cmd=Retrieve&db=PubMed&dopt=Citation&list_uids=10585469

Malenka, R. C., & Bear, M. F. (2004). LTP and LTD: an embarrassment of riches. *Neuron, 44*(1), 5-21. doi:10.1016/j.neuron.2004.09.012

Malinow, R. (2003). AMPA receptor trafficking and long-term potentiation. *Philos Trans R Soc Lond B Biol Sci, 358*(1432), 707-714. doi:10.1098/rstb.2002.1233

Malinow, R., & Tsien, R. W. (1990). Identifying and localizing protein kinases necessary for LTP. *Adv Exp Med Biol, 268*, 301-305. doi:10.1007/978-1-4684-5769-8_33

Mammen, A. L., Kamboj, S., & Huganir, R. L. (1999). Protein phosphorylation of ligand-gated ion channels. *Methods Enzymol, 294*, 353-370.

Man, H. Y. (2011). GluA2-lacking, calcium-permeable AMPA receptors--inducers of plasticity? *Curr Opin Neurobiol, 21*(2), 291-298. doi:10.1016/j.conb.2011.01.001

Manabe, T., Aiba, A., Yamada, A., Ichise, T., Sakagami, H., Kondo, H., & Katsuki, M. (2000). Regulation of long-term potentiation by H-Ras through NMDA receptor phosphorylation. *J Neurosci, 20*(7), 2504-2511. Retrieved from https://www.ncbi.nlm.nih.gov/pubmed/10729330

Manev, H., Favaron, M., Guidotti, A., & Costa, E. (1989). Delayed increase of Ca2+ influx elicited by glutamate: role in neuronal death. *Mol Pharmacol, 36*(1), 106-112. Retrieved from https://www.ncbi.nlm.nih.gov/pubmed/2568579

Manning, G., Whyte, D. B., Martinez, R., Hunter, T., & Sudarsanam, S. (2002). The protein kinase complement of the human genome. *Science, 298*(5600), 1912-1934. doi:10.1126/science.1075762

Mayer, B. J., & Eck, M. J. (1995). SH3 domains. Minding your p's and q's. *Curr Biol, 5*(4), 364-367. Retrieved from https://www.ncbi.nlm.nih.gov/pubmed/7542990

McHugh, T. J., Jones, M. W., Quinn, J. J., Balthasar, N., Coppari, R., Elmquist, J. K., . . . Tonegawa, S. (2007). Dentate gyrus NMDA receptors mediate rapid pattern separation in the hippocampal network. *Science, 317*(5834), 94-99. doi:10.1126/science.1140263

McKay, S., Ryan, T. J., McQueen, J., Indersmitten, T., Marwick, K. F. M., Hasel, P., . . . Komiyama, N. H. (2018). The Developmental Shift of NMDA Receptor Composition Proceeds Independently of GluN2 Subunit-Specific GluN2 C-Terminal Sequences. *Cell Rep, 25*(4), 841-851 e844. doi:10.1016/j.celrep.2018.09.089

Meiselbach, H., Sticht, H., & Enz, R. (2006). Structural analysis of the protein phosphatase 1 docking motif: molecular description of binding specificities identifies interacting proteins. *Chem Biol, 13*(1), 49-59. doi:10.1016/j.chembiol.2005.10.009

Mellacheruvu, D., Wright, Z., Couzens, A. L., Lambert, J. P., St-Denis, N. A., Li, T., . . . Nesvizhskii, A. I. (2013). The CRAPome: a contaminant repository for affinity purification-mass spectrometry data. *Nat Methods, 10*(8), 730-736. doi:10.1038/nmeth.2557

Monyer, H., Burnashev, N., Laurie, D. J., Sakmann, B., & Seeburg, P. H. (1994). Developmental and regional expression in the rat brain and functional properties of four NMDA receptors. *Neuron, 12*(3), 529-540.

Morgan, S. L., & Teyler, T. J. (2001a). Electrical stimuli patterned after the theta-rhythm induce multiple forms of LTP. *J Neurophysiol, 86*(3), 1289-1296. doi:10.1152/jn.2001.86.3.1289

Morgan, S. L., & Teyler, T. J. (2001b). Epileptic-like activity induces multiple forms of plasticity in hippocampal area CA1. *Brain Res, 917*(1), 90-96. doi:10.1016/s0006-8993(01)02913-4

Morris, C. W., Watkins, D. S., Salek, A. B., Edler, M. C., & Baucum, A. J., 2nd. (2018). The association of spinophilin with disks large-associated protein 3 (SAPAP3) is regulated by metabotropic glutamate receptor (mGluR) 5. *Mol Cell Neurosci, 90*, 60-69. doi:10.1016/j.mcn.2018.06.001

Morrison, D. K., Murakami, M. S., & Cleghon, V. (2000). Protein kinases and phosphatases in the Drosophila genome. *J Cell Biol, 150*(2), F57-62. Retrieved from https://www.ncbi.nlm.nih.gov/pubmed/10908587

Moser, M. B., Trommald, M., & Andersen, P. (1994). An increase in dendritic spine density on hippocampal CA1 pyramidal cells following spatial learning in adult rats suggests the formation of new synapses. *Proc Natl Acad Sci U S A, 91*(26), 12673-12675. Retrieved from https://www.ncbi.nlm.nih.gov/pubmed/7809099

Mosley, A. L., Sardiu, M. E., Pattenden, S. G., Workman, J. L., Florens, L., & Washburn, M. P. (2011). Highly reproducible label free quantitative proteomic analysis of RNA polymerase complexes. *Mol Cell Proteomics, 10*(2), M110 000687. doi:10.1074/mcp.M110.000687

Muhammad, K., Reddy-Alla, S., Driller, J. H., Schreiner, D., Rey, U., Bohme, M. A., . . . Sigrist, S. J. (2015). Presynaptic spinophilin tunes neurexin signalling to control active zone architecture and function. *Nat Commun, 6*, 8362. doi:10.1038/ncomms9362

Muly, E. C., Allen, P., Mazloom, M., Aranbayeva, Z., Greenfield, A. T., & Greengard, P. (2004). Subcellular distribution of neurabin immunolabeling in primate prefrontal cortex: comparison with spinophilin. *Cereb Cortex, 14*(12), 1398-1407. Retrieved from http://www.ncbi.nlm.nih.gov/entrez/query.fcgi?cmd=Retrieve&db=PubMed&dopt=Citation&list_uids=15217898

Muly, E. C., Smith, Y., Allen, P., & Greengard, P. (2004). Subcellular distribution of spinophilin immunolabeling in primate prefrontal cortex: localization to and within dendritic spines. *J Comp Neurol, 469*(2), 185-197. Retrieved from http://www.ncbi.nlm.nih.gov/entrez/query.fcgi?cmd=Retrieve&db=PubMed&dopt=Citation&list_uids=14694533

Murphy, D. D., & Segal, M. (1996). Regulation of dendritic spine density in cultured rat hippocampal neurons by steroid hormones. *J Neurosci, 16*(13), 4059-4068. Retrieved from https://www.ncbi.nlm.nih.gov/pubmed/8753868

Murphy, J. A., Stein, I. S., Lau, C. G., Peixoto, R. T., Aman, T. K., Kaneko, N., . . . Zukin, R. S. (2014). Phosphorylation of Ser1166 on GluN2B by PKA is critical to synaptic NMDA receptor function and Ca2+ signaling in spines. *J Neurosci, 34*(3), 869-879. doi:10.1523/JNEUROSCI.4538-13.2014

Nakanishi, H., Obaishi, H., Satoh, A., Wada, M., Mandai, K., Satoh, K., . . . Takai, Y. (1997). Neurabin: a novel neural tissue-specific actin filament-binding protein involved in neurite formation. *J Cell Biol, 139*(4), 951-961. Retrieved from http://www.ncbi.nlm.nih.gov/entrez/query.fcgi?cmd=Retrieve&db=PubMed&dopt=Citation&list_uids=9362513

Norman, E. D., Thiels, E., Barrionuevo, G., & Klann, E. (2000). Long-term depression in the hippocampus in vivo is associated with protein phosphatase-dependent alterations in extracellular signal-regulated kinase. *J Neurochem, 74*(1), 192-198. doi:10.1046/j.1471-4159.2000.0740192.x

Ohshima, T., Ward, J. M., Huh, C. G., Longenecker, G., Veeranna, Pant, H. C., . . . Kulkarni, A. B. (1996). Targeted disruption of the cyclin-dependent kinase 5 gene results in abnormal corticogenesis, neuronal pathology and perinatal death. *Proc Natl Acad Sci U S A, 93*(20), 11173-11178.

Omkumar, R. V., Kiely, M. J., Rosenstein, A. J., Min, K. T., & Kennedy, M. B. (1996). Identification of a phosphorylation site for calcium/calmodulindependent protein kinase II in the NR2B subunit of the N-methyl-D-aspartate receptor. *J Biol Chem, 271*(49), 31670-31678.

Ouimet, C. C., Katona, I., Allen, P., Freund, T. F., & Greengard, P. (2004). Cellular and subcellular distribution of spinophilin, a PP1 regulatory protein that bundles F-actin in dendritic spines. *J Comp Neurol, 479*(4), 374-388. Retrieved from http://www.ncbi.nlm.nih.gov/entrez/query.fcgi?cmd=Retrieve&db=PubMed&dopt=Citation&list_uids=15514983

Pellegrini-Giampietro, D. E., Gorter, J. A., Bennett, M. V., & Zukin, R. S. (1997). The GluR2 (GluR-B) hypothesis: Ca(2+)-permeable AMPA receptors in neurological disorders. *Trends Neurosci, 20*(10), 464-470. doi:10.1016/s0166-2236(97)01100-4

Petito, C. K., Feldmann, E., Pulsinelli, W. A., & Plum, F. (1987). Delayed hippocampal damage in humans following cardiorespiratory arrest. *Neurology, 37*(8), 1281-1286. doi:10.1212/wnl.37.8.1281

Plattner, F., Hernandez, A., Kistler, T. M., Pozo, K., Zhong, P., Yuen, E. Y., . . . Bibb, J. A. (2014). Memory enhancement by targeting Cdk5 regulation of NR2B. *Neuron, 81*(5), 1070-1083. doi:10.1016/j.neuron.2014.01.022

Prabhu Ramya, R., Suma Priya, S., Mayadevi, M., & Omkumar, R. V. (2012). Regulation of phosphorylation at Ser(1303) of GluN2B receptor in the postsynaptic density. *Neurochem Int, 61*(7), 981-985. doi:10.1016/j.neuint.2012.08.016

Qiu, S., Hua, Y. L., Yang, F., Chen, Y. Z., & Luo, J. H. (2005). Subunit assembly of N-methyl-d-aspartate receptors analyzed by fluorescence resonance energy transfer. *J Biol Chem, 280*(26), 24923-24930. doi:10.1074/jbc.M413915200

Ragusa, M. J., Allaire, M., Nairn, A. C., Page, R., & Peti, W. (2011). Flexibility in the PP1:spinophilin holoenzyme. *FEBS Lett, 585*(1), 36-40. doi:10.1016/j.febslet.2010.11.022

Ragusa, M. J., Dancheck, B., Critton, D. A., Nairn, A. C., Page, R., & Peti, W. (2010). Spinophilin directs protein phosphatase 1 specificity by blocking substrate binding sites. *Nat Struct Mol Biol, 17*(4), 459-464. doi:10.1038/nsmb.1786

Ragusa, M. J., Dancheck, B., Critton, D. A., Nairn, A. C., Page, R., & Peti, W. (2010). Spinophilin directs Protein Phosphatase 1 specificity by blocking substrate binding sites. *Nature structural & molecular biology, 17*(4), 459-464. doi:10.1038/nsmb.1786

Raman, I. M., Tong, G., & Jahr, C. E. (1996). Beta-adrenergic regulation of synaptic NMDA receptors by cAMP-dependent protein kinase. *Neuron, 16*(2), 415-421.

Raymond, L. A., Blackstone, C. D., & Huganir, R. L. (1993). Phosphorylation of amino acid neurotransmitter receptors in synaptic plasticity. *Trends Neurosci, 16*(4), 147-153.

Remondes, M., & Schuman, E. M. (2003). Molecular mechanisms contributing to long-lasting synaptic plasticity at the temporoammonic-CA1 synapse. *Learn Mem, 10*(4), 247-252. doi:10.1101/lm.59103

Richman, J. G., Brady, A. E., Wang, Q., Hensel, J. L., Colbran, R. J., & Limbird, L. E. (2001). Agonist-regulated Interaction between alpha2-adrenergic receptors and spinophilin. *J Biol Chem, 276*(18), 15003-15008. Retrieved from http://www.ncbi.nlm.nih.gov/entrez/query.fcgi?cmd=Retrieve&db=PubMed&dopt=Citation&list_uids=11154706

Roche, K. W., Tingley, W. G., & Huganir, R. L. (1994). Glutamate receptor phosphorylation and synaptic plasticity. *Curr Opin Neurobiol, 4*(3), 383-388.

Rothman, S. M., & Olney, J. W. (1995). Excitotoxicity and the NMDA receptor--still lethal after eight years. *Trends Neurosci, 18*(2), 57-58. Retrieved from https://www.ncbi.nlm.nih.gov/pubmed/7537407

Rudolf, R., Bittins, C. M., & Gerdes, H. H. (2011). The role of myosin V in exocytosis and synaptic plasticity. *J Neurochem, 116*(2), 177-191. doi:10.1111/j.1471-4159.2010.07110.x

Ryan, X. P., Alldritt, J., Svenningsson, P., Allen, P. B., Wu, G. Y., Nairn, A. C., & Greengard, P. (2005). The Rho-specific GEF Lfc interacts with neurabin and spinophilin to regulate dendritic spine morphology. *Neuron, 47*(1), 85-100. Retrieved from http://www.ncbi.nlm.nih.gov/entrez/query.fcgi?cmd=Retrieve&db=PubMed&dopt=Citation&list_uids=15996550

Salek, A. B., Edler, M. C., McBride, J. P., & Baucum, A. J., 2nd. (2019). Spinophilin regulates phosphorylation and interactions of the GluN2B subunit of the N-methyl-d-aspartate receptor. *J Neurochem*. doi:10.1111/jnc.14831

Sanz-Clemente, A., Gray, J. A., Ogilvie, K. A., Nicoll, R. A., & Roche, K. W. (2013). Activated CaMKII couples GluN2B and casein kinase 2 to control synaptic NMDA receptors. *Cell Rep, 3*(3), 607-614. doi:10.1016/j.celrep.2013.02.011

Sanz-Clemente, A., Nicoll, R. A., & Roche, K. W. (2013). Diversity in NMDA receptor composition: many regulators, many consequences. *Neuroscientist, 19*(1), 62-75. doi:10.1177/1073858411435129

Sarrouilhe, D., di Tommaso, A., Metaye, T., & Ladeveze, V. (2006). Spinophilin: from partners to functions. *Biochimie, 88*(9), 1099-1113. Retrieved from http://www.ncbi.nlm.nih.gov/entrez/query.fcgi?cmd=Retrieve&db=PubMed&dopt=Citation&list_uids=16737766

Satoh, A., Nakanishi, H., Obaishi, H., Wada, M., Takahashi, K., Satoh, K., . . . Takai, Y. (1998). Neurabin-II/spinophilin. An actin filament-binding protein with one pdz domain localized at cadherin-based cell-cell adhesion sites. *J Biol Chem, 273*(6), 3470-3475. Retrieved from http://www.ncbi.nlm.nih.gov/entrez/query.fcgi?cmd=Retrieve&db=PubMed&dopt=Citation&list_uids=9452470

Schubert, V., & Dotti, C. G. (2007). Transmitting on actin: synaptic control of dendritic architecture. *J Cell Sci, 120*(Pt 2), 205-212. doi:10.1242/jcs.03337

Schuler, H., & Peti, W. (2008). Structure-function analysis of the filamentous actin binding domain of the neuronal scaffolding protein spinophilin. *FEBS J, 275*(1), 59-68. doi:10.1111/j.1742-4658.2007.06171.x

Scott, D. B., Blanpied, T. A., Swanson, G. T., Zhang, C., & Ehlers, M. D. (2001). An NMDA receptor ER retention signal regulated by phosphorylation and alternative splicing. *J Neurosci, 21*(9), 3063-3072.

Scott, J. D., & Pawson, T. (2009). Cell signaling in space and time: where proteins come together and when they're apart. *Science, 326*(5957), 1220-1224. doi:10.1126/science.1175668

Seamon, K. B., & Daly, J. W. (1981). Forskolin: a unique diterpene activator of cyclic AMP-generating systems. *J Cyclic Nucleotide Res, 7*(4), 201-224.

Shipton, O. A., & Paulsen, O. (2014). GluN2A and GluN2B subunit-containing NMDA receptors in hippocampal plasticity. *Philos Trans R Soc Lond B Biol Sci, 369*(1633), 20130163. doi:10.1098/rstb.2013.0163

Sigel, E., Baur, R., & Malherbe, P. (1994). Protein kinase C transiently activated heteromeric N-methyl-D-aspartate receptor channels independent of the phosphorylatable C-terminal splice domain and of consensus phosphorylation sites. *J Biol Chem, 269*(11), 8204-8208.

Skeberdis, V. A., Chevaleyre, V., Lau, C. G., Goldberg, J. H., Pettit, D. L., Suadicani, S. O., . . . Zukin, R. S. (2006). Protein kinase A regulates calcium permeability of NMDA receptors. *Nat Neurosci, 9*(4), 501-510. doi:10.1038/nn1664

Smith-Kinnaman, W. R., Berna, M. J., Hunter, G. O., True, J. D., Hsu, P., Cabello, G. I., . . . Mosley, A. L. (2014). The interactome of the atypical phosphatase Rtr1 in Saccharomyces cerevisiae. *Mol Biosyst, 10*(7), 1730-1741. doi:10.1039/c4mb00109e

Smith, F. D., Oxford, G. S., & Milgram, S. L. (1999). Association of the D2 dopamine receptor third cytoplasmic loop with spinophilin, a protein phosphatase-1-interacting protein. *J Biol Chem, 274*(28), 19894-19900. Retrieved from http://www.ncbi.nlm.nih.gov/entrez/query.fcgi?cmd=Retrieve&db=PubMed&dopt=Citation&list_uids=10391935

Soderling, T. R. (2000). CaM-kinases: modulators of synaptic plasticity. *Curr Opin Neurobiol, 10*(3), 375-380.

Stafstrom-Davis, C. A., Ouimet, C. C., Feng, J., Allen, P. B., Greengard, P., & Houpt, T. A. (2001). Impaired conditioned taste aversion learning in spinophilin knockout mice. *Learn Mem, 8*(5), 272-278. Retrieved from http://www.ncbi.nlm.nih.gov/entrez/query.fcgi?cmd=Retrieve&db=PubMed&dopt=Citation&list_uids=11584074

Stein, I. S., Donaldson, M. S., & Hell, J. W. (2014). CaMKII binding to GluN2B is important for massed spatial learning in the Morris water maze. *F1000Res, 3*, 193. doi:10.12688/f1000research.4660.1

Strack, S., Choi, S., Lovinger, D. M., & Colbran, R. J. (1997). Translocation of autophosphorylated calcium/calmodulin-dependent protein kinase II to the postsynaptic density. *J Biol Chem, 272*(21), 13467-13470. Retrieved from https://www.ncbi.nlm.nih.gov/pubmed/9153188

Swartzwelder, H. S., Risher, M. L., Miller, K. M., Colbran, R. J., Winder, D. G., & Wills, T. A. (2016). Changes in the Adult GluN2B Associated Proteome following Adolescent Intermittent Ethanol Exposure. *PLoS One, 11*(5), e0155951. doi:10.1371/journal.pone.0155951

Swope, S. L., Moss, S. J., Raymond, L. A., & Huganir, R. L. (1999). Regulation of ligand-gated ion channels by protein phosphorylation. *Adv Second Messenger Phosphoprotein Res, 33*, 49-78. Retrieved from https://www.ncbi.nlm.nih.gov/pubmed/10218114

Tang, Y. P., Shimizu, E., Dube, G. R., Rampon, C., Kerchner, G. A., Zhuo, M., . . . Tsien, J. Z. (1999). Genetic enhancement of learning and memory in mice. *Nature, 401*(6748), 63-69. doi:10.1038/43432

Tavalin, S. J., & Colbran, R. J. (2017). CaMKII-mediated phosphorylation of GluN2B regulates recombinant NMDA receptor currents in a chloride-dependent manner. *Mol Cell Neurosci, 79*, 45-52. doi:10.1016/j.mcn.2016.12.002

Terry-Lorenzo, R. T., Elliot, E., Weiser, D. C., Prickett, T. D., Brautigan, D. L., & Shenolikar, S. (2002). Neurabins recruit protein phosphatase-1 and inhibitor-2 to the actin cytoskeleton. *J Biol Chem, 277*(48), 46535-46543. Retrieved from http://www.ncbi.nlm.nih.gov/entrez/query.fcgi?cmd=Retrieve&db=PubMed&dopt=Citation&list_uids=12270929

Thiels, E., Kanterewicz, B. I., Knapp, L. T., Barrionuevo, G., & Klann, E. (2000). Protein phosphatase-mediated regulation of protein kinase C during long-term depression in the adult hippocampus in vivo. *J Neurosci, 20*(19), 7199-7207. Retrieved from https://www.ncbi.nlm.nih.gov/pubmed/11007876

Thiels, E., Norman, E. D., Barrionuevo, G., & Klann, E. (1998). Transient and persistent increases in protein phosphatase activity during long-term depression in the adult hippocampus in vivo. *Neuroscience, 86*(4), 1023-1029. doi:10.1016/s0306-4522(98)00135-3

Tingley, W. G., Ehlers, M. D., Kameyama, K., Doherty, C., Ptak, J. B., Riley, C. T., & Huganir, R. L. (1997). Characterization of protein kinase A and protein kinase C phosphorylation of the N-methyl-D-aspartate receptor NR1 subunit using phosphorylation site-specific antibodies. *J Biol Chem, 272*(8), 5157-5166.

Tovar, K. R., & Westbrook, G. L. (1999). The incorporation of NMDA receptors with a distinct subunit composition at nascent hippocampal synapses in vitro. *J Neurosci, 19*(10), 4180-4188. Retrieved from https://www.ncbi.nlm.nih.gov/pubmed/10234045

Tsien, R. W., & Malinow, R. (1990). Long-term potentiation: presynaptic enhancement following postsynaptic activation of Ca(++)-dependent protein kinases. *Cold Spring Harb Symp Quant Biol, 55*, 147-159. doi:10.1101/sqb.1990.055.01.018

Tsukada, M., Prokscha, A., Oldekamp, J., & Eichele, G. (2003). Identification of neurabin II as a novel doublecortin interacting protein. *Mech Dev, 120*(9), 1033-1043. Retrieved from http://www.ncbi.nlm.nih.gov/entrez/query.fcgi?cmd=Retrieve&db=PubMed&dopt=Citation&list_uids=14550532

Uematsu, K., Futter, M., Hsieh-Wilson, L. C., Higashi, H., Maeda, H., Nairn, A. C., . . . Nishi, A. (2005). Regulation of spinophilin Ser94 phosphorylation in neostriatal neurons involves both DARPP-32-dependent and independent pathways. *J Neurochem, 95*(6), 1642-1652. Retrieved from http://www.ncbi.nlm.nih.gov/entrez/query.fcgi?cmd=Retrieve&db=PubMed&dopt=Citation&list_uids=16300646

Vieira, M. M., Schmidt, J., Ferreira, J. S., She, K., Oku, S., Mele, M., . . . Carvalho, A. L. (2016). Multiple domains in the C-terminus of NMDA receptor GluN2B subunit contribute to neuronal death following in vitro ischemia. *Neurobiol Dis, 89*, 223-234. doi:10.1016/j.nbd.2015.11.007

Virshup, D. M., & Shenolikar, S. (2009). From promiscuity to precision: protein phosphatases get a makeover. *Mol Cell, 33*(5), 537-545. doi:10.1016/j.molcel.2009.02.015

Vogt Weisenhorn, D. M., Roback, L. J., Kwon, J. H., & Wainer, B. H. (2001). Coupling of cAMP/PKA and MAPK signaling in neuronal cells is dependent on developmental stage. *Exp Neurol, 169*(1), 44-55. doi:10.1006/exnr.2001.7651

Wang, J., Liu, S., Fu, Y., Wang, J. H., & Lu, Y. (2003). Cdk5 activation induces hippocampal CA1 cell death by directly phosphorylating NMDA receptors. *Nat Neurosci, 6*(10), 1039-1047. doi:10.1038/nn1119

Wang, X., Zeng, W., Soyombo, A. A., Tang, W., Ross, E. M., Barnes, A. P., . . . Muallem, S. (2005). Spinophilin regulates Ca2+ signalling by binding the N-terminal domain of RGS2 and the third intracellular loop of G-protein-coupled receptors. *Nat Cell Biol, 7*(4), 405-411. Retrieved from http://www.ncbi.nlm.nih.gov/entrez/query.fcgi?cmd=Retrieve&db=PubMed&dopt=Citation&list_uids=15793568

Wang, Y. T., & Salter, M. W. (1994). Regulation of NMDA receptors by tyrosine kinases and phosphatases. *Nature, 369*(6477), 233-235. doi:10.1038/369233a0

Watkins, D. S., True, J. D., Mosley, A. L., & Baucum, A. J. (2019). Correction: Baucum II, Anthony J. et al. Proteomic Analysis of the Spinophilin Interactome in Rodent Striatum Following Psychostimulant Sensitization. Proteomes 2018, 6, 53. *Proteomes, 7*(1). doi:10.3390/proteomes7010007

Waxman, E. A., & Lynch, D. R. (2005). N-methyl-D-aspartate receptor subtypes: multiple roles in excitotoxicity and neurological disease. *Neuroscientist, 11*(1), 37-49. doi:10.1177/1073858404269012

Weeden, C. S. S., Mercurio, J. C., & Cameron, H. A. (2019). A role for hippocampal adult neurogenesis in shifting attention toward novel stimuli. *Behav Brain Res, 376*, 112152. doi:10.1016/j.bbr.2019.112152

Wei, H., Fiskum, G., Rosenthal, R. E., & Perry, D. C. (1997). Global cerebral ischemia and reperfusion alters NMDA receptor binding in canine brain. *Mol Chem Neuropathol, 30*(1-2), 25-39. doi:10.1007/BF02815148

Weisskopf, M. G., Castillo, P. E., Zalutsky, R. A., & Nicoll, R. A. (1994). Mediation of hippocampal mossy fiber long-term potentiation by cyclic AMP. *Science, 265*(5180), 1878-1882. doi:10.1126/science.7916482

Welch, E. J., Jones, B. W., & Scott, J. D. (2010). Networking with AKAPs: context-dependent regulation of anchored enzymes. *Mol Interv, 10*(2), 86-97. doi:10/2/86 [pii]
10.1124/mi.10.2.6

Werling, L. L., Jacocks, H. M., 3rd, Rosenthal, R. E., & Fiskum, G. (1993). Dopamine release from canine striatum following global cerebral ischemia/reperfusion. *Brain Res, 606*(1), 99-105. doi:10.1016/0006-8993(93)91575-d

Winder, D. G., & Sweatt, J. D. (2001). Roles of serine/threonine phosphatases in hippocampal synaptic plasticity. *Nat Rev Neurosci, 2*(7), 461-474. doi:10.1038/35081514

Wong, T. P., Howland, J. G., Robillard, J. M., Ge, Y., Yu, W., Titterness, A. K., . . . Wang, Y. T. (2007). Hippocampal long-term depression mediates acute stress-induced spatial memory retrieval impairment. *Proc Natl Acad Sci U S A, 104*(27), 11471-11476. doi:10.1073/pnas.0702308104

Wu, H., Cottingham, C., Chen, L., Wang, H., Che, P., Liu, K., & Wang, Q. (2017). Age-dependent differential regulation of anxiety- and depression-related behaviors by neurabin and spinophilin. *PLoS One, 12*(7), e0180638. doi:10.1371/journal.pone.0180638

Wu, Y., Chen, C., Yang, Q., Jiao, M., & Qiu, S. (2017). Endocytosis of GluN2B-containing NMDA receptors mediates NMDA-induced excitotoxicity. *Mol Pain, 13*, 1744806917701921. doi:10.1177/1744806917701921

Wyllie, D. J., Livesey, M. R., & Hardingham, G. E. (2013). Influence of GluN2 subunit identity on NMDA receptor function. *Neuropharmacology, 74*, 4-17. doi:10.1016/j.neuropharm.2013.01.016

Yan, Z., Hsieh-Wilson, L., Feng, J., Tomizawa, K., Allen, P. B., Fienberg, A. A., . . . Greengard, P. (1999). Protein phosphatase 1 modulation of neostriatal AMPA channels: regulation by DARPP-32 and spinophilin. *Nat Neurosci, 2*(1), 13-17. Retrieved from http://www.ncbi.nlm.nih.gov/entrez/query.fcgi?cmd=Retrieve&db=PubMed&dopt=Citation&list_uids=10195174

Yang, C. H., Huang, C. C., & Hsu, K. S. (2005). Behavioral stress enhances hippocampal CA1 long-term depression through the blockade of the glutamate uptake. *J Neurosci, 25*(17), 4288-4293. doi:10.1523/JNEUROSCI.0406-05.2005

Zalutsky, R. A., & Nicoll, R. A. (1990). Comparison of two forms of long-term potentiation in single hippocampal neurons. *Science, 248*(4963), 1619-1624. doi:10.1126/science.2114039

Zhang, S., Edelmann, L., Liu, J., Crandall, J. E., & Morabito, M. A. (2008). Cdk5 regulates the phosphorylation of tyrosine 1472 NR2B and the surface expression of NMDA receptors. *J Neurosci, 28*(2), 415-424. doi:10.1523/jneurosci.1900-07.2008

Zheng, X., Zhang, L., Wang, A. P., Bennett, M. V., & Zukin, R. S. (1999). Protein kinase C potentiation of N-methyl-D-aspartate receptor activity is not mediated by phosphorylation of N-methyl-D-aspartate receptor subunits. *Proc Natl Acad Sci U S A, 96*(26), 15262-15267.

Zito, K., Knott, G., Shepherd, G. M., Shenolikar, S., & Svoboda, K. (2004). Induction of spine growth and synapse formation by regulation of the spine actin cytoskeleton. *Neuron, 44*(2), 321-334. Retrieved from http://www.ncbi.nlm.nih.gov/entrez/query.fcgi?cmd=Retrieve&db=PubMed&dopt=Citation&list_uids=15473970